D1.1 – Report on residual biomass characterization, biomass slow pyrolysis and biocoal quality

October 2024

Andrea Salimbeni[1]; Niccolò Pezzati[1]; Davide Mombelli[2]; Sara Scolari[2]

[1] Renewable Energies Consortium for Research and Development (RE-CORD); Scarperia e San Piero (FI), 50038 Italy

[2] Politecnico di Milano (POLIMI); Milano (MI), 20156 Italy

This project has received funding from the European Union's funding programme The Research Fund for Coal and Steel under grant agreement No 101112601. Views and opinions expressed are however those of the author(s) only and do not necessarily reflect those of the European Union or European Research Executive Agency. Neither the European Union nor the granting authority can be held responsible for them.

Table 1: Document information

Document Information	
Project name:	BioRECAST
Full title:	BIObased REsidues Conversion to Advanced fuels for sustainable STeel production
Grant agreement number:	101112601
Deliverable number, name:	1.1, Report on residual biomass characterization, biomass slow pyrolysis and biocoal quality
Lead beneficiary:	2. RE-CORD
Type:	R – Document, report
Delivery date:	Month 9
Dissemination level:	PU - Public
Main author:	Andrea Salimbeni

Table 2: Document history

Version	Date	Changes	Reviewer/ contributor
V1 – first draft	29/07/2024	Document creation	RE-CORD
V2 – second draft	30/09/2024	Paragraph 5 Pilot scale pyrolysis tests comprising pilot scale trial test on SS	RE-CORD
V2 – consolidated version	10/2024	Pilot scale trial tests on AGD, AGW and OFMSW included	RE-CORD
2nd review	xx.xx.xxxx		Company acronym
	xx.xx.xxxx		Company acronym
3rd review	xx.xx.xxxx		Company acronym
Final version	xx.xx.xxxx		Company acronym
Final deliverable submission	xx.xx.xxxx		Company acronym

ACKNOWLEDGMENT & DISCLAIMER

This project has received funding from the European Union's funding program The Research Fund for Coal and Steel under grant agreement No 101112601.

This document has been prepared by BioRECAST project partners as an account of work carried out within the framework of the EC-GA contract No 101112601.

Neither Project Coordinator, nor any signatory party of BioRECAST Project Consortium Agreement, nor any person acting on behalf of any of them:

a) makes any warranty or representation whatsoever, expressed or implied,
   i. with respect to the use of any information, apparatus, method, process, or similar item disclosed in this document, including merchantability and fitness for a particular purpose, or
   ii. that such use does not infringe on or interfere with privately owned rights, including any party's intellectual property, or
   iii. that this document is suitable to any particular user's circumstance; or

b) assumes responsibility for any damages or other liability whatsoever (including any consequential damages, even if the Project Coordinator or any representative of a signatory party of the BioRECAST Project Consortium Agreement has been informed of the possibility of such damages) resulting from your selection or use of this document or any information, apparatus, method, process, or similar item disclosed in this document.

The information and views set out in this report are those of the author(s) and do not necessarily reflect the official opinion of the European Union. Neither the European Union institutions and bodies nor any person acting on their behalf may be held responsible for the use which may be made of the information contained therein.

EXECUTIVE SUMMARY

Steel sector decarbonization is a key challenge for the EU Green deal targets. BioRECAST proposes a “New and improved steelmaking technique”, reusing EAF waste-heat for the on-site conversion of residual biomass into biocoal and sustainable bioenergy, to be used as alternative sustainable fuels for steelmaking process, increasing the sustainability of EAF process. BioRECAST addresses the research objective: “New, sustainable and low-carbon steelmaking and finishing techniques”. The project also aims to the research objective “Decarbonization and Modernization of steel sector”, of the European Green Deal Communication”. The project work plan includes: biocoal production tests in a 100 kg/h plant, biocoal industrial tests in EAFs; pyrogas combustion trials and design of new pyrogas burner to be used in EAFs, and the executive design based on two industrial case studies of a new integrated pyro-EAF steelmaking plant. As a first step, BioRECAST identified a set of biowaste samples commonly produced in urban, industrial and rural areas, potentially suitable for biocoal production to be used in Electric Arc Furnaces. The present report includes the description of the biowaste received, and the characterization performed in laboratory.

This project has received funding from the European Union’s funding programme The Research Fund for Coal and Steel under grant agreement No 101112601. Views and opinions expressed are however those of the author(s) only and do not necessarily reflect those of the European Union or European Research Executive Agency. Neither the European Union nor the granting authority can be held responsible for them.

Table of Contents

FIGURES

TABLES

Table 3: analysis table with reference norms

Parameter	Normative
Moisture	UNI EN ISO 18134-2:2017
Volatiles	UNI EN ISO 18123:2016
Ashes	UNI EN ISO 18122:2016
Fixed carbon (calculation)	UNI EN ISO 1860-2:2005
C, H, N	UNI EN ISO 16948:2015
S (solid matrix)	ASTM D4239-14
S (liquid matrix)	RE-CORD.005
Cl	UNI EN ISO 16994:2017
O (calculation)	UNI EN ISO 16993:2017
Al, B, Ba, Ca, Cd, Co, Cr, Cu, Fe, K, Li, Mg, Mn, Mo, Na, Ni, P, Pb, Si, Ti, V, Zn	UNI EN ISO 16967:2015/UNI EN ISO 16968:2015
HHV	UNI EN ISO 18125:2018
LHV (calculation)	UNI EN ISO 18125:2018
pH	ASTM E70-24
Water content	ASTM E203-08
Coversion factor wet basis/dry basis (calculation)	UNI EN ISO 16993:2017

1 Introduction

The European steel industry represents a major environmental concern, responsible of nearly 190 million tonnes of CO_2 emissions, equal to about 5 % of the overall EU greenhouse gases (GHG) emissions (CATF, 2024), (JRC, 2022). The emissions are related both to a large energy consumption, but also to the dependency of the iron and steel industry on large quantities of coal, mainly used to produce steel by traditional ironmaking processes. Steel is mainly produced by two routes: (i) blast furnace–basic oxygen furnace (BF–BOF) and (ii) electric arc furnace (EAFs) (Mousa, et al., 2016). In 2022, in Europe, the traditional BF-BOF system accounted for about 56.7 % of the EU27 market share, with EAF representing the 43,3 % (EUROFER, 2023). On average, the traditional route consumes around 700-800 kg of coal per ton of hot metal produced (Safarian, 2023; Worldsteel Association, 2023), while the EAF route was considered to consume much less, about 12 kg of coal per t of hot metal (Reichel, et al., 2014). Biogenic carbon sources can contribute to decarbonizing the steel sector and to reduce the EU coal dependency. The use of lignocellulosic biomass as biogenic carbon source to produce biocoal and replace fossil coal has been widely investigated, particularly to replace fossil coal in EAF, and as pulverized coal to be injected in Blast furnaces (PCI) (Salimbeni, et al., 2023; Echterhof, et al., 2014; Echterhof, 2021). The utilization of woody biomass, however, is limited by the reduced availability, and by the high costs of the feedstock, which make the wood-based biocoal not always competitive with the fossil coals, even with the support of the European Emission Trading system.

The utilization of bio-based residues, such as urban, industrial and agricultural biowaste streams, for biocoal production, represents an opportunity to decarbonize the steel sector. In fact, biowastes present much lower market price than biomass and, sometimes, negative value, with a cost related to their valorization. However, the use of biocoals derived from waste materials in the steel sector has been not yet applied, mainly due to the occurrence of harmful elements in the starting feedstock. In fact, in all ironmaking and steelmaking processes coal must comply with specific quality criteria related to its chemical and physical composition. First, the concentration sulfur and phosphorus are highly deleterious elements in steel. Sulphur affects the mechanical properties causing brittleness in the heated state, while phosphorus increases the tendency of a metal to become brittle at reduced temperatures. In the ironmaking and steelmaking furnaces, almost 100% of the phosphorus from raw materials is found in the molten iron, while sulfur is partially transformed in gas, and partially found in the molten slag. Thus, albeit sulfur can be managed by controlling the formation of the blast furnace slag, phosphorus cannot be eliminated during ironmaking and needs to be removed by secondary refining. Other contaminants reducing the coal quality are Zn and Pb, and alkali elements, such as K and Na. Pb impurities might promote redox reactions, create expanding clusters which collapse after cooling and form Pb-containing precipitates. Zn-containing dust seriously affects BF production (Mustafa, et al., 2021). When used in EAF, the coals must be as most inert and refractory as possible at high temperatures and, thus, have the lowest content of volatile matter. On the contrary, a higher volatility is accepted for coal used in blast furnaces. The first step of Task 1.1 of the BioRECAST project was to identify a slate of suitable biowaste streams to be turned into biocoals, based on their composition and the anticipated performances of the pyrolysis and leaching process. In the paragraphs below, the analysis of 8 waste streams is reported. Chemical composition, as well as thermo-gravimetric analysis have been used to determine the optimal pyrolysis conditions to enable the production of biocoals of good quality for the steel sector.

2 Selection of biowastes

Eight biowastes have been selected and characterized. The name, origin and materials description are reported in Table 4.

Table 4: List of biowaste samples

Sample N	Name	Description	Origin
1	OFMSW	Organic Fraction of Municipal Solid Waste	Municipal waste management company
2	GW	Green Waste	Maintenance of gardens and urban areas
3	IS1	Industrial sludge	Sludge from the WWTP of a food industry
4	IS2	Industrial sludge	Sludge from the WWTP of a biochemical industry
5	SS1	Urban sewage sludge	Sludge from a municipal WWTP in Lombardy
6	SS2	Urban sewage sludge	Sludge from a municipal WWTP in Piedmont
7	AGD	Digestate from agrifood sector	Solid residue of anaerobic digestion plant
8	AGW	Lignocellulosic agricultural waste	Olive tree pruning

Waste streams listed 1-8 in Table 4 have heterogeneous and motley composition, especially when it pertains to waste from urban collection such sewage sludge, OFMSW, and GW. However, the characterization performed in this study aimed to identify the most critical aspects and the optimal process conditions to turn them into biocoals. Once the feedstocks are selected for pilot tests and biocoal production campaigns will start, new samples will be collected and analyzed.

2.1 Materials characterization and pretreatment

2.1.1.1 Pretreatment

All the samples have been gathered by RE-CORD, dried and milled. Milling has been performed with the aid of a knife milling unit Retsch SM 300, while the drying was carried out in an oven ArgoLab TCN 200.

Figure 1: Milling unit and oven used for samples pretreatment

2.1.2 Laboratory analysis

The characterization of the different materials selected and listed in Table 4 has been performed with the aid of different instruments and methodologies to determine proximate and ultimate composition as

well as their calorific values. Proximate analysis aimed at the definition of moisture content, ash content, and volatile matter. Ash and volatiles were determined by a LECO TGA701 thermo-gravimetric analyzer (see Figure 2). The ash content of the selected materials has been determined at 550 °C (ash 550) and 710 °C (ash 710); volatiles have been determined as the fraction lost by heating at 900°C for 2 hours. Additionally, a thermogravimetric analysis has been performed on each sample. For this test, three crucibles per sample were charged in the TGA, heated at a heating rate of 7°C/min in by ashing N_2 atmosphere until reaching a temperature of 900°C. The temperature was then kept for 2 hours before cooling the material. The volatilization curves obtained from the analysis have been used to anticipate the material's behavior at different pyrolysis temperatures.

Figure 2: TGA Leco 701, used to determine the volatilization curve of the four waste samples

Ultimate analysis enabled to determine carbon, hydrogen, nitrogen, sulfur, and chlorine contents in the material. The concentration of C, H, N and S was conducted by a CHN-S analyzer (LECO TruSpec CHN and LECO TruSpec S). The oxygen content was calculated as per UNI EN ISO 18125:2018 according to the following equation:

$$O = Ash\ 550 - C - H - N - S$$

Where C, H, N, S represent elements' weight fraction converted on a dry basis. The chlorine content was determined by means of a bomb calorimeter (LECO AC500) pre-treatment and an ion chromatography system (Metrohm 883 Basic IC plus). The higher heating value (HHV) of the feedstock was determined analytically by a bomb calorimeter (LECO AC500).

Fixed carbon represents the recalcitrant fraction of total carbon, i.e. the non-volatile carbon share. Fixed carbon percentage is determined by subtracting ashes and volatiles percentage from total mass, being then defined on a dry basis:

$$Fixed\ carbon\ \left(\%\ \frac{m}{m}\ d.b.\right) = 100 - (Ash\ 710 + volatiles)$$

The concentration of metals and other inorganics in the material was determined after pretreating the solid sample by microwave assisted mineralization system Milestone Start D, thereafter samples have been analyzed by mean of plasma atomic emission spectroscopy (MP-AES, by Agilent 4200 MP-AES). For digesting the solid substrate, the samples have been treated either with aqua regia, or hydrofluoric acid.

2.2 Results of the analysis

All the samples have been characterized at RE-CORD laboratory facility. Being biogenic waste streams, all the samples have been dried in an oven upon delivery. The moisture content of the materials as received is reported in Table 5.

Table 5: Water content of biowaste samples as received

Parameter	Unit	OFMSW	GW	IS1	IS2	SS1	SS2	DIG	AGW
Moisture as received	%wt	69.2	50.1	82.2	30.0	11.5	9.6	70	10.8

Characterization's results after samples' pretreatment are reported in Table 6.

Table 6: Proximate, ultimate analysis and HHV of biowaste samples

Parameter	Unit	OFMSW	GW	IS1	IS2	SS1	SS2	DIG	AGW
Volatiles	%db	75.9	74.4	61.4	64.9	60.0	60.0	69.5	80.2
Volatiles	%d.a.f.*	82.3	79.2	71.5	90.6	83.8	88.5	79.5	81.3
Ash 550	%db	7.8	6.1	14.1	28.4	28.4	32.2	12.6	1.4
Fix. C	%wt	16.3	19.5	24.5	6.7	11.6	7.8	17.9	18.4
C	%wt	45.5	49.2	49.1	38.5	33.7	32.8	43.7	48.8
H	%wt	6.2	6.0	5.4	5.6	5.9	5.6	5.5	5.9
N	%wt	1.5	1.4	4.1	6.8	5.8	5.2	1.3	0.1
S	%wt	0.1	0.1	0.6	3.1	0.9	1.3	0.5	0.1
Cl	%wt	ND	0.0	0.1	0.1	b.d.l.**	0.1	0.3	b.d.l.
HHV	MJ/kg wt	ND	19.5	20.3	17.9	15.1	14.6	16.9	19.5

*Dry ash free basis

** Below detection limit

From data reported in Table 6, it may be observed that the composition of samples can vary significantly depending on their origin, notably when considering carbon content and volatiles. As one could expect, sewage and industrial sludge presented the higher ash content, and the higher volatile content on dry ash free basis. IS2, SS1 and SS2 present a volatile content on dry ash free basis higher than 80%, and an ash content between 28 and 32%.

Graph 1: Concentration of ash and of volatile matter in biowaste samples

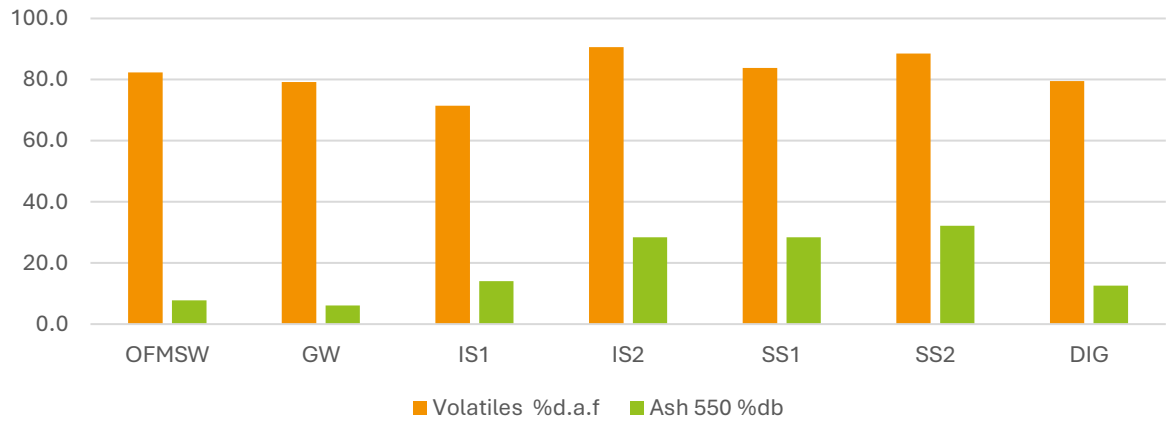

A significant concentration of sulfur was also identified in IS2 (3.1 wt% w.b.), and SS2 (1.3 wt% w.b.). This is to be considered a critical aspect whether the sulfur will remain in the biocoal after the process. A detailed assessment of the inorganic elements in the biowaste streams is reported in Table 7.

Table 7: Concentration of trace elements for different selected biowastes

Element	Unit	OFMSW	GW	IS1	IS2	SS1	SS2	DIG	AGW
Al	mg/kg wt	105	104	3805.4	4076	9382.4	11012	378.9	17.0
B	mg/kg wt	b.d.l.	12	55.4	b.d.l.	b.d.l.	b.d.l.	10.9	b.d.l.
Ba	mg/kg wt	2	26	45.0	39	142.6	192	7.7	7.0
Ca	mg/kg wt	14876	14266	28011	37263	12261.1	18201	34710	4434.0
Cd	mg/kg wt	b.d.l.	b.d.l.	b.d.l.	b.d.l.	b.d.l.	b.d.l.	b.d.l.	b.d.l.
Co	mg/kg wt	b.d.l.	b.d.l.	176	b.d.l.	b.d.l.	b.d.l.	1	b.d.l.
Cr	mg/kg wt	2	0.5	37	68	103	55	5	b.d.l.
Cu	mg/kg wt	4	4	15	71	252	215	23	b.d.l.
Fe	mg/kg wt	596	108	3956	49403	25930	28081	1219	12.0
K	mg/kg wt	7528	6526	2950	2387	4429	2732	14591	1128.0
Li	mg/kg wt	b.d.l.	0.2	1	3	7	7	0	b.d.l.
Mg	mg/kg wt	669	3095	2666	2929	4148	4793	4657	164.0
Mn	mg/kg wt	12	357	553	398	190	155	362	3.0
Mo	mg/kg wt	b.d.l.	b.d.l.	b.d.l.	b.d.l.	b.d.l.	b.d.l.	b.d.l.	b.d.l.
Na	mg/kg wt	2494	94.5	6372	1812	1716	1881	2330	42.0
Ni	mg/kg wt	b.d.l.	b.d.l.	22	15	28	b.d.l.	2	b.d.l.
P	mg/kg wt	964	1535	7245	22419	15600	22153	6265	154.0
Pb	mg/kg wt	b.d.l.	12	b.d.l.	b.d.l.	52	b.d.l.	b.d.l.	b.d.l.
Si	mg/kg wt	421	272	2828	7733	36126	31270	668	15.0
Ti	mg/kg wt	307	1.0	45	90	1152	935	4	b.d.l.
V	mg/kg wt	b.d.l.	b.d.l.	2	5	13	b.d.l.	3	b.d.l.
Zn	mg/kg wt	11	17.5	203	370	612	578	117	b.d.l.
Hg	mg/kg wt	< 1	< 1	< 1	< 1	< 1	< 1	< 1	< 1

Graph 2 shows and draws a comparison of the main elements comprised in the ashes.

Graph 2: Concentration of inorganic elements comprised in the ashes of selected biowastes

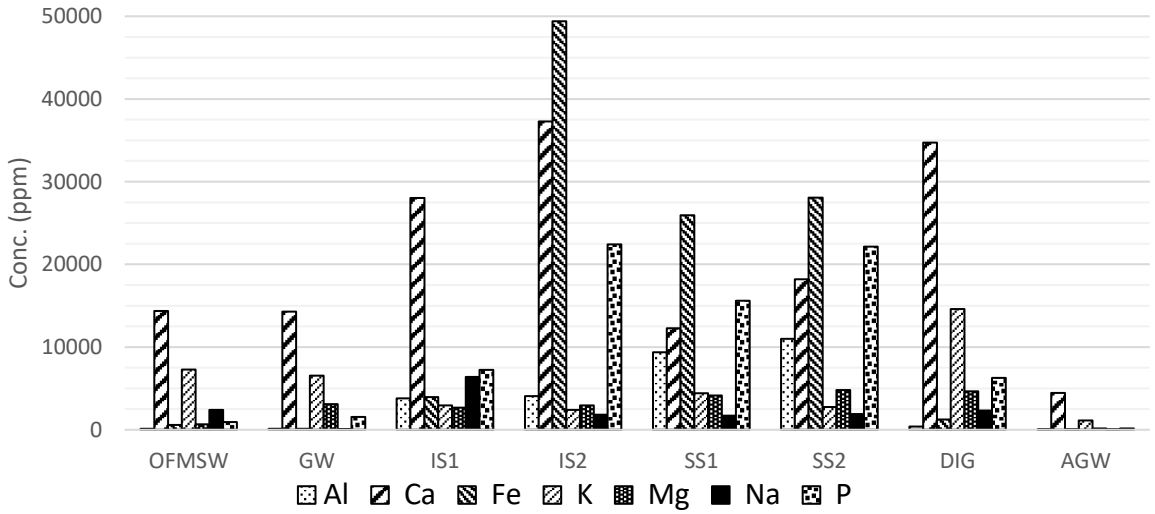

High Ca concentration was found in all selected samples. Moreover, a high concentration of potassium is depicted in the biowaste samples containing lignocellulosic biomass, such as AGW and AGD. Sludge samples (IS1, IS2, SS1 and SS2) contain a significant amount of phosphorus, which must be removed.

2.3 Thermogravimetric analysis

Pyrolysis can be defined as a thermochemical decomposition process during which biomass is heated at moderate or high temperature (typically in the range of 400°-600°C) in the absence of oxygen (Babinszki, et al., 2021). The process always leads to three main products, with proportions that vary based on feedstock nature and process parameters. Namely, a liquid phase, named "pyrolysis – oil", represented by a mixture of condensable organic vapors and water; a gaseous phase, with CH_4, CO, CO_2, H_2 and other gases in different proportions, and a solid carbonaceous material, named char, are obtained. The relative weight of those three main products is strictly dependent on key process parameters, i.e.: RT (Solid residence time), HVRT (Hot Vapor Residence Time), process temperature and HR (Heating Rate). Depending on how these values change, the pyrolysis process can be classified as "slow", "intermediate" or "fast" pyrolysis (see Table 8). Slow thermochemical processing at temperatures below 300 °C is usually defined as "Torrefaction". Among these thermal processes, torrefaction, and slow pyrolysis allow to maximize the solid yield. In fact, both low heating rate and mild temperature foster polymerization reactions leading to solid residue formation. Moreover, a longer hot vapor residence time, i.e. a reduced gas flow affects the char yield as low flow rate provides opportunity for the volatiles to interact with the solid carbonaceous residue and increase the solid yield (Antal & Grønli, 2003).

Table 8: Operative parameters for different thermochemical processes applied to biomass (Salimbeni, et al., 2023)

Parameter	Torrefaction	Gasification	Intermediate Py.	Slow Pyr.
Temperature	200 - 300 °C	800 – 1000 °C	500 – 600 °C	400 – 700 °C
RT	1-2 Hours	<1 hour	<1 hour	1 – 5 hours
HR	1-20 °C/min	High	>20°C/min	0.1 – 20 °C/min
Liquid Yield	5-10%	-	50%	30 - 35%
Gas Yield	15%	85 – 90%	25%	35%
Solid Yield	75-80%	<15%	20-25%	30 - 35%

Torrefaction, thanks to the low process temperature and the long residence time, achieves high solid yields, above 50 % w/w. According to Shankar Tumuluru, et al. 2011 a mass yield of 61.5 % was achieved by torrefaction of willow at 290 °C. Due to the low temperature compared to the slow pyrolysis process, the "torrefied material" has a volatile content above 70 % on dry basis (Ibrahim, et al., 2013). On the contrary, thanks to higher temperatures, slow pyrolysis brings to higher devolatilization of the

feedstock, producing a smaller amount of solid, less volatile and with a higher concentration of stable carbon. Slow pyrolysis is characterized by high temperatures (usually > 400 °C), low heating rate (< 30°C/min) and long biomass retention time (more than 2 hours). In slow pyrolysis, the material is converted into pyro-gas, and a carbon-rich solid. Ashes remain as inert part of the carbon-rich solid. The solid yield is in range of 25-30% of the input organic material, but since ashes don't participate to the reaction, high-ash materials result in higher solid mass yield. In industrial plants this stream is usually burnt to supply the energy required by the pyrolysis process. The carbon-rich solid, herein named "char", is usually characterized by low volatile content (< 25 % db), low oxygen, and a low molar H/C ratio (below 0.7).

The next paragraph depicts the thermogravimetric analysis that has been performed to identify the devolatilization peak of the biowaste samples object of the study.

2.3.1 TGA of sewage sludge (SS) samples

The thermogravimetric analysis of the two sewage sludges presents significant differences. A more rapid and intense weight loss is identified for SS1, compared to SS2. The reason can be related to the fact that SS1 was not digested anaerobically, while SS2 was obtained after that sewage sludge was digested to produce biogas. Both samples show a devolatilization peak at about 350-400 °C, corresponding to the cellulose degradation temperature. At 500°C most of the volatile compound is lost and the devolatilization of the organic matter becomes slower. A further devolatilization peak is identified at about 800°C, probably due to the presence of carbonates.

Figure 3: TGA curve of SS1

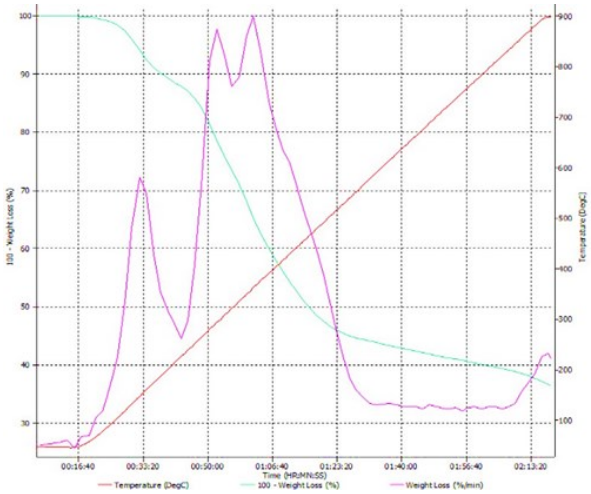

Figure 4: TGA curve of SS2

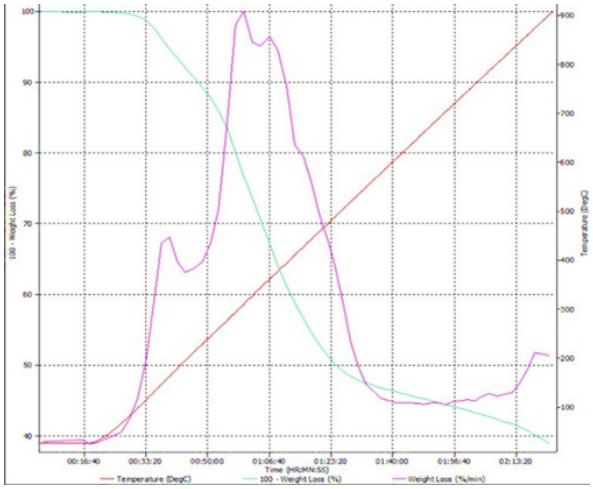

2.3.2 TGA of industrial sludge (IS) samples

The thermo-gravimetric analysis of the industrial sludge samples presents similar results, with the devolatilization peak of IS 1 achieved at lower temperatures (nearly 300°C) than IS2 (between 350 and 400°C). As for the SS, at temperatures above 450 °C most of the volatile matter was lost, with a slow degradation phase starting.

Figure 5: TGA curve of IS1

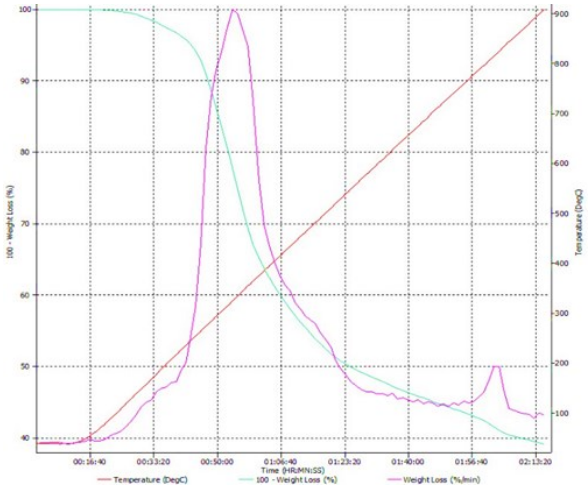

Figure 6: TGA curve of IS2

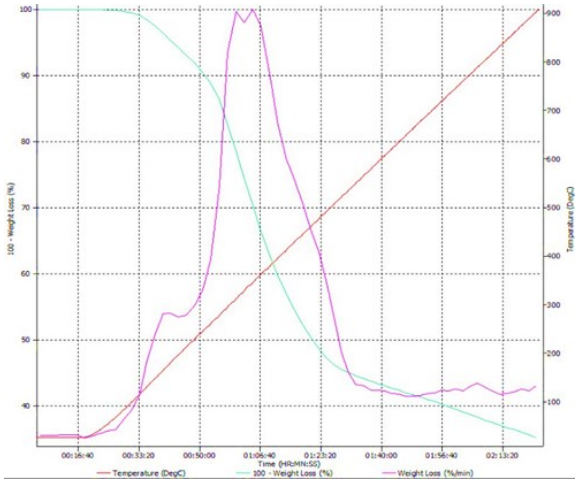

2.3.3 TGA of urban biowaste samples (OFMSW + AGW)

The biowaste samples derived from urban collection: OFMSW and GW, present similar curves. One difference might be noticed as of the GW showing a more visible devolatilization peak at low temperature, probably related to the hemicellulose contained in the material. At temperatures above 400°C, both materials show a very rapid devolatilization, while the weight loss becomes slower after 500°C, as for the other investigated samples

Figure 7: TGA curve of OFMSW

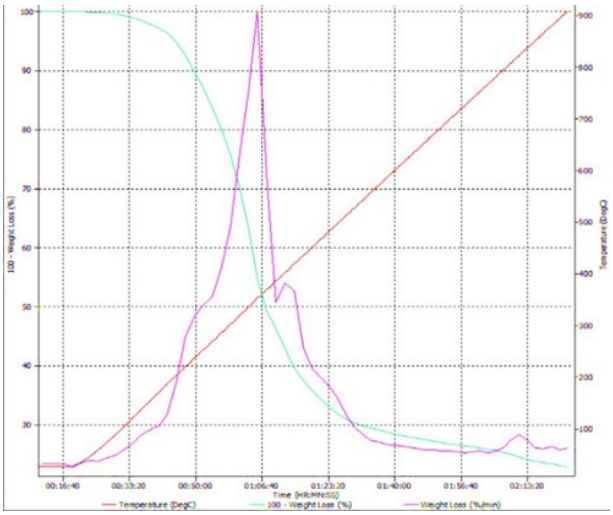

Figure 8: TGA curve of GW

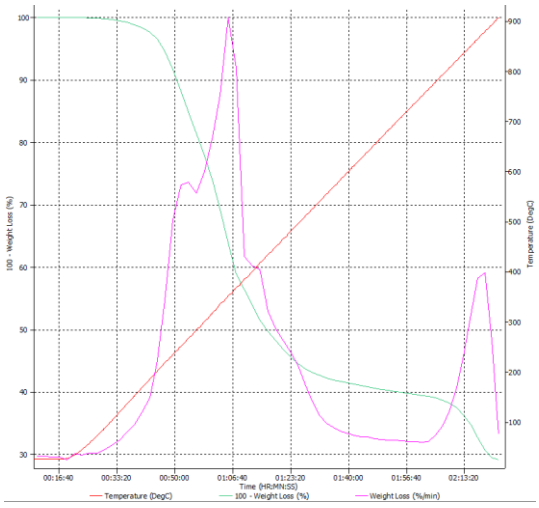

2.3.4 TGA of agricultural digestate (AGD) and olives pruning (AGW)

The same test performed on the agricultural waste derived from the anaerobic digestion of manure and straw, show similar curve than industrial sludge samples, with a very rapid weight loss at 300-350°C, and a stabilization of the curve above 400°C.

Figure 9: TGA curve of AGD and AGW

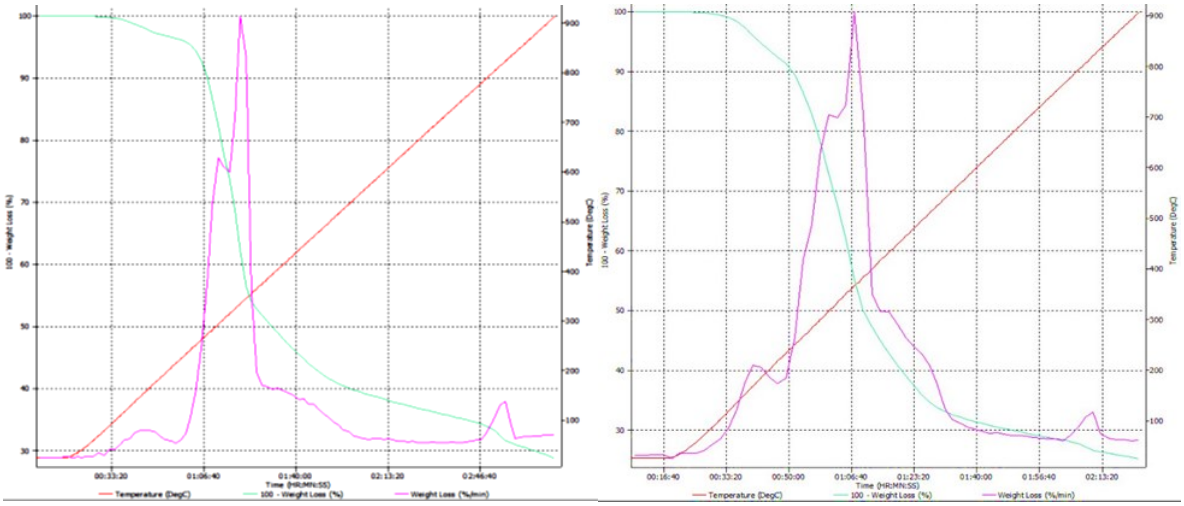

3 Selection of starting materials

The results obtained after characterizing the eight selected feedstocks brought to the identification of four samples which will be object of pilot scale tests. The four types of biowaste streams that have been chosen based upon their characteristics, their costs and their availability are listed below:

- AGD: the digestate, represents a residue of the anaerobic digestion plants, largely available everywhere in Europe, and its market value is considered lower than a woody biomass
- AGW: the olive pruning, represents the best quality material, from which high quality biocoal is obtained.
- OFMSW: the organic fraction of municipal solid waste, demonstrated to have reduced inorganics and a valuable quality as precursor of biocoal. The negative cost of this feedstock makes it interesting for the project
- SS1: sewage sludge, given the high availability and the high disposal cost, represents a strategic residue to be valorized for EU. The high concentration of phosphorus will require to perform chemical leaching, as part of the integrated process.

4 Pyrolysis for suitable biocoal quality

4.1 Methodology

As previously mentioned, four out of the eight types of waste listed in Table 4 were subjected to lab-scale pyrolysis using LECO TGA701. Namely, an overall of 48 TGA tests were carried out on waste 1 (OFMSW), waste 5 (SS1), waste 7 (AGD) and waste 8 (AGW). On each material, four different temperatures have been tested: 450°C, 550°C, 600°C and 650°C and three different residence times have been evaluated: 20 minutes, 1 hour and 2 hours were investigated at each temperature. The feedstock was loaded into 17 cm^3 crucibles and 10 $L \cdot min^{-1}$ N_2 flow was maintained through the test to ensure inert atmosphere inside the furnace. The tests were monitored using TGA701 Software 1.4. Table 9 sums up the experimental pattern adopted during the lab-scale pyrolysis tests.

Figure 10: LECO TGA701 used for pyrolysis tests

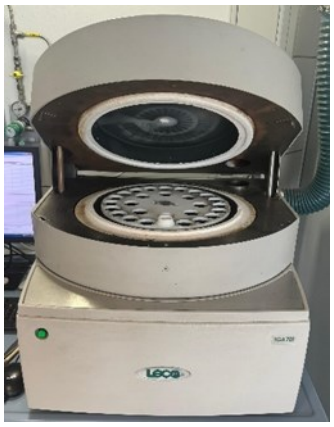

Table 9: Summary table for TGA conditions on selected waste streams

ID	T (°C)	t (min)	HR ($°C \cdot min^{-1}$)	Feedstock description
1	**450**	**20**	**20**	OFMSW
2	**450**	**20**	**20**	SS1
3	**450**	**20**	**20**	AGD
4	**450**	**20**	**20**	AGW
5	**450**	**60**	**20**	OFMSW
6	**450**	**60**	**20**	SS1
7	**450**	**60**	**20**	AGD
8	**450**	**60**	**20**	AGW
9	**450**	**120**	**20**	OFMSW
10	**450**	**120**	**20**	SS1
11	**450**	**120**	**20**	AGD
12	**450**	**120**	**20**	AGW
13	**550**	**20**	**20**	OFMSW
14	**550**	**20**	**20**	SS1
15	**550**	**20**	**20**	AGD
16	**550**	**20**	**20**	AGW
17	**550**	**60**	**20**	OFMSW
18	**550**	**60**	**20**	SS1
19	**550**	**60**	**20**	AGD
20	**550**	**60**	**20**	AGW
21	**550**	**120**	**20**	OFMSW
22	**550**	**120**	**20**	SS1
23	**550**	**120**	**20**	AGD

24	**550**	**120**	**20**	AGW
25	**600**	**20**	**20**	OFMSW
26	**600**	**20**	**20**	SS1
27	**600**	**20**	**20**	AGD
28	**600**	**20**	**20**	AGW
29	**600**	**60**	**20**	OFMSW
30	**600**	**60**	**20**	SS1
31	**600**	**60**	**20**	AGD
32	**600**	**60**	**20**	AGW
33	**600**	**120**	**20**	OFMSW
34	**600**	**120**	**20**	SS1
35	**600**	**120**	**20**	AGD
36	**600**	**120**	**20**	AGW
37	**650**	**20**	**20**	OFMSW
38	**650**	**20**	**20**	SS1
39	**650**	**20**	**20**	AGD
40	**650**	**20**	**20**	AGW
41	**650**	**60**	**20**	OFMSW
42	**650**	**60**	**20**	SS1
43	**650**	**60**	**20**	AGD
44	**650**	**60**	**20**	AGW
45	**650**	**120**	**20**	OFMSW
46	**650**	**120**	**20**	SS1
47	**650**	**120**	**20**	AGD
48	**650**	**120**	**20**	AGW

TGA-derived chars were analyzed aiming to characterize their proximate and ultimate composition and to assess also their calorific value. As already described in paragraph 2.1.2 working on biowastes streams, also for thereof char proximate analyses were carried out using LECO TGA701 thermo-balance previously employed for pyrolytic char production. Moisture was determined according to UNI EN ISO 18134-2:2017; volatiles determination followed UNI EN ISO 18123:2016; ashes were evaluated at 550°C and 815°C according to UNI EN ISO 18122:2016. Fixed carbon was calculated as the difference between 100 and the sum of moisture (M), volatiles (V) and ashes (A) at 550°C as per UNI EN ISO 1860-2:2005.

$$Fixed\ C = 100 - M - V - A_{550}$$

Elemental analysis employed LECO TruSpec CHN for determination of C, H and N following UNI EN ISO 16948:2015 and LECO TruSpec S for assessing S according to ASTM D4239-14. The gross calorific value (HHV) was defined using a bomb calorimeter LECO AC500 as per UNI EN ISO 18125:2018. All the data referring to the char's composition were obtained on '*air dried*' material and converted into *'dry basis'* through calculation as per UNI EN ISO 16993:2017, H conversion formula solely differs from others.

$$X_{db} = \frac{100 \cdot X_{ad}}{100 - M}$$

$$H_{db} = \frac{100 \cdot \left(H_{ad} - \frac{M}{8.937}\right)}{100 - M}$$

Where X is the generic quantity to be converted, *db* and *ad* stand respectively for "dry basis" and "air dried".

Oxygen was determined as the difference between 100 and the sum of ashes at 550°C and C, H, N, S converted on dry basis. Net calorific value (LHV) was calculated using dry basis converted data following formula given in UNI EN ISO 18125:2018.

$$O_{db} = 100 - A_{550} - C_{db} - H_{db} - N_{db} - S_{db}$$

$$LHV = HHV - 0.2122 \cdot H_{db} - 0.0008 \cdot (O_{db} + N_{db}) \equiv \left[\frac{MJ}{kg}\right]$$

4.2 Products quality

The analysis that has been performed allowed to investigate and to get deeper understanding of the qualitative profile of the chars that have been obtained. Chars from AGW show the highest content of total carbon (80÷90 wt%, dry basis), while sewage sludge derived chars have the lowest share of total carbon (32÷36 wt%, dry basis) with the char retaining high amounts of ashes up to 62 wt% on dry basis. OFMSW and AGD derived chars have intermediate amounts of total carbon ranging respectively between 64÷73 wt% and 52÷59 wt%. Looking at the results, it can be noticed that by and large that under equal temperature conditions; C (%) is inversely proportional to the residence time that fosters organic carbon loss through volatilization as one can expect. A few exceptions must be highlighted though. Total carbon increases with residence time for replicated tests on OFMSW at 600°C (see test 25, 29, 33). This being an isolated case and considering the high oxygen content (see sample 25) might be ascribed to the high heterogeneity of the OFMSW sample. It is also noteworthy that working with AGW, total carbon remains pretty much constant with time under the same temperature, but it rises notably as the latter increases. One may notice that in all these cases just mentioned, where carbon is low, higher oxygen content occurs. Moisture levels stay constant for all the char samples and data are reported dry basis, so high oxygen occurrence cannot be due to water content. Higher oxygen levels may be attributed to the presence of partially oxidized compounds, such as humic acids whose occurrence is promoted by bacterial degradation which is likely to happen considering OFMSW and AGW wastes. Such species contain in their structures several hydroxy and carboxylic functionalities that are readily lost through C-C or C-OH bond cleavage promoted by thermal activation. In this case the higher the temperature the higher the rate of decarboxylation or dihydroxylation. These mechanisms promote the removal of volatile compounds such as CO_2 and water originating from the organic substrate without negatively affecting the carbon content that on the other hand thanks to free-radicals mechanism involved during the thermal degradation can undergo polymerization producing fixed carbon matrix. In the case of SS1 total C content decreases with time and temperature, while ashes build up as both parameters increase. Looking at sludge pyrolysis tests one can notice the oxygen level of the chars produced during SS1 pyrolysis decreasing with temperature. Both carbon and oxygen decrease with time and temperature might be ascribed to the loss of CO_2 originating from inorganic carbonates possibly used during the conditioning stages of the sludge. CO_2 removal in this case affects evenly oxygen and carbon content while fostering ashes occurrence.

Graph 3: ultimate composition of selected biowaste derived char: (a) OFMSW derived; (b) SS derived; (c) AGD derived; (d) AGW derived

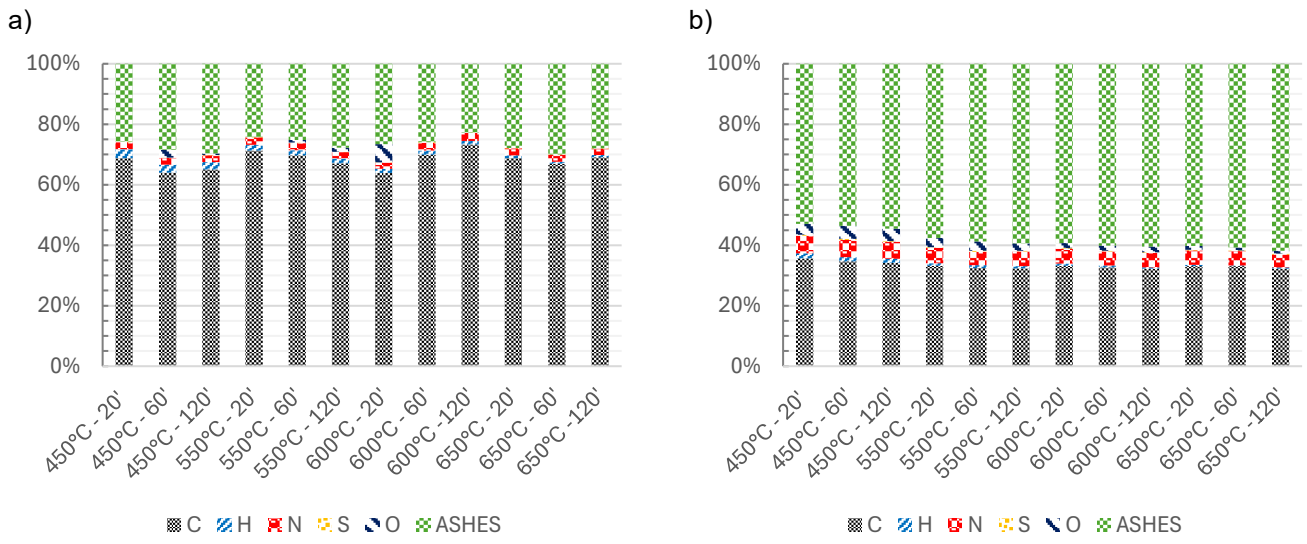

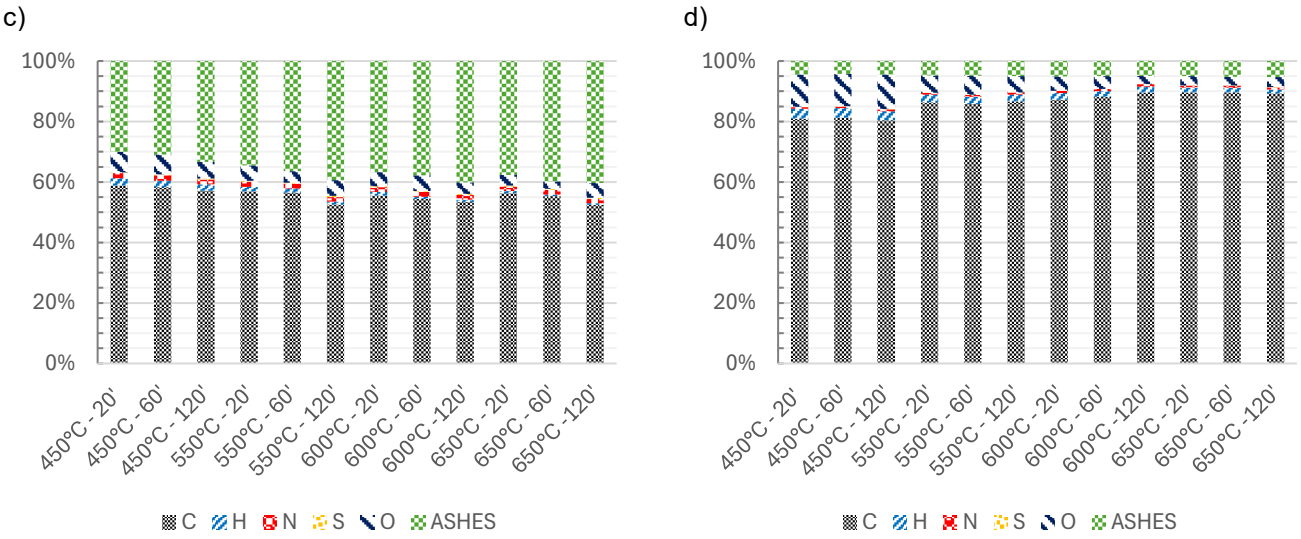

AGW-derived chars also retain the highest content of fixed C. The latter can reach up to 96% of the total C when harshest conditions (i.e. 650°C 60' and 120') are applied for pyrolysis. In this case, as stated above, after removal of small moieties attached to the organic matrix producing some gases, high temperature and long residence time promote repolymerization reactions of macroradicals that can originate from highly complex structures such as those that can be found in humic acids, polyphenols, and lignin that are arguably comprised within pruning derived substate. Not least, the type of waste used for char production affects markedly the ratio of volatile and fixed carbon as it is highlighted in Graph 4. OFMSW-derived chars withhold the highest amount of volatile carbon with volatile to fixed C ratio reaching up to 0.56 that means slightly more than half of the fixed carbon. OFMSW comprises high shares of biodegradable plastic bags and paper napkins. Under the chemical profile both are made up of polymeric compounds, the former being predominantly polyesters and the latter being composed primarily of cellulose. During pyrolysis these species are likely to undergo random cleavage of the polymeric backbone, chain-stripping and unzipping reactions that promote molecular weight reduction while volatile carbon content is slightly affected as new low molecular weight compounds are steadily formed with a rate that is likely to be similar or even exceed the one at which repolymerization occurs leading to coking and therefore the appearance of fixed carbon.

Graph 4: Volatile C to Fixed C ratio

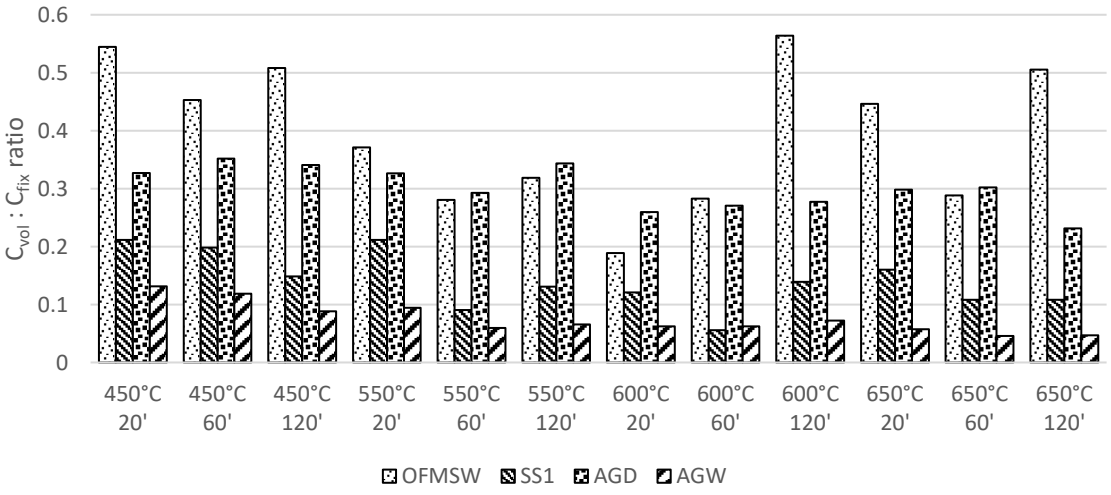

By and large calculating molar O:C and H:C ratios all char samples meet high rank coals standards falling near the anthracite-like material area. This makes the chars suitable for high-level purposes in steelmaking sector or catalytic supports production.

Graph 5: Van Krevelen diagrams depicting overall char samples produced during TGA tests on selected wastes: OFMSW, SS, digestate, pruning.

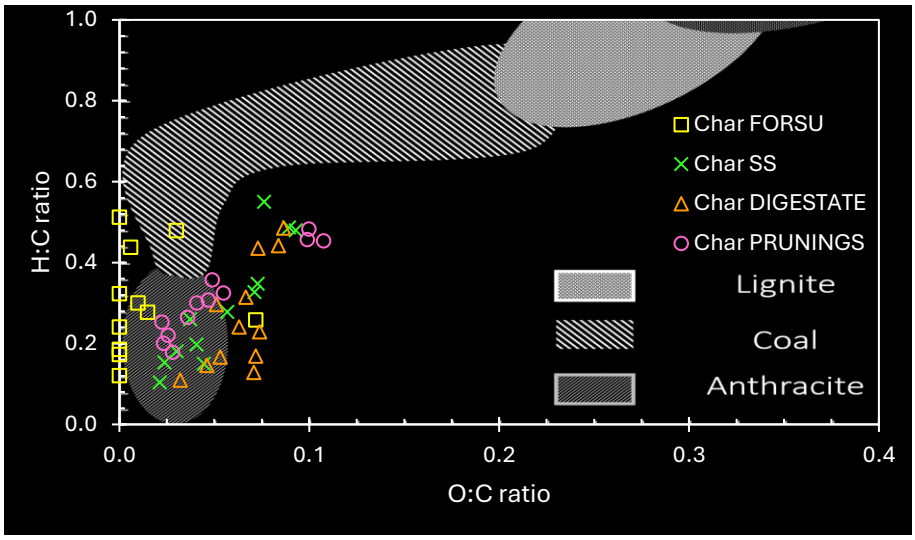

Both H and O levels in the char reduce with time and temperature at which pyrolysis tests are carried out. Longer residence time and higher temperature boost the free-radical mechanism that occurs during pyrolysis promoting the removal of oxygen and hydrogen in the form of •OH, •OOH, •H radicals with coking occurring through termination process driven by C• coupling.

Graph 6: Van Krevelen diagrams for TGA-derived char samples from OFMSW

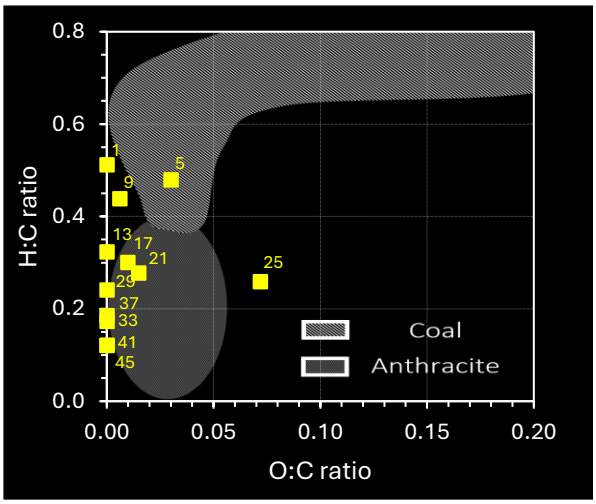

Graph 7: Van Krevelen diagrams for TGA-derived char samples from Sewage sludge

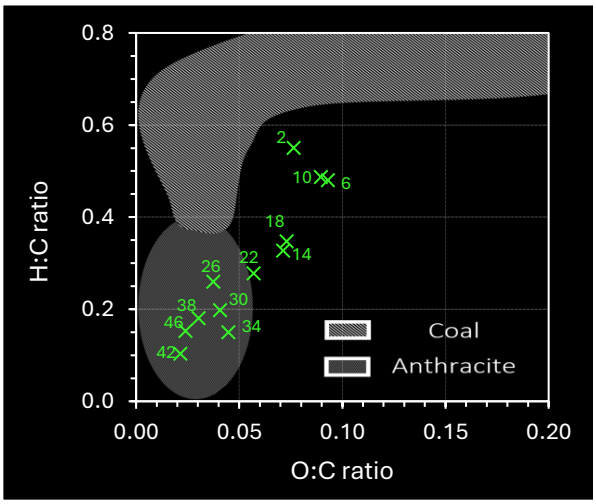

Graph 8: Van Krevelen diagrams for TGA-derived char samples from Agricultural digestate

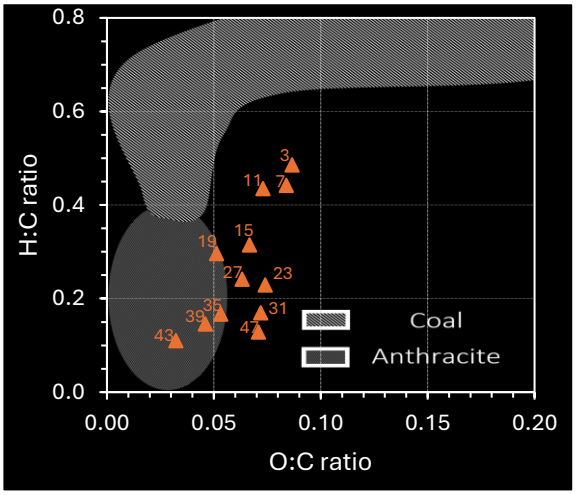

Graph 9: Van Krevelen diagrams for TGA-derived char samples from olive prunings

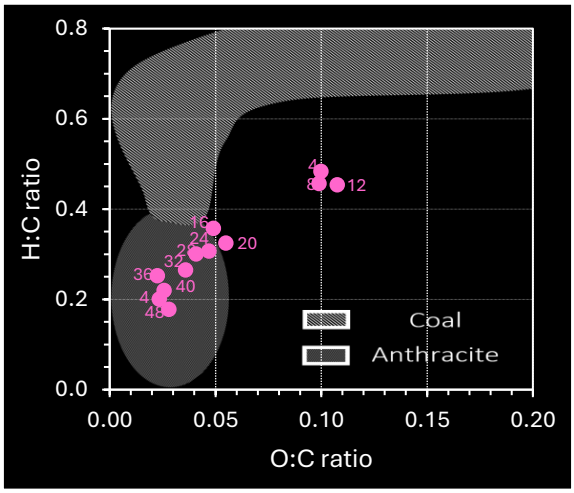

4.3 Mass and energy balance

4.3.1 TGA Yields

Yields are calculated according to the following equation:

$$Y(\%) = \frac{M_f}{M_i} \cdot 100$$

where M_f represents the residual mass inside the crucible after the pyrolysis, M_i being instead the feedstock put inside the crucible before the TGA test. The yields reported below are the average result, the confidence interval is calculated using *t-Student's* values with 95% confidence level as per IUPAC recommendation.

Table 10: TGA yields for pyrolysis test on OFMSW

Product	TGA conditions	TGA Yields	C.I.$_{95\%}$
1	450°C - 20' – 20°·min^{-1}	**34%**	**± 5%**
5	450°C - 60'– 20°·min^{-1}	**34%**	**± 3%**
9	450°C - 120'– 20°·min^{-1}	**33%**	**± 6%**
13	550°C - 20'– 20°·min^{-1}	**29%**	**± 3%**
17	550°C - 60'– 20°·min^{-1}	**28%**	**± 3%**
21	550°C - 120'– 20°·min^{-1}	**29.8%**	**± 0.9%**
25	600°C - 20'– 20°·min^{-1}	**30%**	**± 3%**
29	600°C - 60'– 20°·min^{-1}	**29%**	**± 2%**
33	600°C -120'– 20°·min^{-1}	**29%**	**± 5%**
37	650°C - 20'– 20°·min^{-1}	**29%**	**± 2%**
41	650°C - 60'– 20°·min^{-1}	**28%**	**± 2%**

45	650°C -120'– 20°·min^{-1}	**29%**	±	**4%**

Graph 10: TGA yields for pyrolysis test on OFMSW; data are reported in Table 10

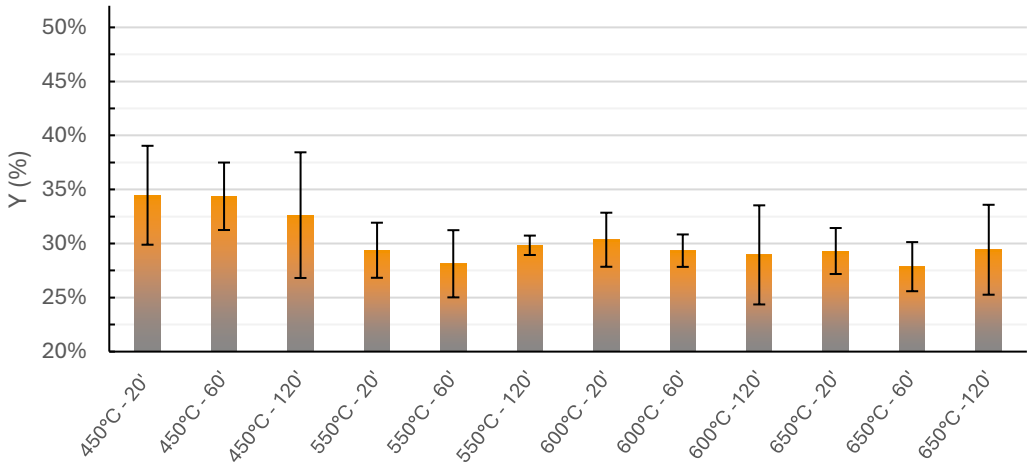

As one can notice from Graph 10 large confidence intervals indicate low reproducibility of the pyrolysis test, arguably due to the high heterogeneity of the substrate.

Table 11: TGA yields for pyrolysis test on SS

Product	TGA conditions	TGA Yields	C.I.$_{95\%}$	
2	450°C - 20' – 20°·min^{-1}	**50.4%**	±	**0.2%**
6	450°C - 60'– 20°·min^{-1}	**48.8%**	±	**0.2%**
10	450°C - 120'– 20°·min^{-1}	**48%**	±	**2%**
14	550°C - 20'– 20°·min^{-1}	**45.8%**	±	**0.1%**
18	550°C - 60'– 20°·min^{-1}	**45.0%**	±	**0.4%**
22	550°C - 120'– 20°·min^{-1}	**44.5%**	±	**0.9%**
26	600°C - 20'– 20°·min^{-1}	**44.8%**	±	**0.2%**
30	600°C - 60'– 20°·min^{-1}	**44.24%**	±	**0.03%**
34	600°C -120'– 20°·min^{-1}	**44%**	±	**1%**
38	650°C - 20'– 20°·min^{-1}	**44.1%**	±	**0.3%**
42	650°C - 60'– 20°·min^{-1}	**43.5%**	±	**0.2%**
46	650°C -120'– 20°·min^{-1}	**43.2%**	±	**0.3%**

Graph 11: TGA yields for pyrolysis test on SS; data are reported in Table 11

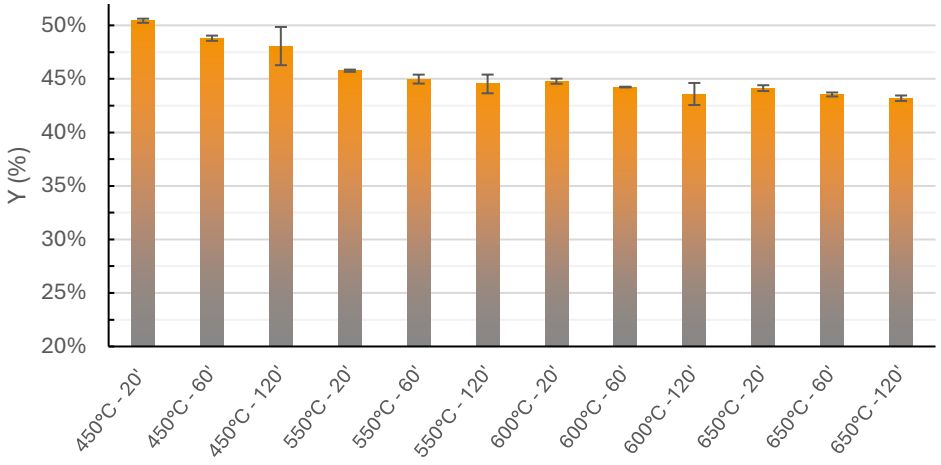

Table 12: TGA yields for pyrolysis test on digestate (AGD)

Product	TGA conditions	TGA Yields	C.I.$_{95\%}$	
3	450°C - 20' – 20°·min^{-1}	**39.9%**	±	**0.3%**
7	450°C - 60'– 20°·min^{-1}	**38.6%**	±	**0.2%**
11	450°C - 120'– 20°·min^{-1}	**36.5%**	±	**0.8%**
15	550°C - 20'– 20°·min^{-1}	**36.9%**	±	**0.3%**
19	550°C - 60'– 20°·min^{-1}	**34.2%**	±	**0.3%**
23	550°C - 120'– 20°·min^{-1}	**32.5%**	±	**0.5%**
27	600°C - 20'– 20°·min^{-1}	**35.0%**	±	**0.1%**
31	600°C - 60'– 20°·min^{-1}	**33.8%**	±	**0.2%**
35	600°C -120'– 20°·min^{-1}	**31.7%**	±	**0.3%**
39	650°C - 20'– 20°·min^{-1}	**34.4%**	±	**0.3%**
43	650°C - 60'– 20°·min^{-1}	**32.8%**	±	**0.3%**
47	650°C -120'– 20°·min^{-1}	**31.4%**	±	**0.6%**

Graph 12: TGA yields for pyrolysis test on digestate; data are reported in Table 12

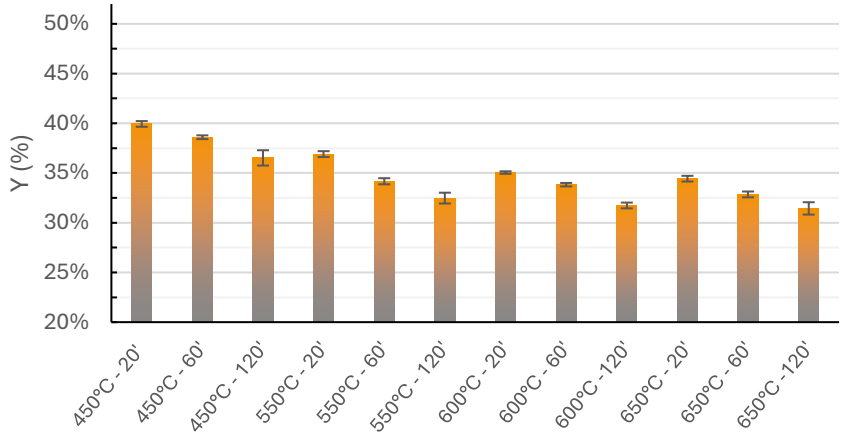

Table 13: TGA yields for pyrolysis test on pruning (AGW)

Product	TGA conditions	TGA Yields	C.I.$_{95\%}$
4	450°C - 20' – 20°·min^{-1}	**28.1%**	± **0.1%**
8	450°C - 60'– 20°·min^{-1}	**26.8%**	± **0.1%**
12	450°C - 120'– 20°·min^{-1}	**26.09%**	± **0.07%**
16	550°C - 20'– 20°·min^{-1}	**24.6%**	± **0.1%**
20	550°C - 60'– 20°·min^{-1}	**23.8%**	± **0.2%**
24	550°C - 120'– 20°·min^{-1}	**23.29%**	± **0.06%**
28	600°C - 20'– 20°·min^{-1}	**23.81%**	± **0.03%**
32	600°C - 60'– 20°·min^{-1}	**23.28%**	± **0.09%**
36	600°C -120'– 20°·min^{-1}	**22.6%**	± **0.1%**
40	650°C - 20'– 20°·min^{-1}	**23.29%**	± **0.09%**
44	650°C - 60'– 20°·min^{-1}	**22.8%**	± **0.1%**
48	650°C -120'– 20°·min^{-1}	**22.1%**	± **0.2%**

Graph 13: TGA yields for pyrolysis test on digestate; data are reported in Table 13.

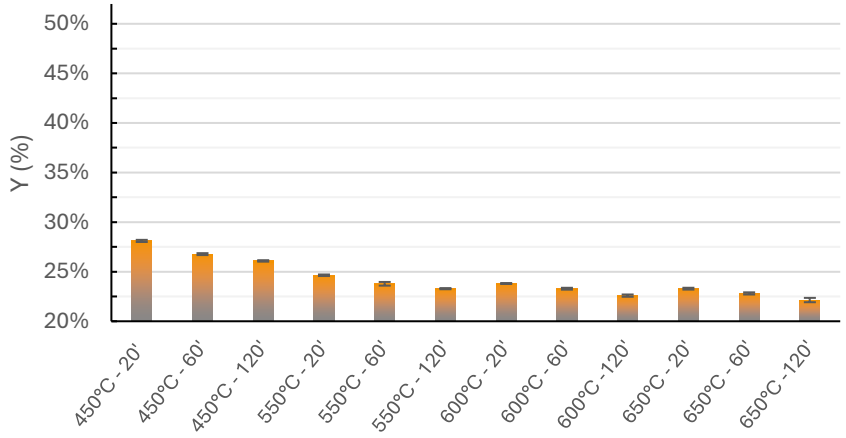

The yields reported in the graphs above are representative of the nature of the feedstock. Substrates with higher contaminants content such as SS1 and OFMSW guarantee higher yields thanks to major shares of ashes in the feedstock. This while positively impacts the mass balance output on the other hand it returns a char with lower carbon content. On the opposite working with a near-pristine organic based feedstock such as AGW it is possible to achieve the highest carbon content in the char whose mass yield is bound to be negatively impacted.

Graph 14: TGA yields for pyrolysis test at 450°C; effect of waste processed and residence time. OFMSW ; SS1 ; AGD ; AGW

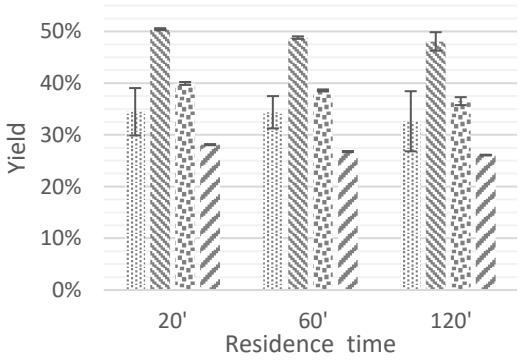

Graph 15: TGA yields for pyrolysis test at 550°C; effect of waste processed and residence time. OFMSW ; SS1 ; AGD ; AGW

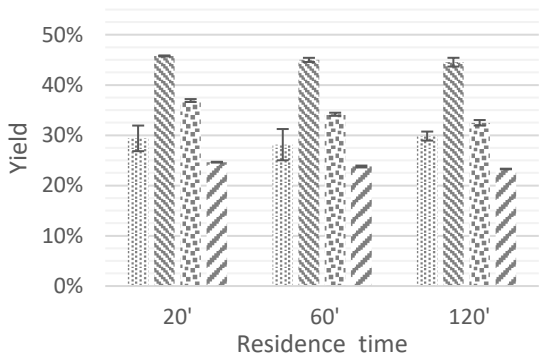

Graph 16: TGA yields for pyrolysis test at 600°C; effect of waste processed and residence time. OFMSW ; SS1 ; AGD ; AGW .

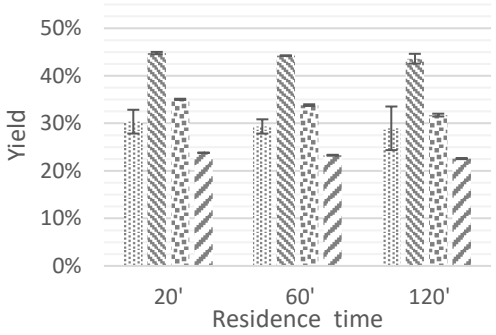

Graph 17: TGA yields for pyrolysis test at 650°C; effect of waste processed and residence time. OFMSW ; SS1 ; AGD ; AGW .

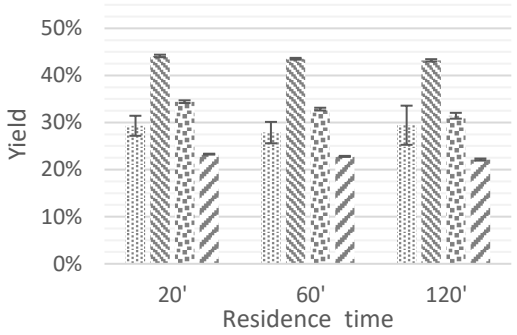

Graph 14-Graph 17 show the effect of residence time under same temperature conditions on mass yield for the four types of waste investigated. As discussed above, the nature of the feedstock markedly affects the yield. Residence time under same temperature and feedstock has no significant impact on the process yield. With this respect shorter residence time can be considered as an optimized parameter for the process.

From Graph 18 one can notice that temperature is a slightly more impactful parameter for mass yield compared to residence time. Notably for pyrolysis tests performed on SS1 and AGW the output variation with T is sensibly more significant than the variation with time. Considering the quality of the char products described in the previous section, optimized qualitative and quantitative output can be met performing the process at 550°C.

Graph 18: TGA yields for pyrolysis test; effect of temperature.

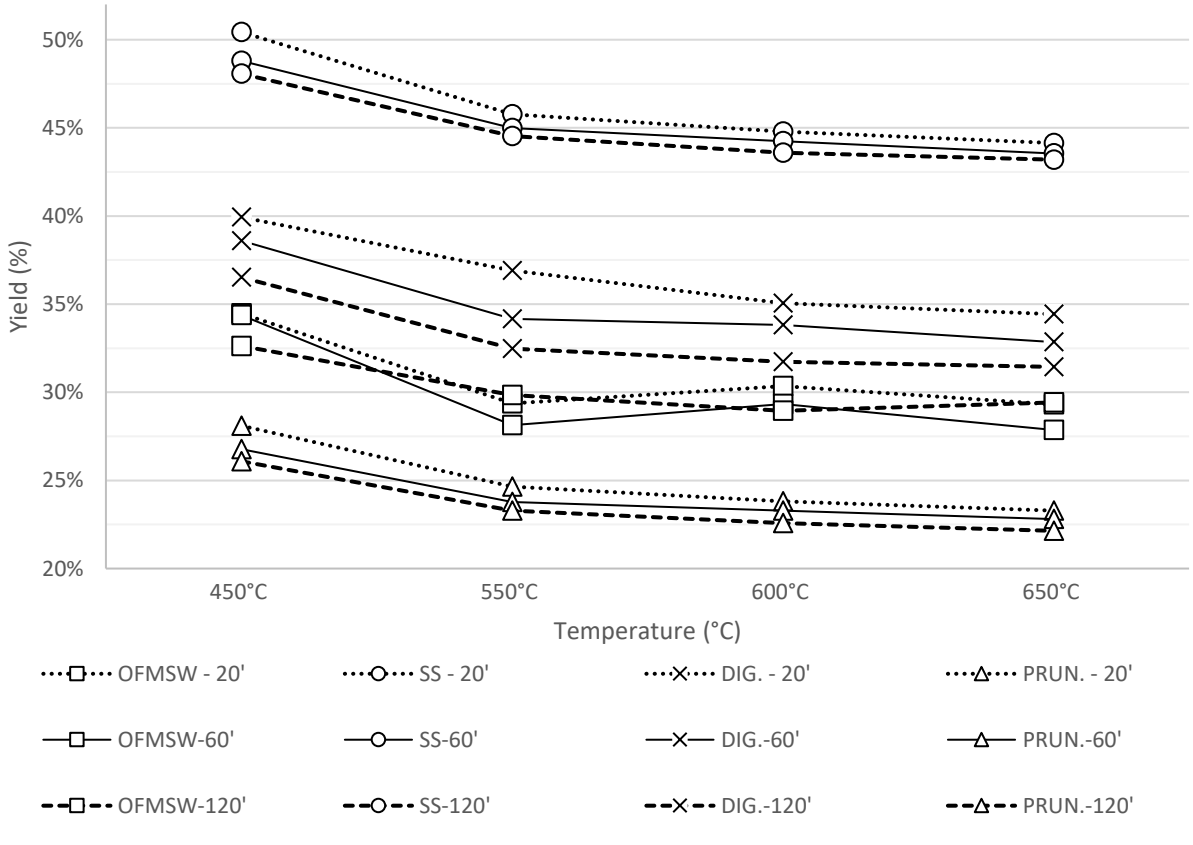

Gross calorific values are reported in Graph 19-Graph 22 to give a broad idea of the enthalpic content stored within the char samples. The results can give a rough qualitative esteem of the product but cannot be used in this stage for a quantitative investigation of the energy balance due to high uncertainty of the data stressed out by wide confidence intervals produced by limited analysis replicate for an appropriate statistic. The intervals of confidence are calculated with at 95% confidence level N-1=1, where N-1 is the degree of freedom with N the number of events of the statistical sample.

The lowest gross calorific values are noticed for SS1 derived chars. High mass yields and high ash content reduce significantly the energetic density of these samples. AGD-derived chars' HHV resembles that of common wood. HHVs for OFMSW and AGW derived chars draw closer to the values of graphitic and coke like materials.

Graph 19: OFMSW derived char's HHV values.

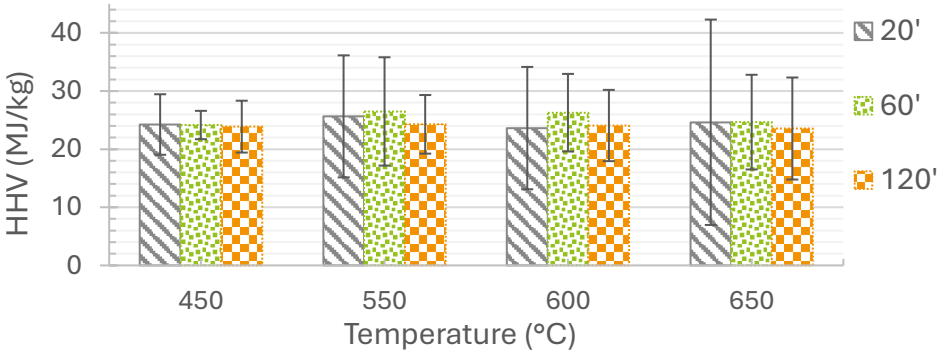

Graph 20: SS derived char's HHV values.

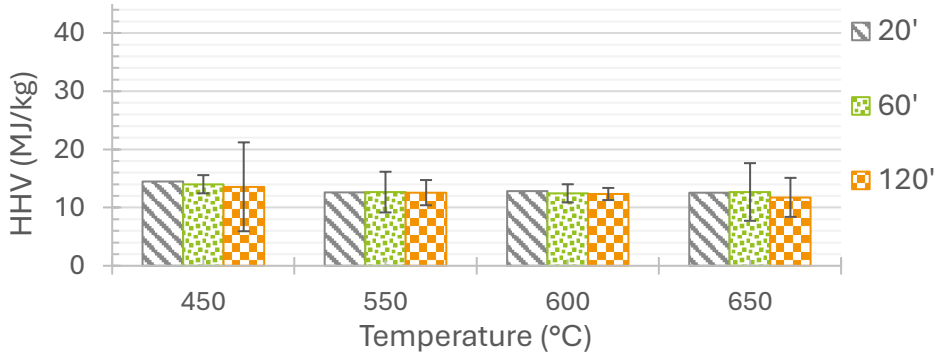

Graph 21: AGD derived char's HHV values

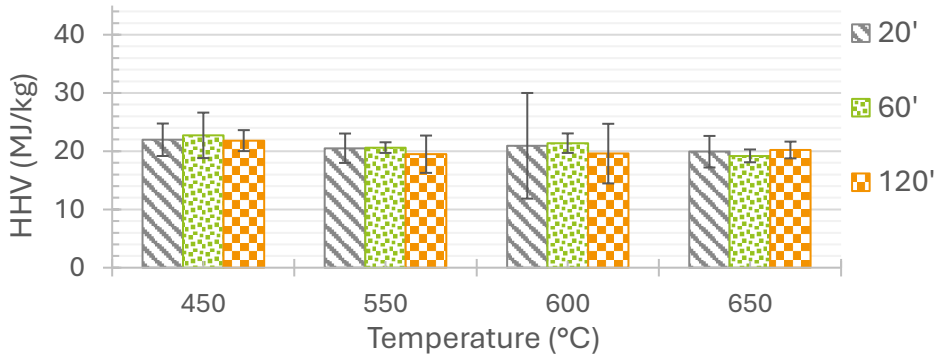

Graph 22: AGW derived char's HHV values

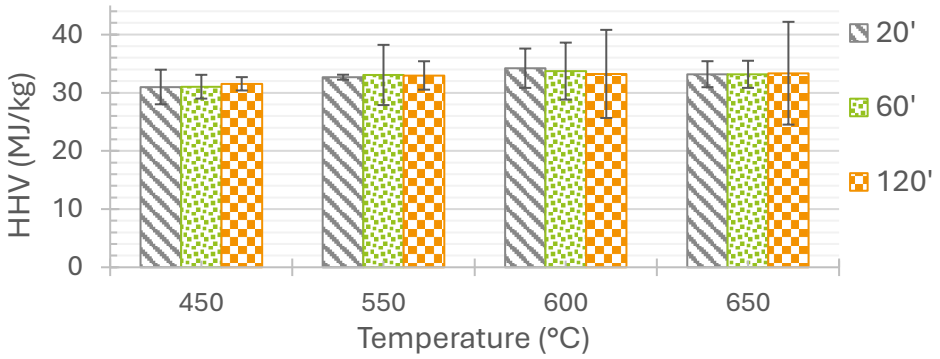

5 Pilot scale pyrolysis tests

Four pilot-scale pyrolysis trials were anticipated to be performed on selected biowaste streams listed in paragraph 4 (i.e. SS, OFMSW, AGW, AGD). The slow pyrolysis pilot-scale tests have been performed with the aid of two different slow pyrolysis pilot plants located at RE-CORD's experimental area (REC-PARK, Scarperia e San Piero, 50038, FI, Italy). Differentiating the trials on two distinct units was due to special maintenance to the smaller pilot unit owned by RE-CORD which was meant to be used at the beginning. However, as the smaller unit was unavailable during the last months for maintenance activities, further tests were carried out on a larger unit already present at the facility, which was expected to be used later in this project. The small 3 $kg \cdot h^{-1}$ auger type slow pyrolysis plant, named SPYRO (see Figure 11) was used to perform the pilot-scale test on SS. This unit, once back in November, will be also used to perform three more small scale tests. The pilot-scale trials on AGD and AGW have been carried out in a 100 $kg \cdot h^{-1}$ rotary kiln slow pyrolysis pilot plant, named PYROK (see Figure 12). A minimum of 2 kg of biowaste was anticipated to be processed in every single test. Eventually, during SPYRO SS slow pyrolysis trial roughly 10 kg of dry biowaste have been processed. On the other hand, during PYROK tests, due to the larger capacity of the plant, feedstock amounts required to be significantly increased, up to hundreds of kg order.

Table 14: Pilot scale slow pyrolysis trials summary

Biowaste	Pilot plant for trial	Type	Capacity (kg/h)	Processed material (kg)
SS	SPYRO	Auger	3	10.3
AGW	PYROK	Rotary kiln	100	351.4
AGD	PYROK	Rotary kiln	100	297.0
OFMSW	PYROK	Rotary kiln	100	TBD

Additional trials are ongoing in the large plant with digested OFMSW, as well as new tests are planned over the next few months of the project. Pilot-scale trial on OFMSW is still pending and will be carried out either on SPYRO or PYROK depending on circumstances. In summary, new tests with AGW, OFMSW, and AGD will be processed with SPYRO. While a new test with SS will be likely processed with PYROK.

Figure 11: Auger-type 3 kg/h slow pyrolysis pilot plant (SPYRO) at REC-PARK

Figure 12: Rotary kiln 100 kg/h slow pyrolysis pilot plant (PYROK) at REC-PARK

Optimized conditions highlighted during lab scale TGA tests (i.e. about 550°C, 20' residence time) have been implemented during pilot scale trials, but it is worth noticing that some adjustments were due according to the specific operability of the leveraged pilot-scale unit. Therefore, some of the setpoints that are adopted may slightly differ from the specific operative parameters within a range deemed as reasonable.

5.1 Pilot scale methodology

For the tests in SPYRO unit, the sample was dried before feeding it to the slow pyrolysis pilot scale unit. When PYROK (100 kg/h plant) was used, feedstock was processed as received, thus with variable moisture. To assess both energy and mass balance track is kept of input and output quantities involved in each single trial. The energy balance of the process is evaluated based on feedstock's mass input and HHV as well as on char's yield and HHV, according to the following equation:

$$E_{bc} = \frac{HHV_{bc}}{HHV_f} \cdot Y_{bc} \cdot 100$$

Where E_{bc} is the energetic contribution stored in the char, HHV_{bc} is the calorific content of the char, HHV_f is the calorific content of the feedstock and Y_{bc} is the mass yield of the solid fraction (i.e. char). The energetic content stored in the pyro-gas (E_{pg}) can be calculated by difference according to the following equation:

$$E_{pg} = 100 - E_{bc}$$

For mass balance the yields are given as follows.

$$Y_i = \frac{M_i}{M_f} \cdot 100$$

Where "i" is the generic product of the pyrolysis which can either be the solid, the liquid or the flue-gas (and any of their combination or any of their constituents), "f" is the feedstock and "M" is the mass. The solid product (char) and the condensates (bio-oil) are collected for further analysis aimed at their characterization. The solid is characterized in its moisture, volatiles and ash content, CHNS and inorganic elements composition, calorific value and porosity. The analysis performed on the solid are carried out with the same methodology depicted in previous section 4.1. The condensable product fraction (bio-oil) was collected with the aid of a fractioned condensation unit (FCU) placed downstream of the reactor. For lab characterization a share of the condensates is subject to phase separation with the aid of a separatory funnel aimed at recovery of separated aqueous phase (AP) and organic phase (OP). The AP and OP are characterized in their ultimate composition according to UNI EN ISO 16948:2015 for CHN characterization. Sulphur (S) content was determined according to internal method

RE-CORD.005. Chlorine (Cl) content has been determined according to UNI EN ISO 16994:2017. The calorific density (HHV) has been determined according to UNI EN ISO 18125:2018. Water content and pH have been determined according to ASTM E203-08 and ASTM E70-24 respectively. Permanent gases through FCU are sent to online analysis with MicroGC 990 Agilent running two modules simultaneously: module A equipped with MolSieve5A 10M×0.25MM×30UM BF column (oven 80°C) fluxed with Ar (1.4 bar) for detection of H2, O2, N2, CH4 e CO and module B equipped with Poraplot U FS 10M×0.25MM×8UM BF (oven 70°C) fluxed with He (1.4 bar) for detection of CO2, C2H4, C2H6, C2H2, H2S, C3H8, iC4, nC4. The MicroGC is run by using Soprane CDS v.3.0.12 SRA Instruments.

5.1.1 SPYRO operability

The biowaste is fed to the unit through a hopper placed on top of the reactive unit. The pyrolysis temperature is achieved by means of three electric heaters. The temperature of the process is monitored thanks to three thermocouples (T5, T4, T3) installed along the length of the auger. A N_2 (5 $L \cdot min^{-1}$) flow is sparged inside the chamber to maintain an inert atmosphere as well as to operate as gas carrier. Gas sparging is controlled through the aid of an electro valve regulating the gas stream from the gas cylinder, the gas flow is regulated by using LabVIEW™2017 (17.0.1f3, National Instruments). Residence time inside the reaction chamber is regulated by properly setting the auger's speed. A simplified PFD of the SPYRO unit is represented in Figure 13.

Figure 13: PFD of SPYRO slow pyrolysis pilot unit owned and operated by RE-CORD

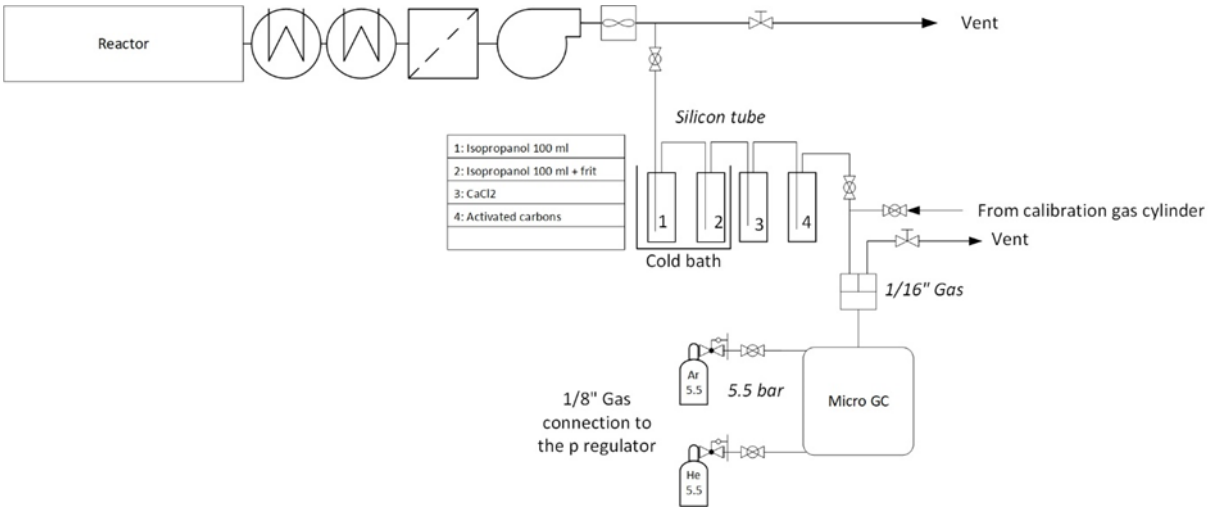

5.1.2 PYROK operability

The feed is carried by a screw system which transports the material from a 3,000 L loading hopper to an inlet section to the furnace delimited by two clapet plates which open alternately dropping the feedstock and limiting the input of air. Pyrolysis occurs in a cylindric chamber, which consists of a rotating drum heated indirectly by using the irradiation and convection of the fumes produced by the gas burner ("muffle") placed below the drum. The temperature inside the reactor is monitored with the aid of a strain gauge. The reactor is kept at a slightly negative pressure through a high temperature fan that allows the extraction of the pyro-gas. The char produced inside the drum is extracted by a fixed-speed auger conveyor and the char is cooled by a water sprayer (1.2 L/min) that moistens the solid to prevent the risk of fire when it is collected inside the big-bag placed at the end of the screw. For the sake of completeness, the flowsheet of the PYROK is given in Figure 14.

Figure 14: PFD of PYROK slow pyrolysis pilot unit owned and operated by RE-CORD

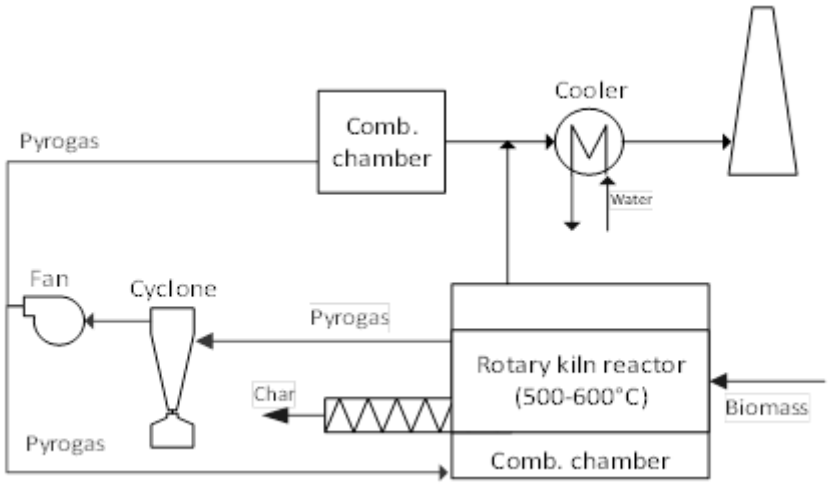

5.2 SPYRO trial

5.2.1 SS pilot scale slow pyrolysis trial

Sewage sludge treated in this stage was provided by a company operating wastewater treatment plant in northern Italy (see Figure 15).

Figure 15: Sludge processed during SS pilot scale slow pyrolysis trial

5.2.1.1 Characteristics of the processed sludge

The composition of the sludge is reported in Table 15:

Table 15: Characterization of SS used during slow pyrolysis pilot-scale test

Parameter	Value		C.I.$_{95\%}$	Unit
Moisture	**2.83**	±	0.03	wt.%, wb
Volatiles	**50.5**	±	0.1	wt.%, db
Ashes 550°C	**40.4**	±	0.3	wt.%, db

Ashes 710°C	**39.8**	±	0.4	wt.%, db
Fixed C	**9.1**	±	0.4	wt.%, db
C	**31.2**	±	0.2	wt.%, db
H	**4.48**	±	0.04	wt.%, db
N	**4.4**	±	0.1	wt.%, db
S	**1.5**	±	0.1	wt.%, db
Cl	**0.06**	±	0.02	wt.%, db
O	**18.0**	±	0.5	wt.%, db
Al	**37018**	±	10035	ppm, db
B	**b.d.l.**	±	n/a	ppm, db
Ba	**268**	±	9	ppm, db
Ca	**25236**	±	14709	ppm, db
Cd	**b.d.l.**	±	n/a	ppm, db
Co	**b.d.l.**	±	n/a	ppm, db
Cr	**999**	±	213	ppm, db
Cu	**496**	±	3	ppm, db
Fe	**13598**	±	711	ppm, db
K	**4353**	±	887	ppm, db
Li	**14**	±	2	ppm, db
Mg	**2720**	±	1442	ppm, db
Mn	**244**	±	45	ppm, db
Mo	**b.d.l.**	±	n/a	ppm, db
Na	**3218**	±	267	ppm, db
Ni	**232**	±	185	ppm, db
P	**29199**	±	1956	ppm, db
Pb	**125**	±	19	ppm, db
Si	**71449**	±	7502	ppm, db
Ti	**1396**	±	104	ppm, db
V	**25**	±	20	ppm, db
Zn	**1424**	±	118	ppm, db
HHV	**13.2**	±	0.3	MJ/kg, db

Proximate characterization of the selected sludge is in line with the average composition of stabilized sewage sludge reported by the literature. The volatiles content falls at the lower-end margin of the organic matter content and the ashes precisely centred in the mineral matter range (Kacprzak, et al., 2017). Ultimate analysis is aligned with other composition ranges reported in the literature (Gao, et al., 2020). The elemental ratios O:C and H:C, when plotted on a Van Krevelen diagram, reveal the

composition of SS falling just above of the boundaries of the biomass region, with O content being in between that of a biomass and a peat, but H being rather high (see Graph 29). This may be owed to high ash content which can be deemed rather high compared to other biowastes. As the inorganic metallic oxides, hydroxides, carbonates, phosphates maintain oxygen level high, they do not directly affect hydrogen content. In such this way, the O:C can be slightly or significantly increased, mainly depending on the fraction of carbonates which comprise inorganic C besides O. At the same time the H:C ratio does not change but remains as it would be in the organic fraction alone. The high ash content causes the composition of the feedstock in analysis to shift right towards the biomass region from a more lipid-based characteristic area which would be reasonable for the composition of the organic share of a municipal sewage sludge. High inorganic content also accounts for quite low reported calorific density.

High ash content also anticipates relatively high char yields. However, the derived char will see the ash content increased even further. For this reason, subsequent post-treatment intended at removing the inorganic fraction contamination (e.g. leaching treatment) will be needed to upgrade the quality of the char.

Graph 23: Proximate composition of SS used during slow pyrolysis pilot-scale test

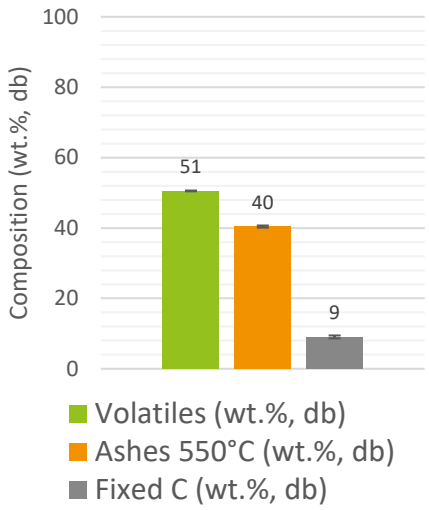

Graph 24: Ultimate composition of SS used during slow pyrolysis pilot-scale test.

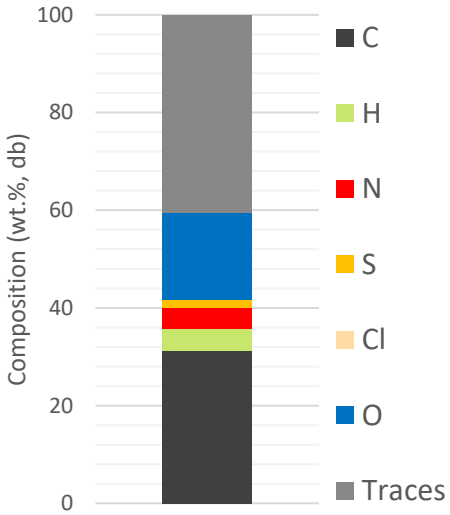

Graph 25: Trace elements in SS used during slow pyrolysis pilot-scale test

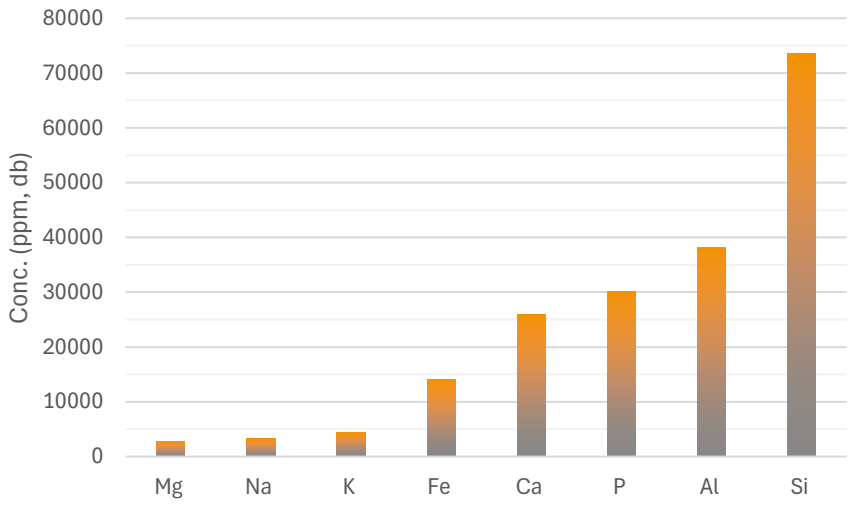

5.2.1.2 Description of the test on SS

Overall, 10.355 kg dry basis of sewage sludge from a wastewater treatment plant located in Lombardy (Italy) have been used for this trial. The SS was received with 23.7 wt% moisture content and dried at 105°C with ArgoLab TCN 200 oven. The operative temperature of T5, T4 and T3 has been set at 550°C. Auger speed has been set on 1.8 rpm such to ensure 15 minutes residence time inside pyrolysis chamber. N_2 flow has been set on 5 $L \cdot min^{-1}$ corresponding to 0.4 kg/h mass flow rate. Condensates have been recovered separately in condenser 1, 2, 3 ESP and pipelines 2-3 and 3-ESP and later merged. A 63% share of the condensates was recovered from condenser 1, 13% and 12% shares of condensates were recovered respectively from condenser 2 and condenser 3, 10% share of the condensates came from ESP section. Char yield turned out to be slightly higher than what emerged from TGA preliminary tests listed in Table 11 and equal to 56%. Condensates yield resulted equal to 24%. Gas yield was calculated by difference equal to 20%.

Table 16: Slow pyrolysis pilot-scale test on SS mass yields

Slow pyrolysis conditions	Product	Mass balance
550-550-550°C-15'; N_2: 5 $L \cdot min^{-1}$; 1.8 rpm	**Char**	**56%**
	Oil	**24%**
	Flue gas	**21%**

Graph 26: Products distribution from slow pyrolysis pilot-scale test on SS

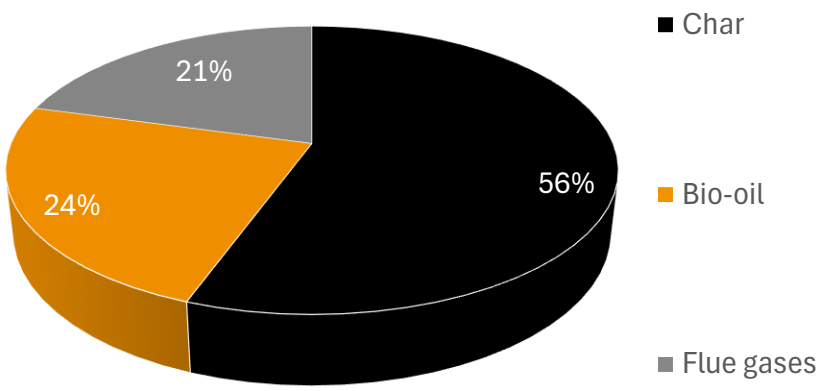

Figure 16: Char (SSC) produced after pilot-scale pyrolysis of sewage sludge (SS)

Compared to the preliminary test under the same conditions, the char produced during the pilot scale trial has higher ash content (73.1 ± 1.2 wt.% db at 550°C) as previously anticipated based on ash level in the feedstock. The latter figure is 28% higher than what was found for the char produced during lab-scale test (57.5 wt% db ashes at 550°C).

Table 17: Proximate composition of char produced during pilot scale slow pyrolysis on SS

Parameter	Value (wt.%, db *)		C.I.$_{95\%}$
Moisture	**1.6**	±	n/d
Volatiles	**13.6**	±	0.5
Ashes 550°C	**73.1**	±	1.2
Ashes 710°C	**72.0**	±	1.1
Fixed C	**13.3**	±	1.1

** Values are given on db (dry basis) except for moisture content.*

While the ashes appear higher, volatiles are consistent when drawing a comparison between the two SS-derived chars produced during pilot and lab-scale trials (13.6% v. 13.7%, db), respectively. Thus, C content results lower for char produced during pilot scale pyrolysis trial compared to the char produced under the same conditions during TGA test, the former being 23.3 ± 1.1 wt.% db (see Table 18) against 33.0 ± 0.3 wt% db for the char produced during preliminary investigations. From ultimate analysis one can also infer H and N content to be respectively 45% and 44% lower for char obtained during pilot scale trial compared to TGA test while S content results roughly 5 times higher. O content for char obtained during pilot scale trial is negligible.

Table 18: Ultimate composition of char produced during pilot scale slow pyrolysis on SS

Parameter	Value (wt.%, db)		C.I.$_{95\%}$
C	**23.3**	±	1.1
H	**0.6**	±	0.1
N	**2.8**	±	0.3

S	**1.3**	±	0.1
Cl	**0.07**	±	0.03

The calorific value of the char obtained during pilot scale trial compared to the counterpart produced during preliminary lab scale test results 30% lower.

Table 19: Calorific value of char from SS slow pyrolysis pilot-scale test

Parameter	Value (MJ/kg, db)		$C.I._{95\%}$
HHV	**8.89**	±	0.07
LHV	**8.77**	±	0.07

All the aforementioned differences between SS-derived chars produced during pilot and lab scale trials can be attributed to a good extent to the high ash content in the SS batch used during the pilot scale trial. Despite being both sewage sludges from municipal WWTPs, they have been provided by different wastewater treatment companies located in northern Italy. For the sake of clarity, ash content in the feedstock used during the pilot scale test equals 40.4 ± 0.3 wt.% db compared to that of the SS used during preliminary test which was just 28.4 ± 0.2 wt.% db, which is a 44% higher ash content for the former one compared to the latter one.

Alkali metals, earth-alkali metals, Fe, P, Al, and Si are the main inorganic impurities derived from the ashes in the char produced during the pilot scale pyrolysis trial. Major contaminant is Si which achieve 85,700 ppm db content. Si removal can be though even after some post-treatment. Other trace elements (e.g. Na, K, Mg, Fe, P, Ca, Al) can be removed through leaching.

Table 20: Inorganic trace elements characterization for char derived from SS slow pyrolysis pi8lot scale trial

Element	Value (ppm, db)
Al	58637
Ba	531
Ca	38247
Cr	1157
Cu	753
Fe	22423
K	7301
Li	19
Mg	8695
Mo	19
Na	5346
P	33642
Si	85689
Ti	2606
Zn	2499

Graph 27: Trace elements in char from SS slow pyrolysis pilot-scale test

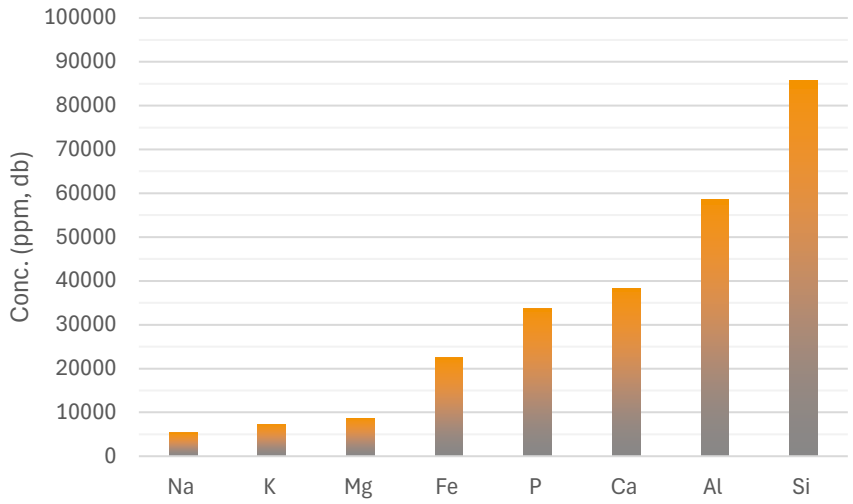

5.2.1.3 Assessment of pilot scale test on sewage sludge

In accordance with the equations reported in paragraph 5.1 the energy balance is split 37% and 63% respectively between the solid and the pyro-gas.

Graph 28: Energy balance for SS slow pyrolysis pilot-scale trial

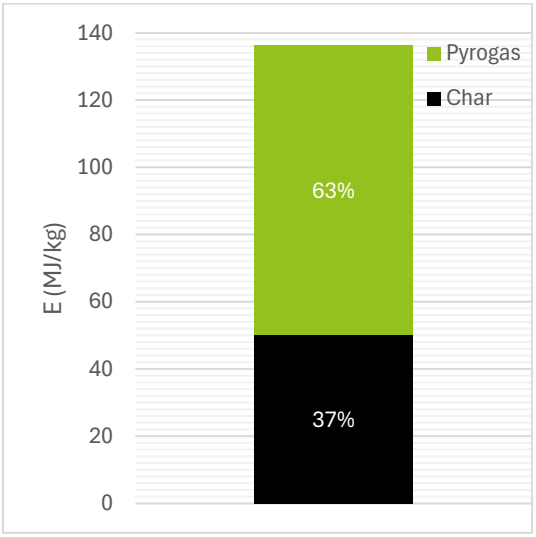

The test on sewage sludge enabled us to obtain reliable quantity of char, but with a chemical composition not considered suitable for a use in the steelmaking process. In fact, the C content of 23 % and the high ash content (72% db), avoid the classification of this char as a bio-coal. Moreover, a high concentration of contaminants could affect the steel quality during the EAF operations. For this reason, a chemical upgrading by acid leaching will be performed. Moreover, the sludge used resulted rich in Cr, and other heavy metals. The reason can stay in the fact that this sludge was contaminated by other sludges of industrial origins. Therefore, in addition to leaching tests, further char will be produced with a SS of more standard quality, like that adopted for the lab scale trials.

Graph 29: Van Krevelen diagram showing sewage sludge (SS) and sewage sludge char (SSC) placements.

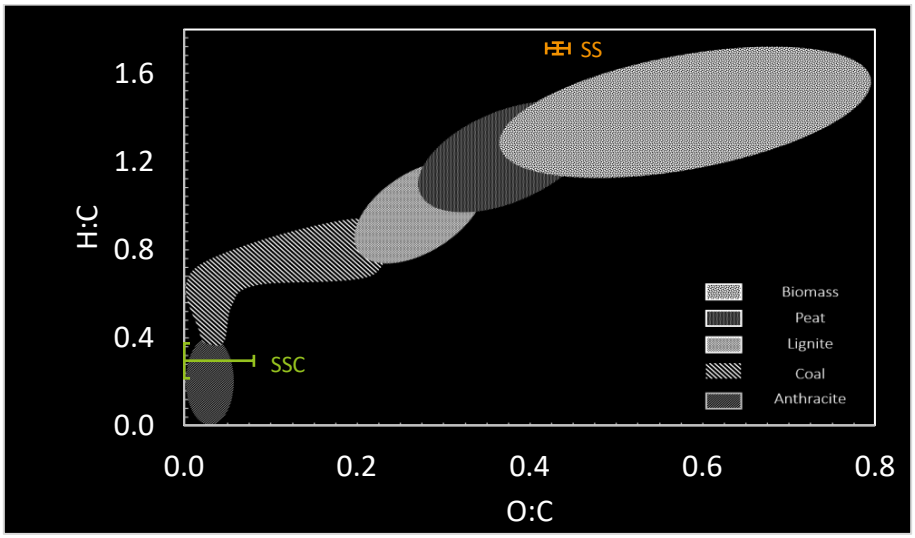

5.3 PYROK trials

Two PYROK pilot scale trials have been performed. AGW and AGD biowastes have been processed. The description and assessment of the two tests are reported below in section 5.3.1 and section 5.3.2.

5.3.1 AGW pilot scale slow pyrolysis trial

The green waste processed consisted of a pelletized straw batch collected in Finland (see Figure 17).

Figure 17: Pelletized straw sample processed during AGW pilot scale slow pyrolysis trial.

5.3.1.1 Characterization of the processed green waste

The proximate and ultimate composition of the straw processed along with its trace elements content and calorific density are reported in Table 21.

Table 21: Characterization of AGW used during slow pyrolysis pilot-scale test

Parameter	Value		C.I.$_{95\%}$	Unit
Moisture	**0.9**	±	0.4	wt.%, wb
Volatiles	**72.7**	±	0.6	wt.%, db
Ashes 550°C	**8.6**	±	0.5	wt.%, db
Ashes 815°C	**8.2**	±	0.6	wt.%, db
Fixed C	**18.6**	±	0.2	wt.%, db
C	**45.3**	±	0.3	wt.%, db
H	**5.8**	±	0.1	wt.%, db
N	**0.9**	±	0.4	wt.%, db
S	**0.1**	±	0.04	wt.%, db
Cl	**0.3**	±	0.1	wt.%, db
O	**39**	±	5	wt.%, db
Al	**261**	±	n/d	wt.%, db
Ba	**25**	±	8	wt.%, db
Ca	**5866**	±	821	wt.%, db
Cd	**<1**	±	n/d	wt.%, db
Co	**<2**	±	n/d	wt.%, db
Cr	**<5**	±	n/d	wt.%, db
Cu	**<5**	±	n/d	wt.%, db
Fe	**448**	±	134	wt.%, db
K	**6492**	±	909	wt.%, db
Li	**<5**	±	n/d	wt.%, db
Mg	**998**	±	140	wt.%, db
Mn	**43**	±	13	wt.%, db
Mo	**<2**	±	n/d	wt.%, db
Na	**695**	±	97	wt.%, db
Ni	**<5**	±	n/d	wt.%, db
P	**1246**	±	n/d	wt.%, db
Pb	**<5**	±	n/d	wt.%, db
Ti	**<5**	±	n/d	wt.%, db
V	**<5**	±	n/d	wt.%, db
Zn	**19**	±	6	wt.%, db

HHV	**18.0**	±	0.2	MJ/kg, db

The composition of the material treated is generally consistent with that of other green agricultural wastes reported in the literature. Volatiles share is typically reported to fall around 74%-84%. The ashes typically can range from 3% to 19% (e.g. rice husk) and in this specific case they fall within the range. Fixed carbon is also in line with other evidence reported in the literature and little different from the values found for grapes (20%), tobacco (19%), corn cob (15-17%) (Trninić, et al., 2016). Both proximate and ultimate composition of the AGW used closely resemble that of a batch of municipal green waste collected from Rockhampton landfill (QLD, Australia) (Kabir, et al., 2015).

Graph 30: Proximate composition of AGW used during slow pyrolysis pilot-scale test

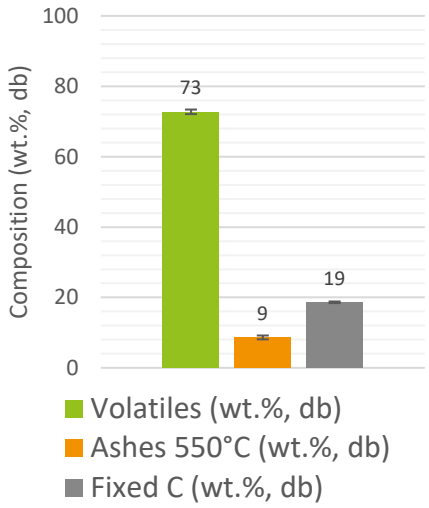

Graph 31: Ultimate composition of AGW used during slow pyrolysis pilot-scale test

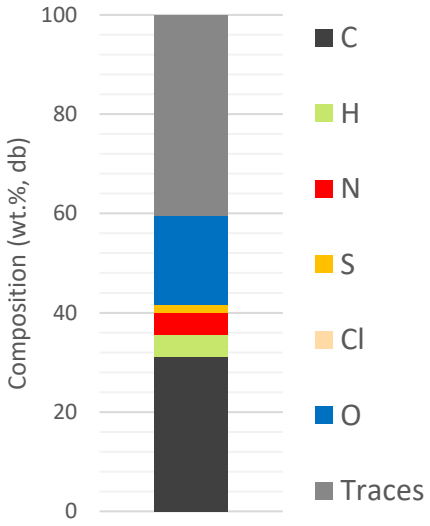

Graph 32: Trace elements in AGW used during slow pyrolysis pilot-scale test

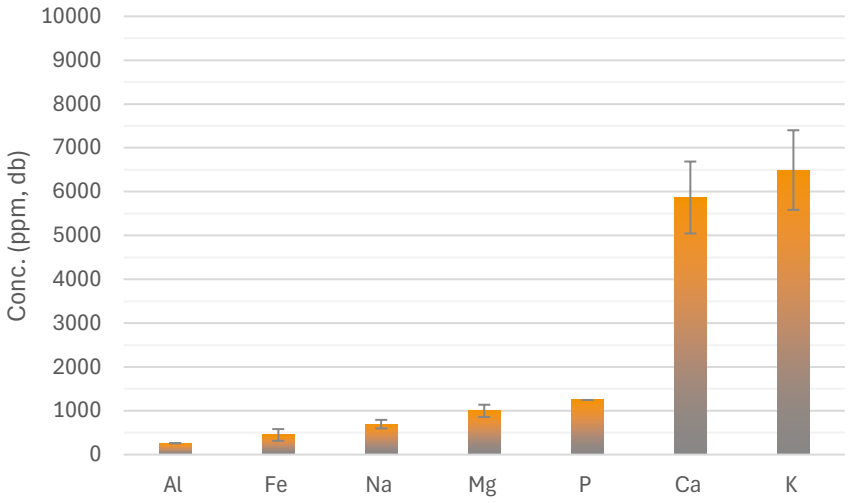

5.3.1.2 Description of the test on AGW

The feedstock as received was loaded to the hopper to be processed for a total amount of 351 kg corresponding to roughly 322 kg dry matter. The temperature of the kiln was set at 500°C. It is worth mentioning that, by prior knowledge developed internally by RE-CORD during PYROK operations the actual operating temperature deviates positively from the setpoint, so a setpoint of 500°C conceivably

allows to reach an operating temperature close to the optimum value stated in the previous section (i.e., 550°C). The kiln was operated at 4.8 rpm, which in this specific case leads to roughly 40 minutes residence time. During lab-scale tests 20' residence time was identified as optimal, but this figure does not consider the heating ramp which requires roughly 30 minutes to bring the system to the setpoint temperature. By and large, the entire temperature program during lab-scale trials took up to 50 minutes. This latter figure is consistent with the actual residence time achieved during pilot scale trial.

The trial produced 115 kg of dry solid (see Figure 18) product divided as follows: 96% produced as main solid, and 4% recovered as powder from the cyclone. The condensates to flue gases ratio (L/G) in the pyrogas was calculated to be 0.884. By and large, 111 kg of bio-oil and 125 kg of flue gases were produced. The mass balance of the trial is summarized in Table 22.

Char yield is higher for pilot scale trial compared to the lab-scale test. A 36% yield based on dry feedstock has been achieved in former case against 25% char yield in the latter case (see test 16 Table 13). Both the values do not differ much from the yield values of char from slow pyrolysis of lignocellulosic waste material reported by other authors (Kung, et al., 2015). Under similar pyrolysis conditions, the typical range for solid yields during pyrolysis of agricultural green residues can extend in a quite large span from 22% up to even 50% accordingly to the specific biomass treated (Hawash, et al., 2017; Tanoh, et al., 2020).

Table 22: Slow pyrolysis pilot-scale test on AGW mass yields

Slow pyrolysis conditions	Product	Mass balance*
500°C, 4.8 rpm, 40'	**Char**	**33%**
	Oil	**32%**
	Flue gas	**36%**

*based on feedstock as received (not db)

Graph 33: Products distribution from slow pyrolysis pilot-scale test on AGW (please note: mass balance is calculated on feedstock ar)

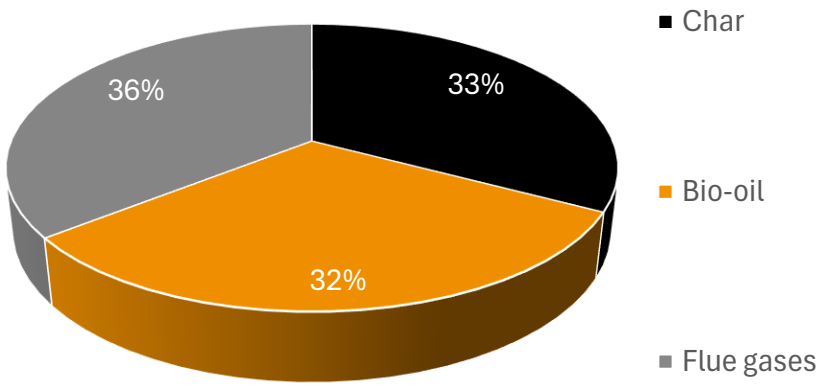

Figure 18: Char (AGWC) produced after pilot-scale pyrolysis of pelletized straw (AGW)

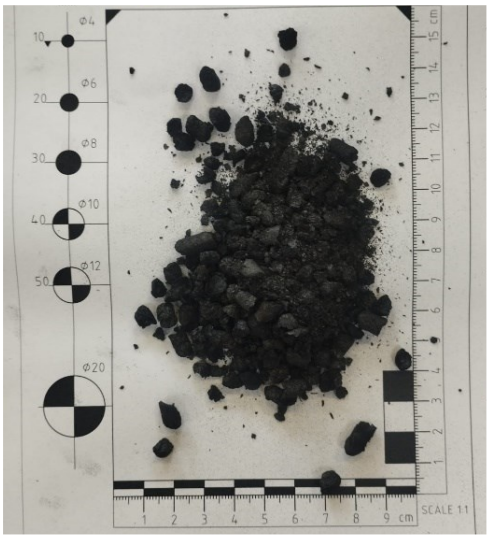

Figure 19: Bottle of bio-oil recovered after AGW pilot scale pyrolysis test

Volatiles and ash contents in the char resemble those found by other authors when processing other agricultural green waste such as rice husk processed under similar conditions (i.e. 450°-550°C) (Pariyar, et al., 2020). Fixed C content 59% is consistent with other observations available in the literature for chars produced during pyrolysis at 500°C on a variety of green waste substrates such as wood, bark, leaves, shells and straw (Yang, et al., 2017).

Table 23: Proximate composition of char produced during pilot scale slow pyrolysis on AGW

Parameter	Value (wt.%, db*)		C.I.$_{95\%}$
Moisture	**1.2**	**±**	**0.1**
Volatiles	**12.2**	**±**	**0.2**
Ashes 550°C	**28.6**	**±**	**0.2**
Ashes 710°C	**26.8**	**±**	**1.0**
Fixed C	**59.3**	**±**	**0.1**

** Values are given on db (dry basis) except for moisture content.*

Ultimate composition highlights quite a good carbon content (i.e. 64%).

Table 24: Ultimate composition of char produced during pilot scale slow pyrolysis on AGW

Parameter	Value (wt.%, db)		C.I.$_{95\%}$
C	**64.3**	**±**	**1.5**
H	**2.0**	**±**	**0.2**
N	**1.31**	**±**	**0.02**
S	**0.11**	**±**	**0.02**
Cl	**0.5**	**±**	**0.6**
O	**3.5**	**±**	**4.8**

Table 25: Calorific value of char from AGW slow pyrolysis pilot-scale test

Parameter	Value (MJ/kg, db)		C.I.$_{95\%}$
HHV	**24.4**	±	0.8
LHV	**24.0**	±	0.8

Major inorganic contaminants comprise alkali and earth-alkali metals which can be subsequently quite easily removed by an acidic treatment to upgrade the char into coal.

Table 26: Inorganic trace elements characterization for char derived from AGW slow pyrolysis pi8lot scale trial

Element	Value (ppm, db)
Al	863
Ba	83
Ca	19391
Fe	1481
K	21460
Mg	3299
Mn	142
Na	2297
P	4119
Zn	63

Graph 34: Trace elements in char from AGW slow pyrolysis pilot-scale test

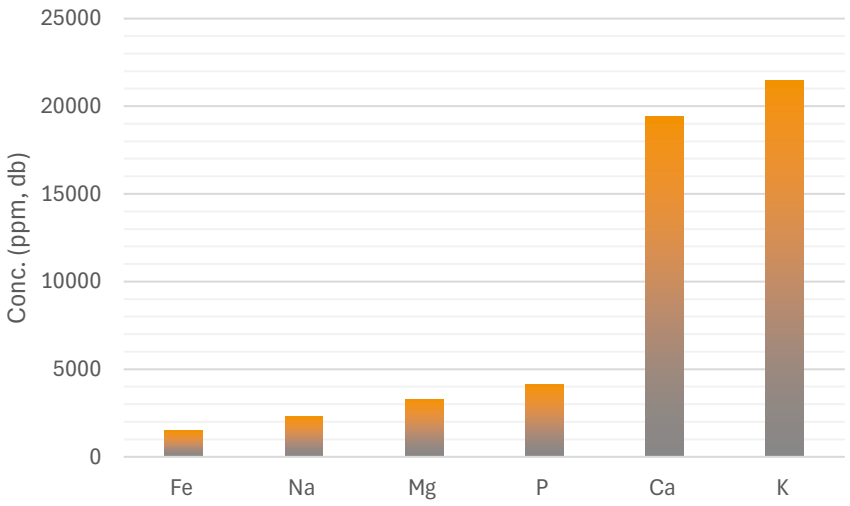

5.3.1.3 *Assessment of pilot scale test on agricultural green waste*

In accordance with the equations reported in paragraph 5.1 the energy balance is split 48% and 52% respectively between the solid and the pyrogas.

Graph 35: Energy balance for AGW slow pyrolysis pilot-scale trial

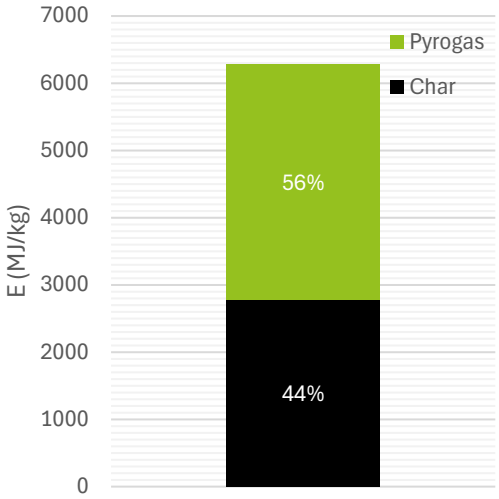

The char produced during the pilot scale trial on AGW has good carbon content (64%) comprising 59% of fixed C, with moderate amount of ashes 29%. Considering the inorganic contaminants can be removed by subsequent acidic leaching, the char produced has good potential to be upgraded to bio-coal. The elemental O:C and H:C ratios for the char, 0.04 and 0.37 respectively, allow to allocate the char produced within the boundaries of an anthracite/coal like material in the Van Krevelen diagram.

Graph 36: Van Krevelen diagram showing agricultural green waste (AGW) and AGW char (AGWC) placements.

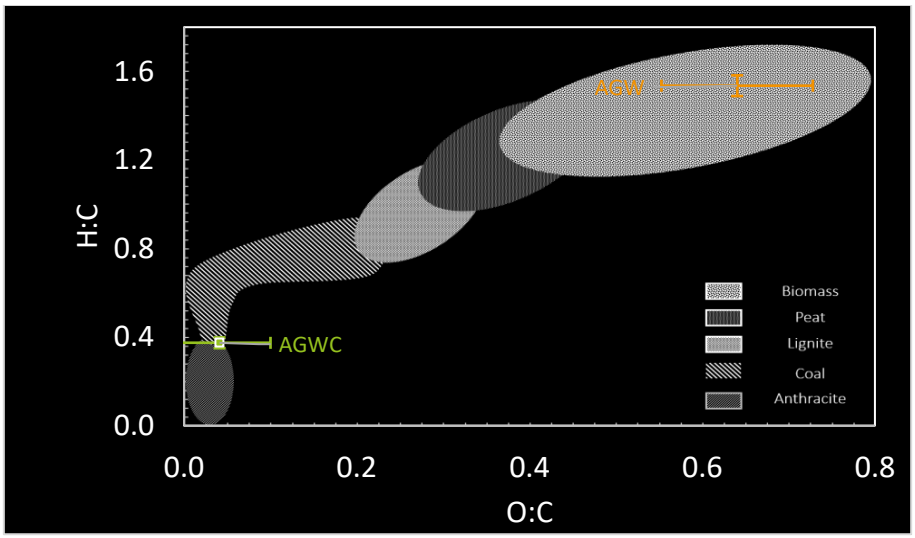

5.3.2 AGD pilot scale slow pyrolysis trial

The AGD used for the trial was based on pelletized solid digestate purchased from a company located in northern Italy operating an anaerobic digestion plant.

Figure 20: Pelletized solid digestate processed during AGD pilot scale slow pyrolysis trial.

5.3.2.1 Characterization of the processed solid digestate

Table 27 summarises the physical (calorific density) and chemical properties (proximate, ultimate and trace elements composition) of the pelletized solid digestate processed during pilot scale trial on AGD.

Table 27: Characterization of AGD used during slow pyrolysis pilot-scale test

Parameter	Value		C.I.$_{95\%}$	Unit
Moisture	**0.5**	±	0.3	wt.%, wb
Volatiles	**64.7**	±	0.2	wt.%, db
Ashes 550°C	**13.8**	±	0.2	wt.%, db
Ashes 815°C	**13.6**	±	0.1	wt.%, db
Fixed C	**21.5**	±	0.3	wt.%, db
C	**45.3**	±	0.1	wt.%, db
H	**5.7**	±	0.2	wt.%, db
N	**1.5**	±	0.1	wt.%, db
S	**0.45**	±	0.01	wt.%, db
Cl	**0.3**	±	0.1	wt.%, db
O	**32.9**	±	0.4	wt.%, db
Al	**350**	±	n/d	wt.%, db
Ba	**25**	±	8	wt.%, db
Ca	**13278**	±	1859	wt.%, db
Cd	**<1**	±	n/d	wt.%, db
Co	**<2**	±	n/d	wt.%, db
Cr	**<5**	±	n/d	wt.%, db

Cu	**24**	±	7	wt.%, db
Fe	**1349**	±	405	wt.%, db
K	**13302**	±	1862	wt.%, db
Li	**<5**	±	n/d	wt.%, db
Mg	**8278**	±	1159	wt.%, db
Mn	**125**	±	38	wt.%, db
Mo	**3**	±	1	wt.%, db
Na	**1209**	±	169	wt.%, db
Ni	**<5**	±	n/d	wt.%, db
P	**9497**	±	n/d	wt.%, db
Pb	**<5**	±	n/d	wt.%, db
Ti	**13**	±	n/d	wt.%, db
V	**<5**	±	n/d	wt.%, db
Zn	**88**	±	26	wt.%, db
HHV	**18.4**	±	1.2	MJ/kg, db

Usually, solid digestate studies focus on matrices produced during the digestion of manure or civil sludge which typically have a higher ash content and lower C content than the material treated hereby (Petrovič, et al., 2021; Hung, et al., 2017). Digestate derived from agricultural waste might achieve carbon content increase with reduced ashes when manure and crops or green waste are mixed together as it could be the case.

Graph 37: Proximate composition of AGD used during slow pyrolysis pilot-scale test

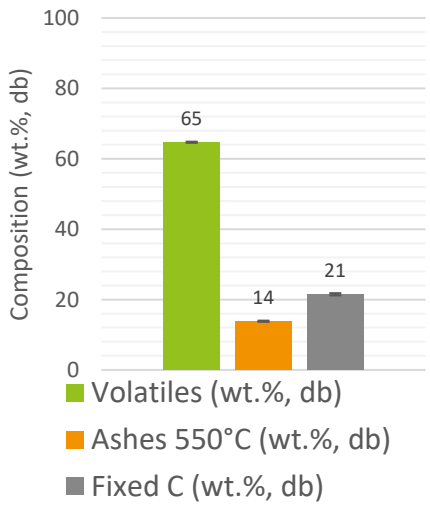

Graph 38: Ultimate composition of AGD used during slow pyrolysis pilot-scale test

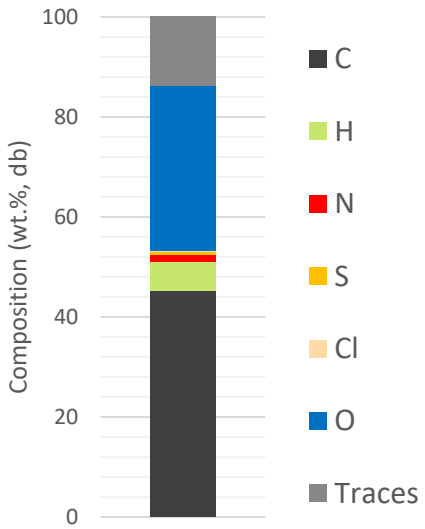

Graph 39: Trace elements in AGD used during slow pyrolysis pilot-scale test

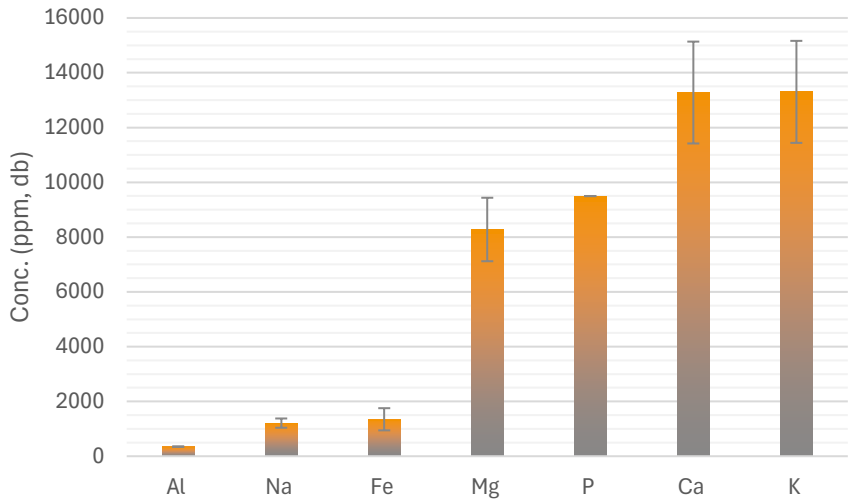

5.3.2.2 Description of the test on AGD

The pelletized solid digestate as received was fed to the pyrolysis unit. A total of 280 kg of material with 14% moisture content was processed. The set-point temperature has been set to 500°C: As stated above in section 5.3.1.2, an operating temperature close to the optimum value (550°C) can be achieved by setting the oven temperature to 500°C. The kiln was set on a speed equal to 4 rpm which ensures roughly 80 minutes of residence time inside the pyrolysis oven. One should bear in mind that while optimum residence time during lab scale pyrolysis tests was noticed to be 20 minutes, this value does not consider the temperature ramp that was set on 20°C·min^{-1} to reach 550°C. Considering the time span required during lab-scale tests to bring the system up to operating temperature, the total residence time inside the pyrolysis chamber is around 50 minutes. The scaling-up context allows for the discrepancy between this latter value and the actual figure (i.e. 80') to be deemed as acceptable.

Total operation process time was 5.4 hours. Pyrogas sampling was carried out for 1.4 hours.

Out of 241 kg of dry feedstock the slow pyrolysis pilot scale test produced 41.5 kg of dry AGD char (AGDC) at the stationary state plus other 50.1 kg dry char during transitory and shutdown. Overall char production equals 91.6 kg of dry material which gives 38 wt.% solid yield based on dry biomass input. This latter figure well approximates the value that was observed during lab-scale test (see test 15 Table 12). The match between these two values is a good validation of the process scalability. The global mass balance based on the feedstock as received gives 33% solid yield and 67% pyrogas yield. The pyrogas composition has a calculated L/G ratio equal to 1.046. This value enables us to estimate bio-oil production around 96 kg (i.e. 34% yield) and flue gases production around 92 kg (i.e. 33% yield). The mass balance of the trial is summarized in Table 28.

Table 28: Slow pyrolysis pilot-scale test on AGD mass yields

Slow pyrolysis conditions	Product	Mass balance*
500°C, 4 rpm, 80'	**Char**	**33%**
	Bio-oil	**34%**
	Flue gas	**33%**

* Based on feedstock as received (not db)

Graph 40: Products distribution from slow pyrolysis pilot-scale test on AGD (please note: mass balance is calculated on feedstock ar)

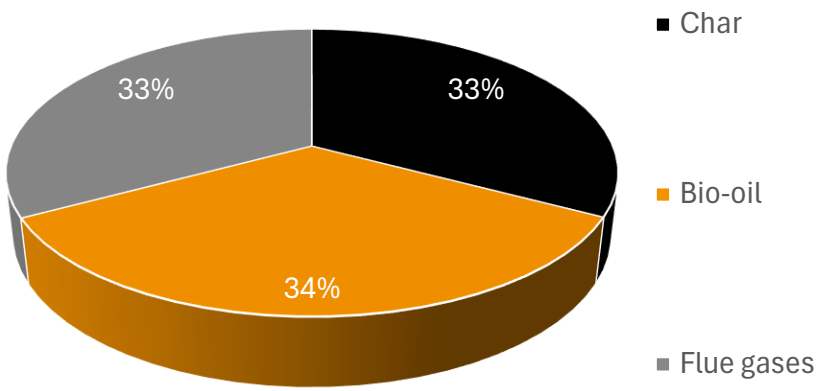

Char's proximate composition is not too different from the one of the char produced during AGW treatment. This can be an evidence that the solid digestate treated derived from a mixed substrate of manure and agricultural green waste.

Table 29: Proximate composition of char produced during pilot scale slow pyrolysis on AGD

Parameter	Value (wt.%, db)		$C.I._{95\%}$
Moisture	**0.73**	±	0.07
Volatiles	**12.06**	±	0.23
Ashes 550°C	**35.89**	±	0.35
Ashes 710°C	**35.14**	±	0.28
Fixed C	**52.05**	±	0.15

** Values are given on db (dry basis) except for moisture content.*

Carbon content is relatively high and quite similar to the content of C in char derived from AGW.

Table 30: Ultimate composition of char produced during pilot scale slow pyrolysis on AGD

Parameter	Value (wt.%, db)		$C.I._{95\%}$
C	**56.8**	±	0.3
H	**1.6**	±	0.1
N	**1.50**	±	0.04
S	**0.30**	±	0.02
Cl	**0.5**	±	0.4
O	**3.3**	±	2.0

Table 31: Calorific value of char from AGD slow pyrolysis pilot-scale test

Parameter	Value (MJ/kg, db)		C.I.$_{95\%}$
HHV	**21.1**	±	0.2
LHV	**20.7**	±	0.2

Table 32: Inorganic trace elements characterization for char derived from AGD slow pyrolysis pi8lot scale trial

Element	Value (ppm, db)
Al	908
Ba	65
Ca	34458
Cu	62
Fe	3501
K	34520
Mg	21482
Mn	324
Mo	8
Na	3137
P	24646
Ti	34
Zn	228

Graph 41: Trace elements in char from AGD slow pyrolysis pilot-scale test

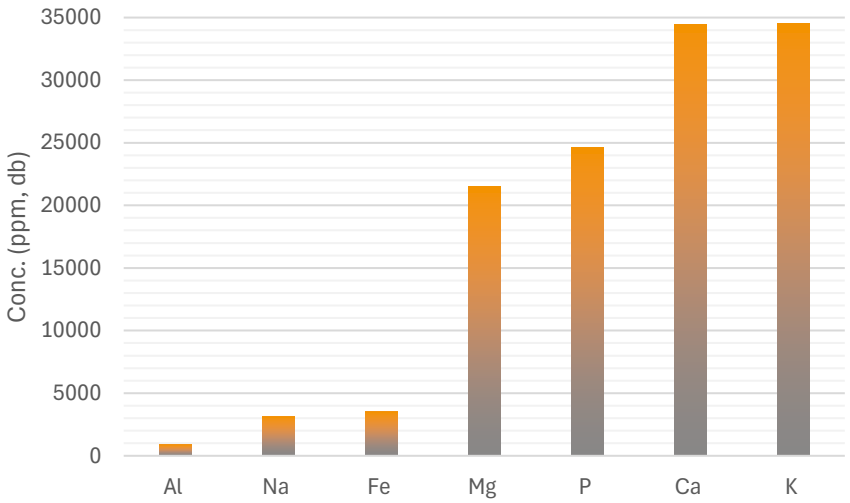

The condensates have been recovered during the test. The organic and the aqueous phase have been separated and analysed. Table 33 and Table 34 summarize the characterization of the organic and water phases respectively.

Table 33: Characterization of the organic phase recovered from bio-oil derived from slow pyrolysis on AGD

Parameter	Value		C.I.$_{95\%}$	Unit
Water	**21.6**	±	0.4	wt.%, wb
C	**75.1**	±	1.4	wt.%, db
H	**7.57**	±	0.09	wt.%, db
N	**4.4**	±	0.2	wt.%, db
S	**0.86**	±	0.02	wt.%, db
Cl	**0.08**	±	0.07	wt.%, db
O	**12.1**	±	1.4	wt.%, db
HHV	**33.3**	±	0.5	MJ/kg, db
LHV	**31.5**	±	0.5	MJ/kg, db
pH	**6.17**	±	0.01	

Graph 42: Composition of the bio-oil's organic phase (OP) recovered after slow pyrolysis on AGD

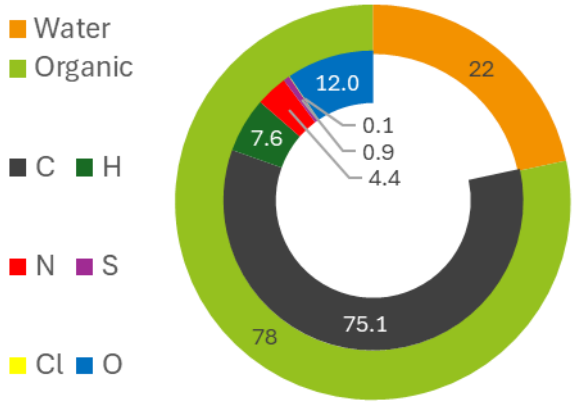

Table 34: Characterization of the aqueous phase recovered from bio-oil derived from slow pyrolysis on AGD

Parameter	Value		C.I.$_{95\%}$	Unit
Water	**88.5**	±	2.0	wt.%, wb
C	**45.2**	±	0.6	wt.%, db
H	**0.1**	±	0.3	wt.%, db
N	**12.1**	±	0.3	wt.%, db
S	**2.42**	±	0.03	wt.%, db

Cl	**0.50**	±	0.06	wt.%, db
O	**39.9**	±	0.5	wt.%, db
HHV	**2.5**	±	0.2	MJ/kg, wb
pH	**7.25**	±	0.02	

Graph 43: Composition of the bio-oil's aqueous phase (AP) recovered after slow pyrolysis on AGD

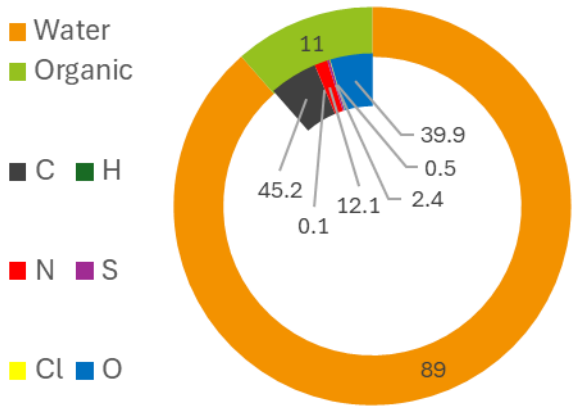

5.3.2.3 Assessment of pilot scale test on solid digestate

In accordance with the equations reported in paragraph 5.1 the energy balance is split 38% and 62% respectively between the solid and the pyrogas.

Graph 44: Energy balance for AGD slow pyrolysis pilot-scale trial

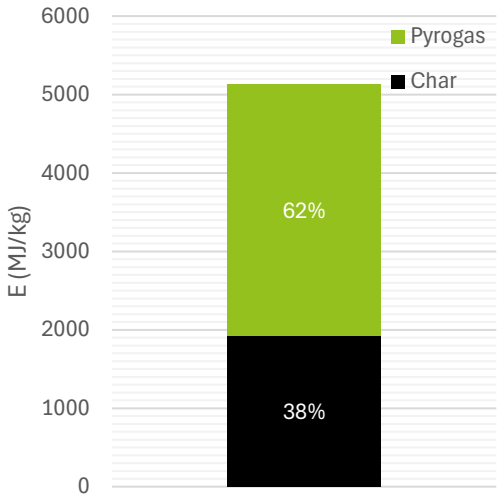

The char produced during the pilot scale trial on AGD has good carbon content (57%) comprising 52% of fixed C, with 36% ashes. The inorganic contaminants, mainly comprising alkali, earth alkali, iron and phosphorus can be removed by subsequent acidic leaching ensuring upgrading to bio-coal. The elemental O:C and H:C ratios for the char, 0.04 and 0.33 respectively, allow to allocate the char produced within the boundaries of an anthracite like material in the Van Krevelen diagram.

Graph 45: Van Krevelen diagram showing agricultural green waste (AGD) and AGD char (AGDC) placements.

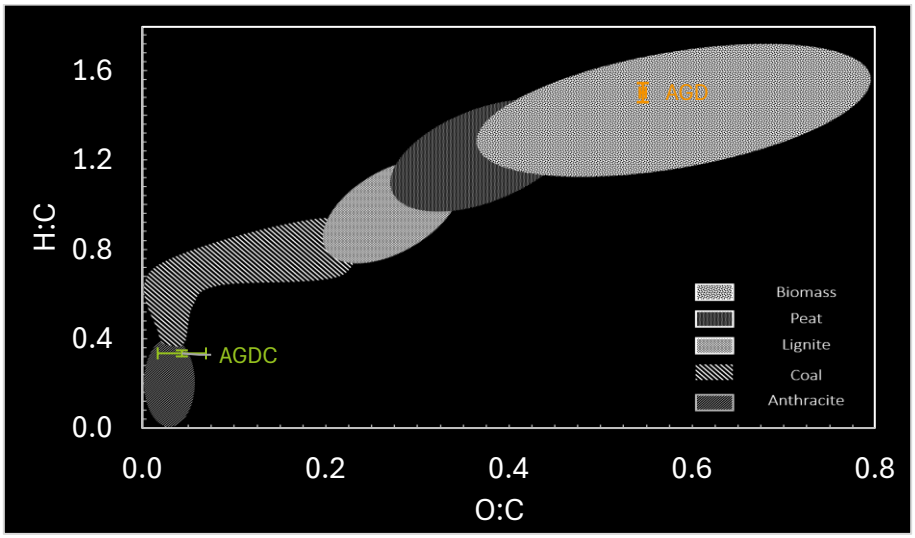

6 Conclusion

The results of the laboratory tests showed that residence time does not have any significant impact on bio-coal quality, and mass yield. On the contrary, temperature seems to influence more the process and the product quality. Working at 450 °C leads to production of a bio-coal comprising higher volatile fraction, preserving more oxygenated compounds in the material compared to counterparts produced at higher temperatures. Biocoal's samples produced between 550 and 650 °C present similar features, worth mentioning that the bio-coal from AGW shows higher HHV and higher C content for higher temperatures. For biocoal obtained in the range between 550°C and 650°C from SS, or OFMSW no significant difference has to be mentioned

All the bio-coals produced above 550°C showed a composition resembling the anthracite-bituminous coal quality, according to Van Krevelen. As expected, bio-coal from AGW presents low ashes and, thus, good value for being used in the steel sector. Only alkali elements in the ash represent a limit, which can be solved by leaching process. On the contrary, AGD, OFMSW, and even more SS, present too high ash content, which is concentrated in the coal after pyrolysis. Consequently, post treatment by acid leaching is needed to increase the HHV and carbon content, and to reduce the concentration of elements such as P, K, Mg, Na and Ca. The test performed on sewage sludge showed a high mass yield, as expected, but produced a low-quality char, mainly composed of inorganics. The use of this char in steelmaking is considered not feasible. However, further chemical leaching tests will be performed on this char to remove the inorganics and upgrade it to a suitable quality for the EAF.

As a next step, further pilot scale pyrolysis tests are planned, including:

- Sewage sludge test in PYROK – 550°C, RT: 20 minutes, HR: 20°C/min
- Digestate test in PYROK – 550°C, RT: 20 minutes, HR: 20°C/min
- OFMSW test in SPYRO and PYROK– 550°C, RT: 20 minutes, HR: 20°C/min
- AGW test in SPYRO and PYROK – 600°C, RT: 20 minutes, HR: 20°C/min

For each of the char produced, chemical leaching tests will be performed at pilot scale, so that to increase the char quality to a biocoal-grade composition, and to obtain reliable amount of steel grade biocoal for being used in EAF.

The description of the new pyrolysis tests and of the char chemical leaching trials will be included in the next deliverable D1.2.

7 References

Antal, M. J. & Grønli, M., 2003. The Art, Science, and Technology of Charcoal Production. *Ind. Eng. Chem. Res.,* 42(8), pp. 1619-1640.

Babinszki, B. et al., 2021. Effect of slow pyrolysis conditions on biocarbon yield and properties: Characterization of the volatiles. *Bioresource Technology,* Volume 338, p. 125567.

CATF, 2024. *Transforming the European Steel Sector to Net Zero.* [Online] Available at: https://www.catf.us/resource/transforming-european-steel-sector-net-zero/#:~:text=An%20important%20part%20of%20the,of%20the%20EU's%20annual%20emissions. [Consultato il giorno 07 2024].

Echterhof, T., 2021. Review on the Use of Alternative Carbon Sources in. *Metals,* 11(222).

Echterhof, T., Demus, T., Schulten, M. N. Y. & & Pfeifer, H., 2014. *Substituting fossil carbon sources in the electric arc and cupola furnace with biochar.* Teesside University: Middlesbrough, UK., s.n.

EUROFER, 2023. *European Steel in Figures 2023.* [Online] Available at: https://www.eurofer.eu/publications/brochures-booklets-and-factsheets/european-steel-in-figures-2023 [Consultato il giorno 07 2024].

Gao, N., Kamran, K., Quan, C. & Williams, P. T., 2020. Thermochemical conversion of sewage sludge: A critical review. *Progress in Energy and Combustion Science,* Volume 79, p. 100843.

Hawash, S., Farah, J. Y. & El-Diwani, G., 2017. Pyrolysis of agriculture wastes for bio-oil and char production. *Journal of Analytical and Applied Pyrolysis,* Volume 124, pp. 369-372.

Hung, C.-Y.et al., 2017. Characterization of biochar prepared from biogas digestate. *Waste Management,* Volume 66, pp. 53-60.

Ibrahim, R. H., Darvell, L. I., Jones, J. M. & Williams, A., 2013. Physicochemical characterisation of torrefied biomass. *Journal of Analytical and Applied Pyrolysis,* Volume 103, pp. 21-30.

JRC, 2022. *EU climate targets: how to decarbonise the steel industry.* [Online] Available at: https://joint-research-centre.ec.europa.eu/jrc-news-and-updates/eu-climate-targets-how-decarbonise-steel-industry-2022-06-15_en#_ftn1 [Consultato il giorno 07 2024].

Kabir, M. J., Chowdhury, A. A. & Rasul, M. G., 2015. Pyrolysis of municipal green waste: a modelling, simulation and experimental analysis. *Energies,* Volume 8, pp. 7522-7541.

Kacprzak, M. et al., 2017. Sewage sludge disposal strategies for sustainable development. *Environmental Reasearch,* Volume 156, pp. 39-46.

Kung, C.-C., Kong, F. & Choi, Y., 2015. Pyrolysis and biochar potential using crop residues and agricultural wastes in China. *Ecological Indicators,* Volume 51, pp. 139-145.

Mousa, E., Wang, C., Riesbeck, J. & Larsson, M., 2016. Biomass applications in iron and steel industry: An overview of challenges and opportunities. *Renewable and Sustainable Energy Reviews,* Volume 65, pp. 1247-1266.

Mustafa, S. et al., 2021. Effect of Lead and Zinc Impurities in Ironmaking and the Corresponding Removal Methods: A Review. *Metals,* 11(3), p. 407.

Pariyar, P., Kumari, K., Jain, M. K. & Jadhao, P. S., 2020. Evaluation of change in biochar properties derived from different feedstock and pyrolysis temperature for environmental and agricultural application. *Science of The Total Environment,* Volume 713, p. 136433.

Petrovič, A. et al., 2021. Pyrolysis of Solid Digestate from Sewage Sludge and Lignocellulosic Biomass: Kinetic and Thermodynamic Analysis, Characterization of Biochar. *Sustainability,* Volume 13, p. 9642.

Reichel, T., Demus, T., Echterhof, T. & Pfeifer, H., 2014. *Increasing the sustainability of the steel production in the electric arc furnace by substituting fossil coal with biochar.* s.l.:s.n.

Safarian, S., 2023. To what extent could biochar replace coal and coke in steel industries?. *Fuel,* Volume 339, p. 127401.

Salimbeni, A., Lombardi, G., Rizzo, A. & Chiaramonti, D., 2023. Techno-Economic feasibility of integrating biomass slow pyrolysis in an EAF steelmaking site: A case study. *Applied Energy,* Volume 339, p. 120991.

Shankar Tumuluru, J. et al., 2011. A review on biomass torrefaction process and product properties for energy applications. *Industrial Biotechnology,* 7(5), pp. 384-401.

Tanoh, T. S. et al., 2020. Green Waste/Wood Pellet Pyrolysis in a Pilot-Scale Rotary Kiln: Effect of Temperature on Product Distribution and Characteristics. *Energy & Fuels,* 34(3), pp. 3336-3345.

Trninić, M., Jovović, A. & Stojiljković, D., 2016. A steady state model of agricultural waste pyrolysis: A mini review. *Waste Management & Research,* 34(9), pp. 851-865.

Worldsteel Association, 2023. *Fact sheet. Steel and raw materials,* s.l.: s.n.

Yang, X. et al., 2017. Thermal Properties of Biochars Derived from Waste Biomass Generated by Agricultural and Forestry Sectors. *Energies,* Volume 10, p. 469.

8 Annex I - Calculation of activation energy of pyrolysis process

Micro-TGA-DTA tests were performed on the four biomass matrixes that have shown the best chemical properties to be converted into char suitable for steelmaking applications. The four samples are listed below:

C.24.125.001: digestate (AGD)

RES.21.027.008: prunings (AGW)

RES.24.067.001: Organic Fraction of Municipal Solid Waste (OFMSW)

RES.23.077.005: Sewage sludge (SS)

The TGA-DTA tests were conducted in a Perkin Elmer Q6000 SDT under 100 ml/min of nitrogen atmosphere by setting three different heating rate (15, 20 and 25 °C/min) from room temperature to the set temperature (450 or 650 °C, respectively) and maintaining the set point for 20 or 120 minutes as a function of the temperature. In Table 13, experimental plan is summarized for a total number of tests equal to 24. The analysis was conducted to determine the activation energy of the pyrolysis process according to the Kissinger–Akahira–Sunose (KAS) method given its wide diffusion in the biomass pyrolysis kinetics studies[1]. The final equation derived using the Doyle approximation method is given in Equation 1.

$$ln\left(\frac{\beta_i}{T_{ai}^2}\right) = ln\left(\frac{A_a R}{E_a g(a)}\right) - \frac{E_a}{RT_{ai}} \qquad (1)$$

where β (in K/min) correspond to the heating rate, T (in K) to the temperature, A (in 1/s) to the Arrhenius pre-exponential factor, R to the gas constant (8.314 J/mol K), E_a (in J/mol) to the apparent activation energy, $g(a)$ is constant at a given value of conversion and the subscripts i and a denotes the heating rate and value of conversion, respectively. The apparent activation energy is obtained by plotting $ln(\beta_i/T^2_{ai})$ versus $1000/T_{ai}$ for a given value of conversion, where the slope is equal $-E_a/R$.

Table 35. Experimental plan for the determination of pyrolysis activation energy

Biomass sample	Heating rate [°C/min]	Target temperature [°C]	Dwelling time [min]
C.24.125.001: digestate	15, 20, 25	450	20
		650	120
RES.21.027.008: prunings	15, 20, 25	450	20
		650	120
RES.23.077.005: civil mud	15, 20, 25	450	20
		650	120
RES.24.067.001: OFMSW	15, 20, 25	450	20
		650	120

In the following figures (Figure 21 from to Figure 44) the thermogram of the four biomasses at the different testing conditions are reported. Thermogravimetric curve (TG) is reported in red while its first derivate (dTG) is reported in green. Heat flow signal (DTA) is reported in blue.

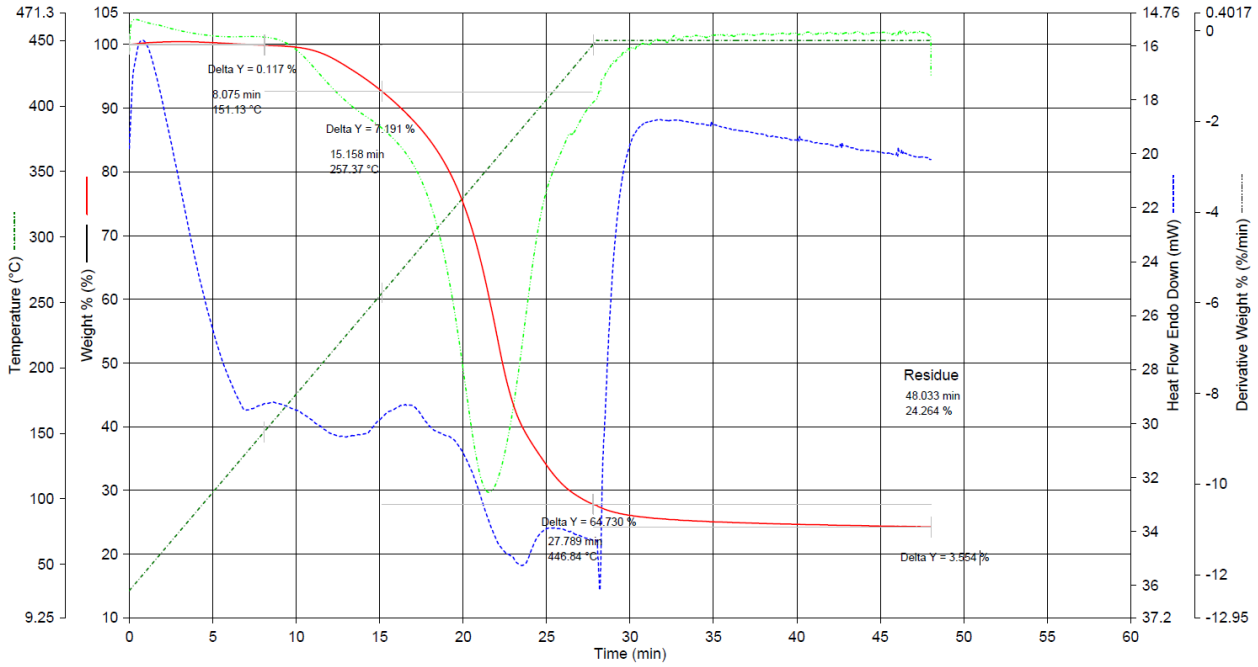

Figure 21. TGA-DTA results of OFMSW at 450 °C x 20 min at 15 °C/min.

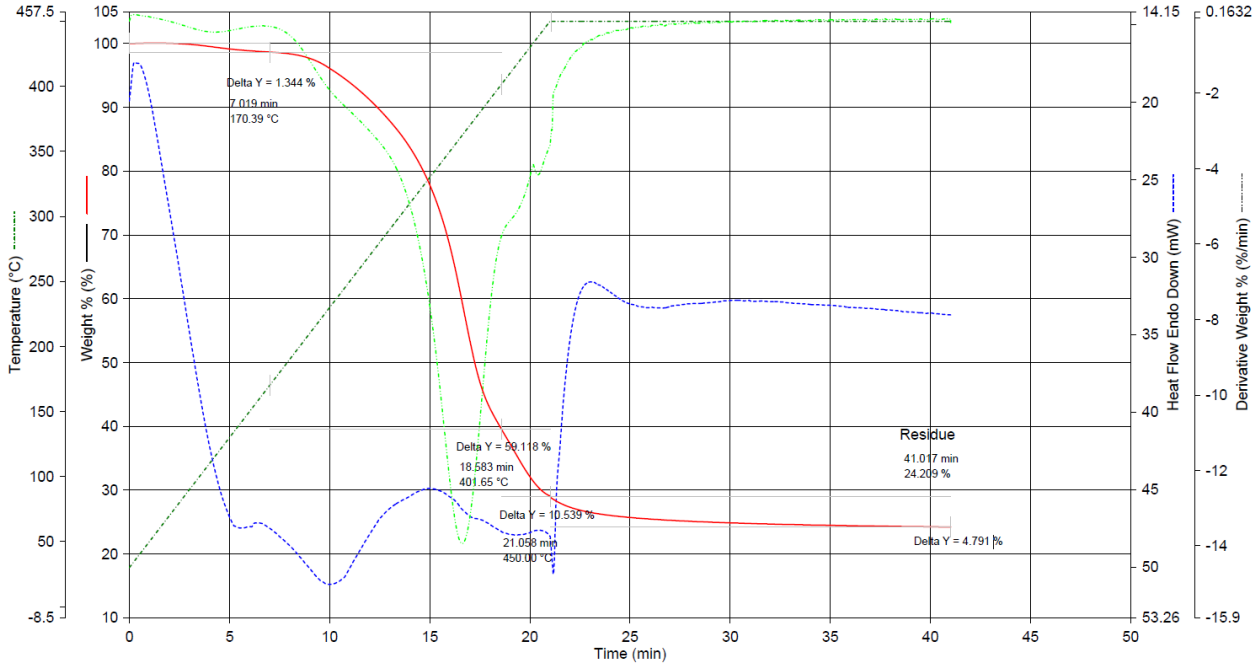

Figure 22. TGA-DTA results of OFMSW at 450 °C x 20 min at 20 °C/min.

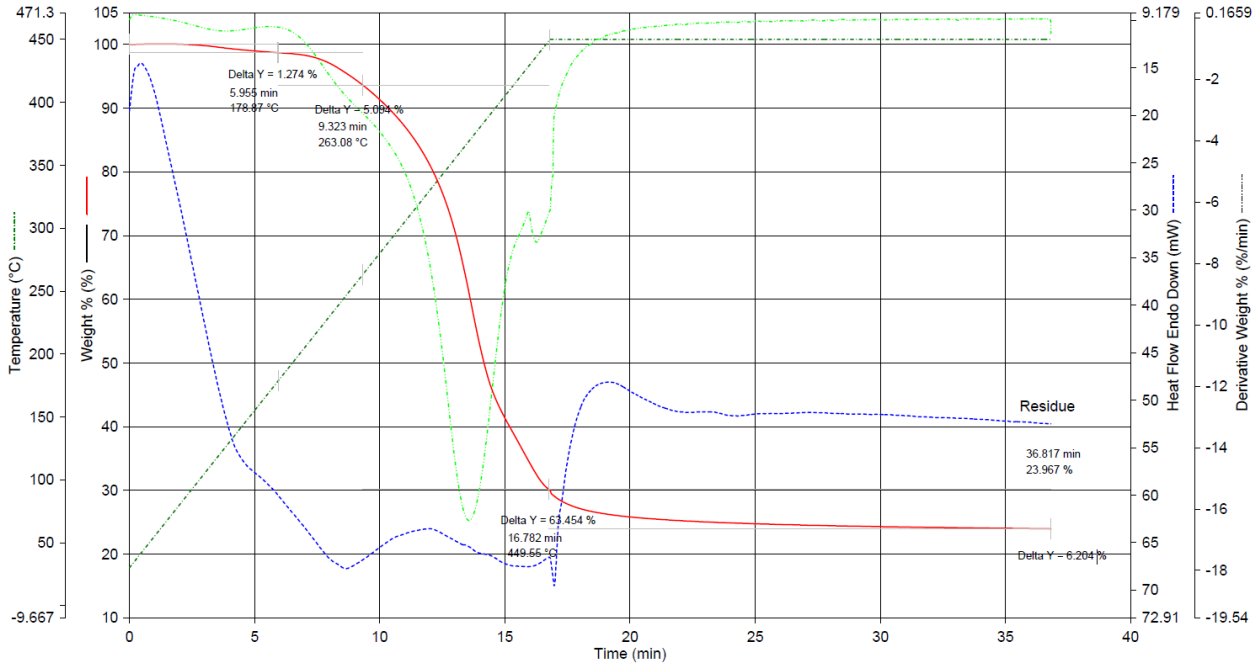

Figure 23. TGA-DTA results of OFMSW at 450 °C x 20 min at 25 °C/min.

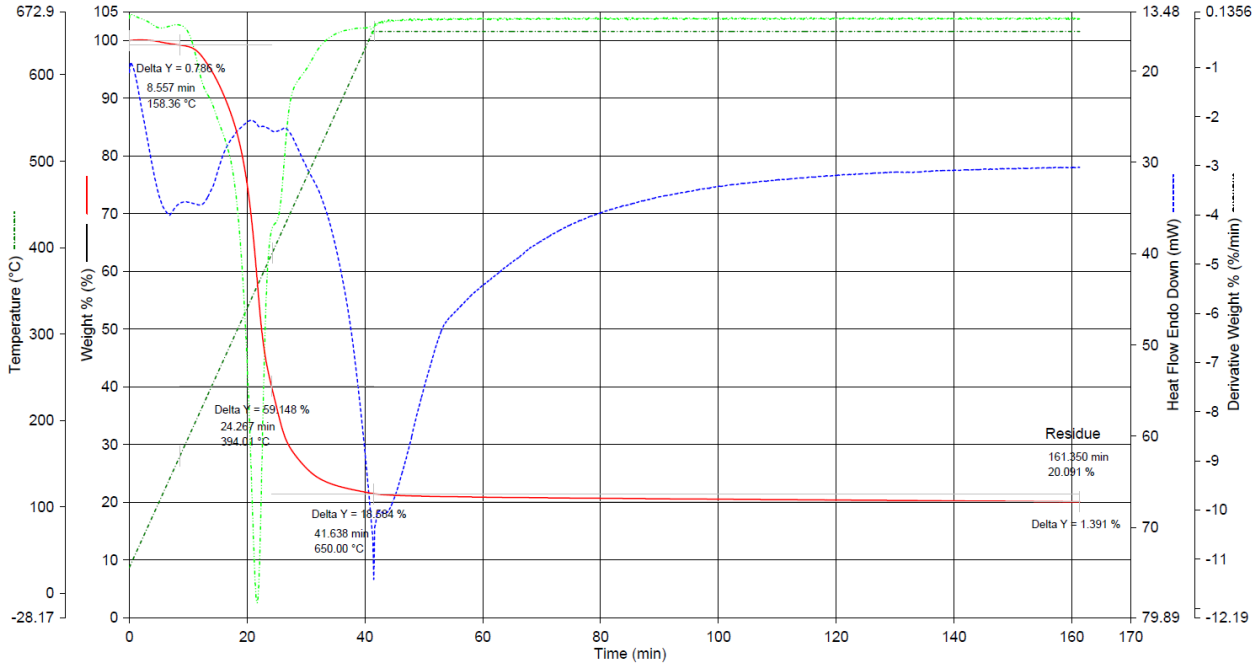

Figure 24. TGA-DTA results of OFMSW at 650 °C x 120 min at 15 °C/min.

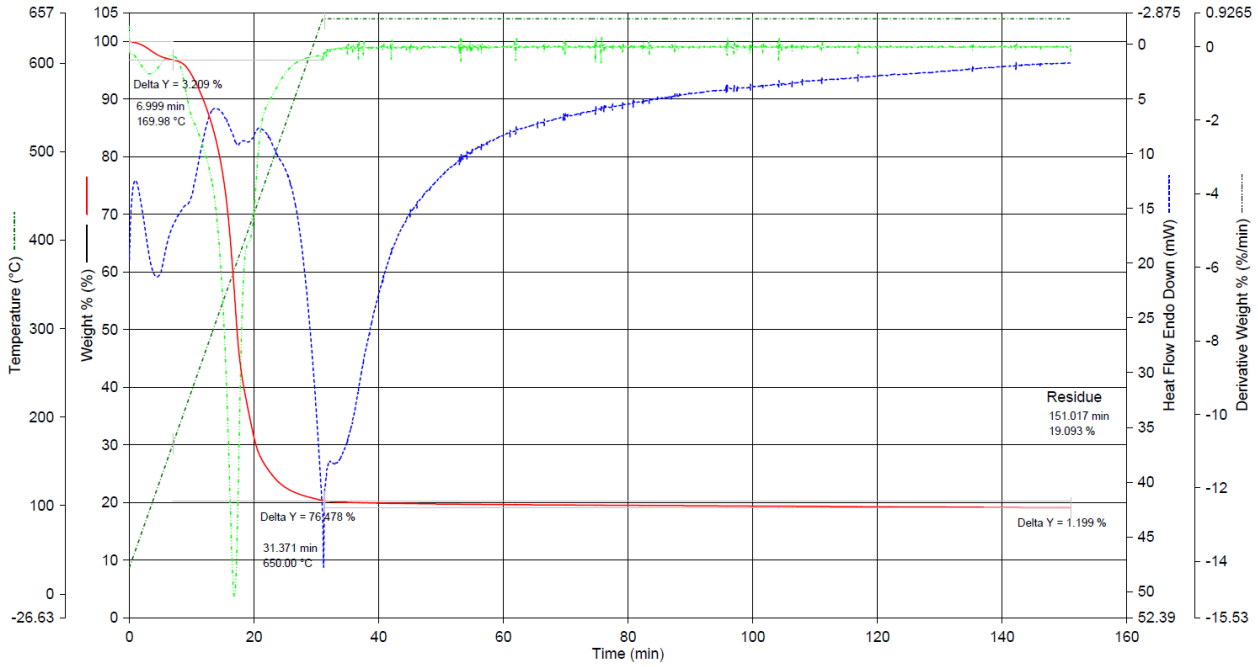

Figure 25. TGA-DTA results of OFMSW at 650 °C x 120 min at 20 °C/min.

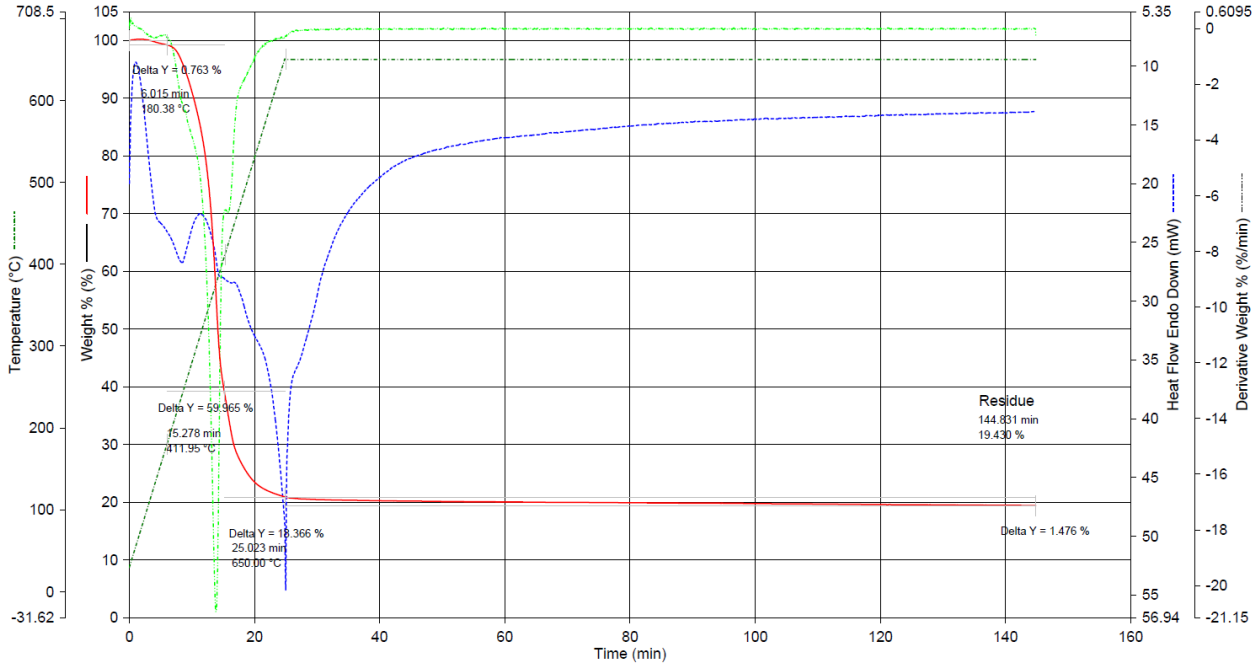

Figure 26. TGA-DTA results of OFMSW at 650 °C x 120 min at 25 °C/min.

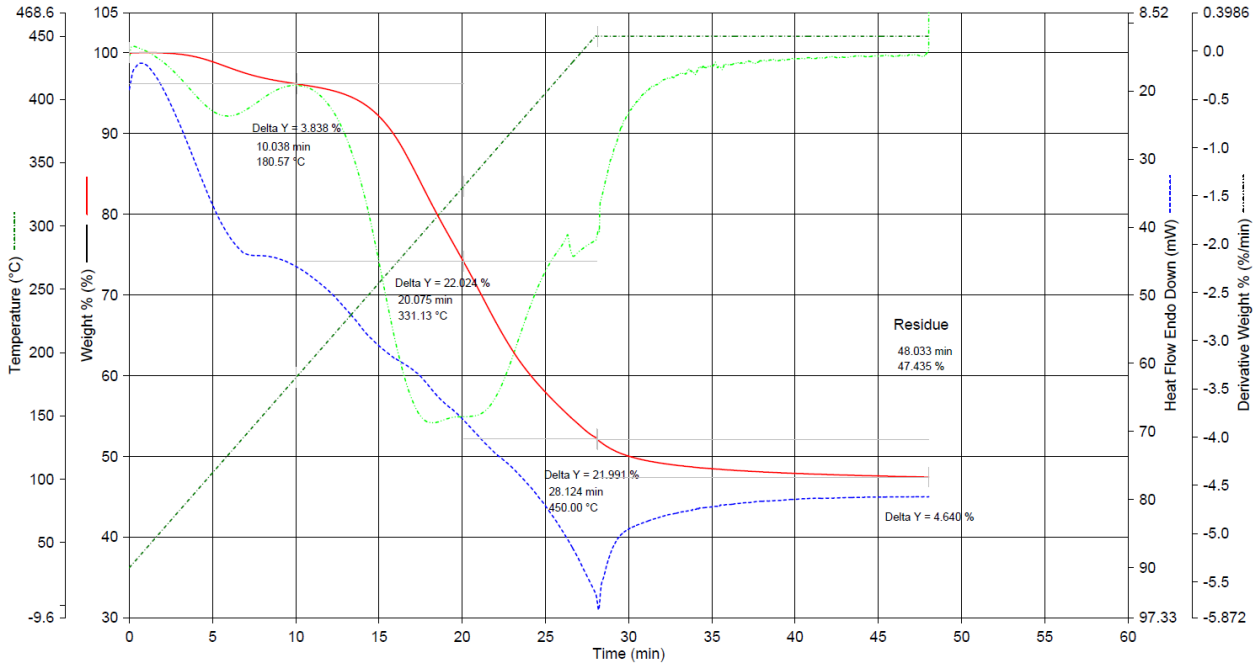

Figure 27. TGA-DTA results of civil mud at 450 °C x 20 min at 15 °C/min.

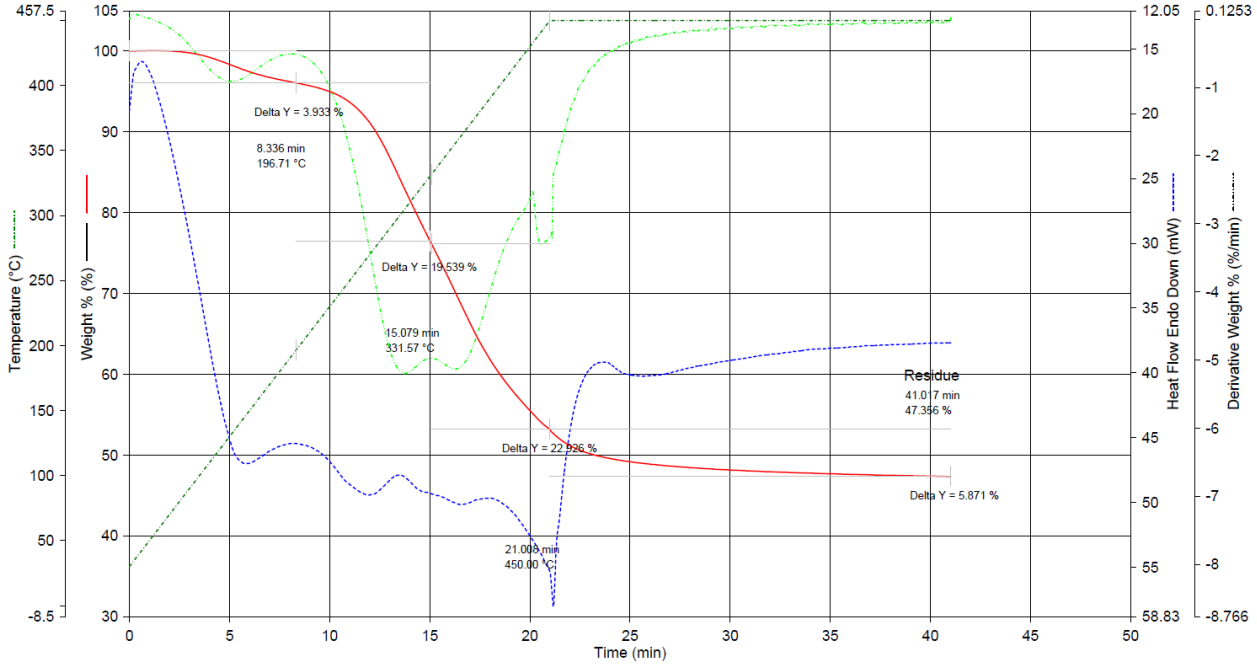

Figure 28. TGA-DTA results of civil mud at 450 °C x 20 min at 20 °C/min.

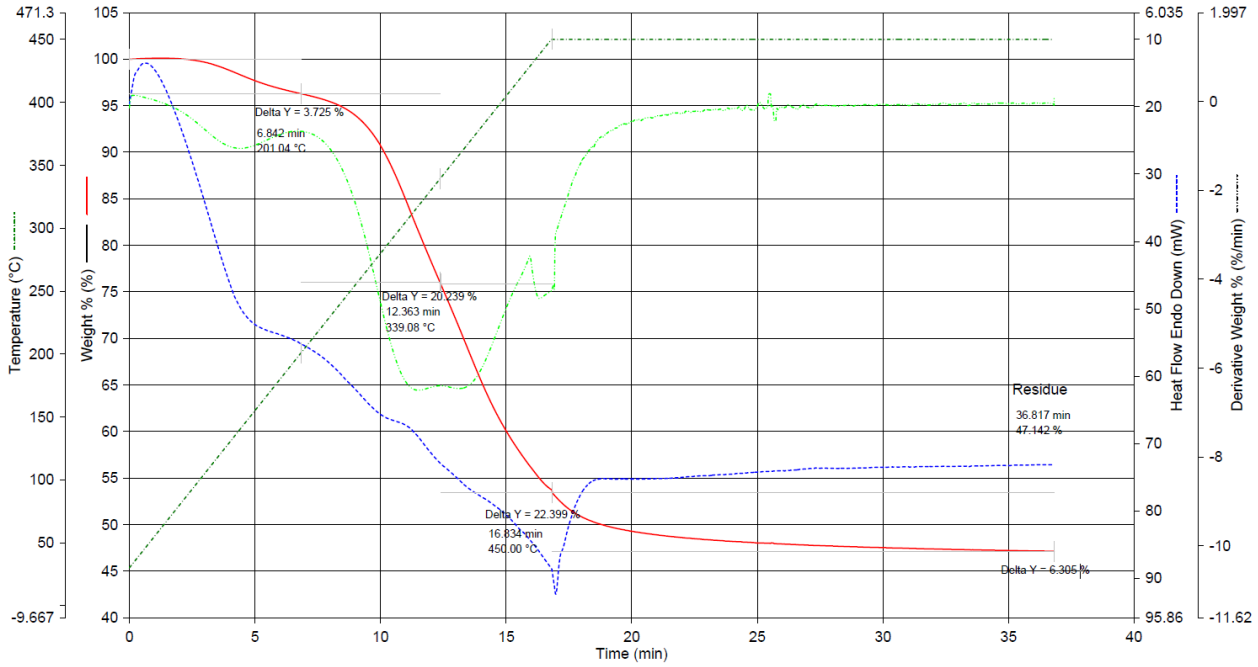

Figure 29. TGA-DTA results of civil mud at 450 °C x 20 min at 25 °C/min.

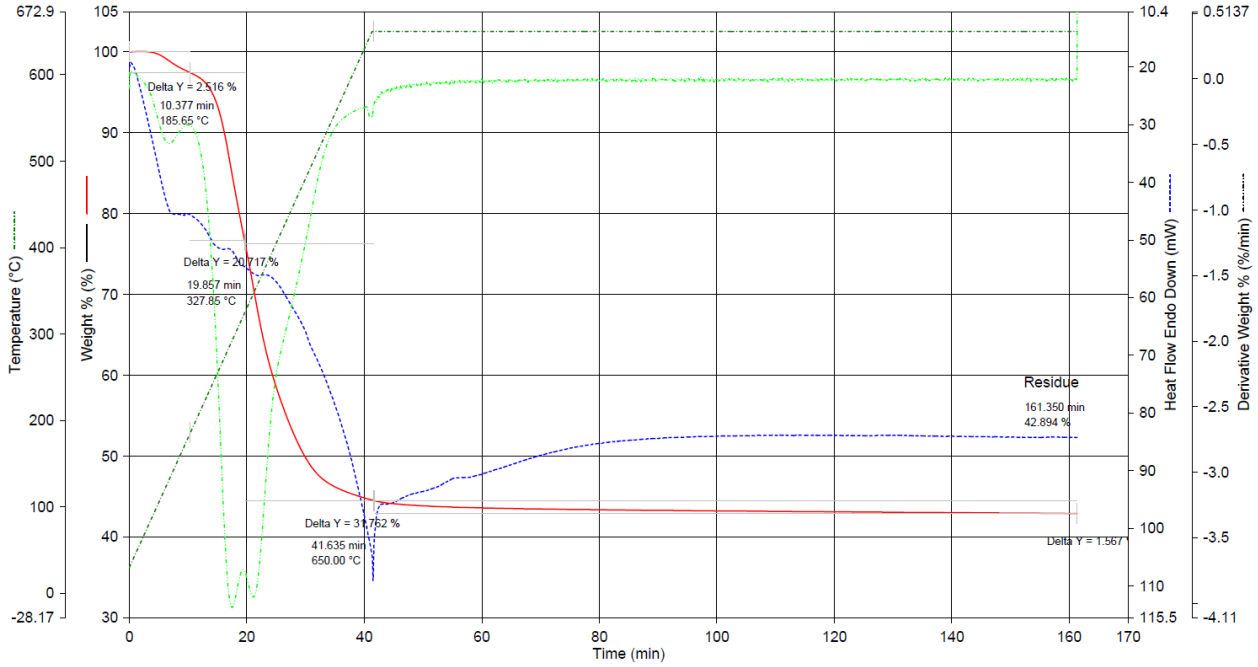

Figure 30. TGA-DTA results of civil mud at 650 °C x 120 min at 15 °C/min.

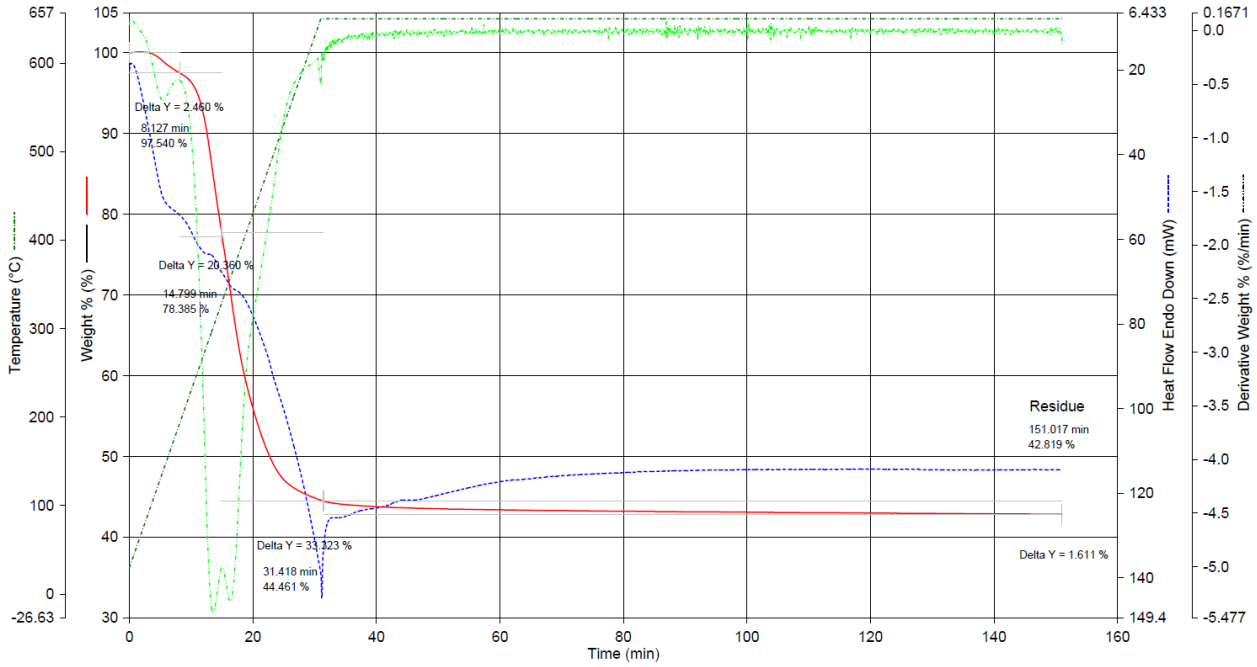

Figure 31. TGA-DTA results of civil mud at 650 °C x 120 min at 20 °C/min.

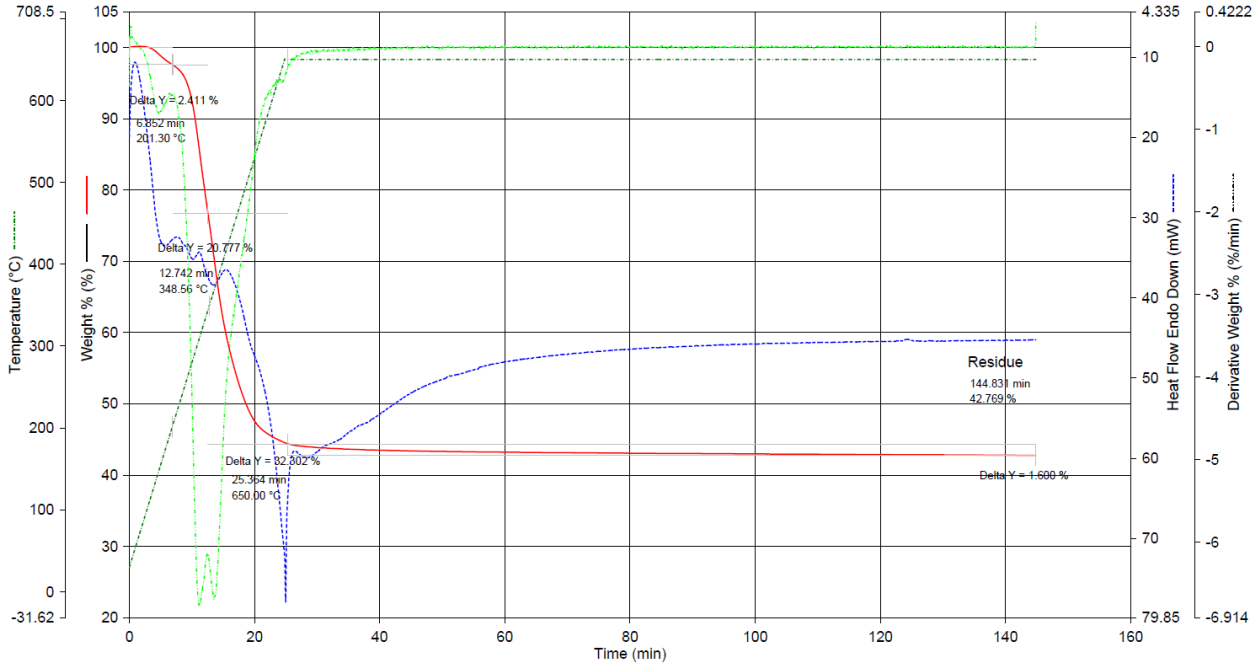

Figure 32. TGA-DTA results of civil mud at 650 °C x 120 min at 25 °C/min.

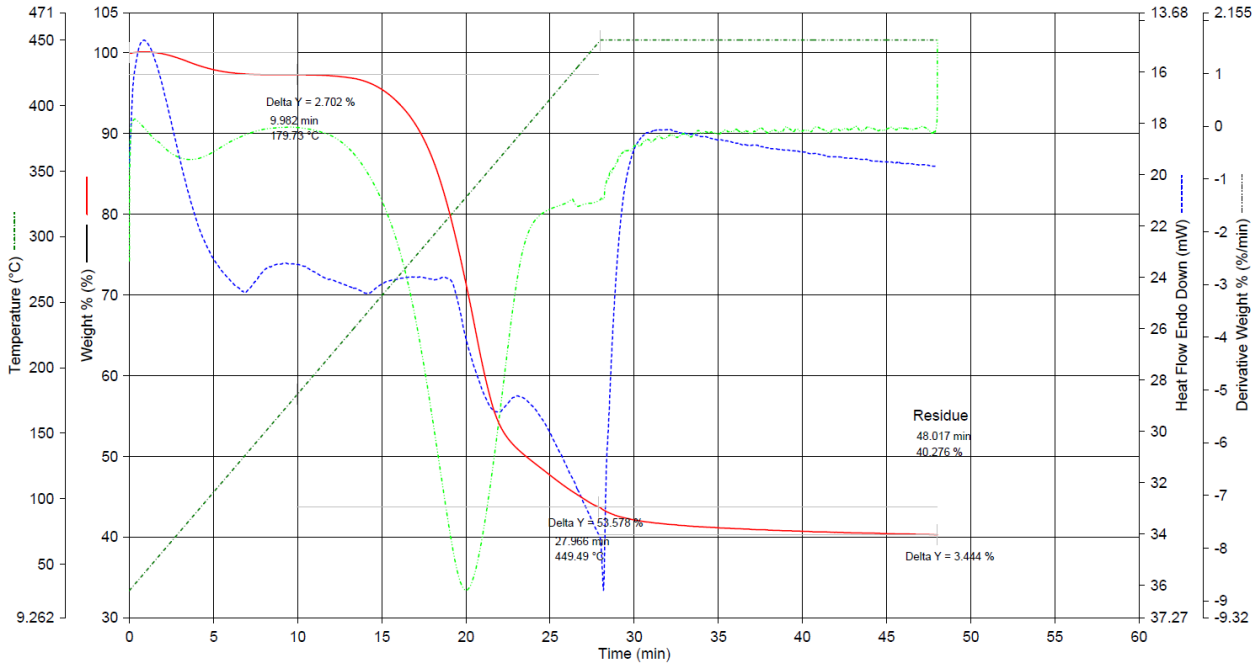

Figure 33. TGA-DTA results of digestate at 450 °C x 20 min at 15 °C/min.

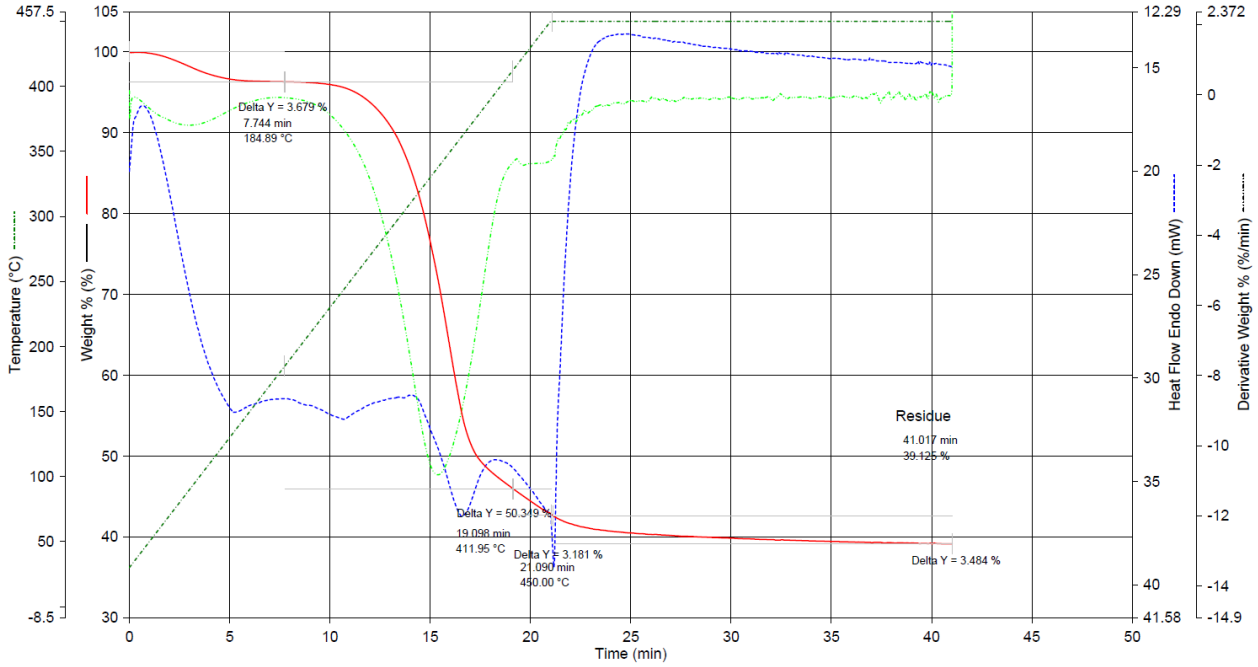

Figure 34. TGA-DTA results of digestate at 450 °C x 20 min at 20 °C/min.

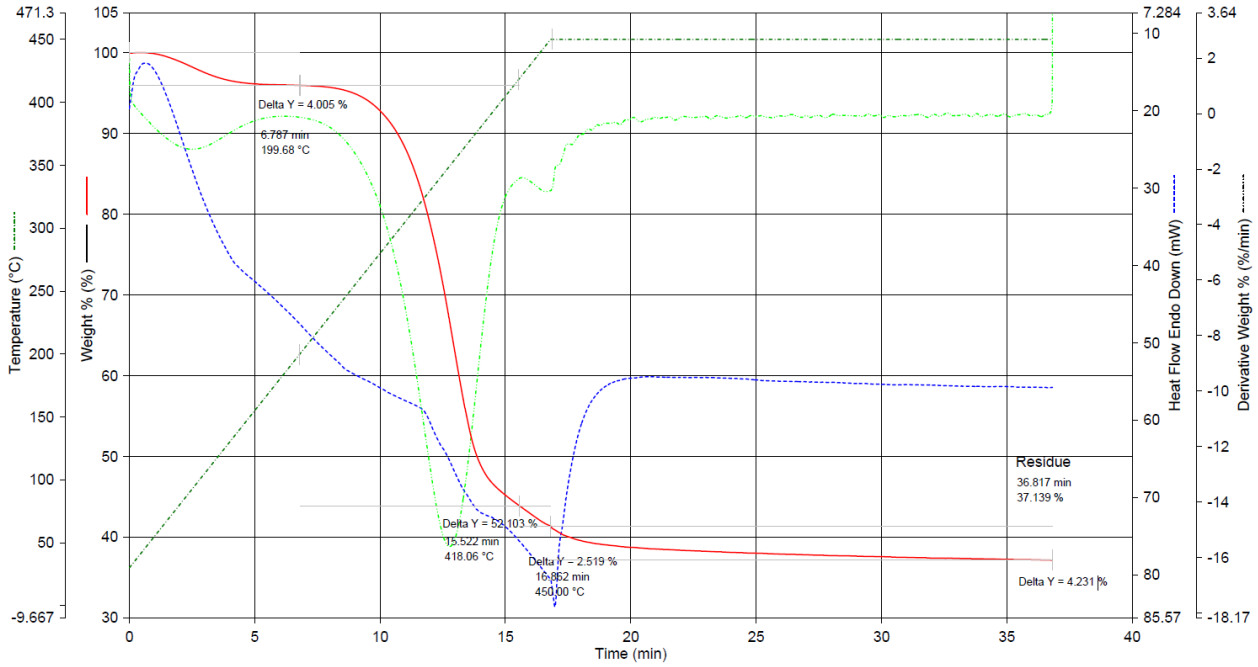

Figure 35. TGA-DTA results of digestate at 450 °C x 20 min at 25 °C/min.

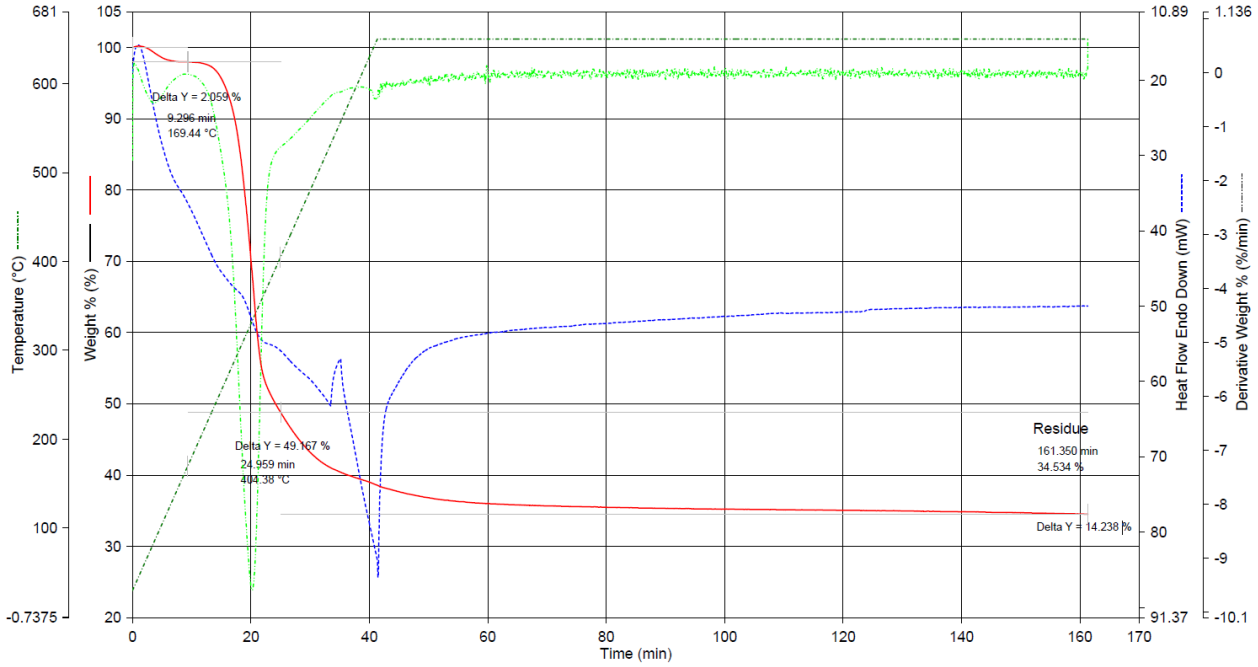

Figure 36. TGA-DTA results of digestate at 650 °C x 120 min at 15 °C/min.

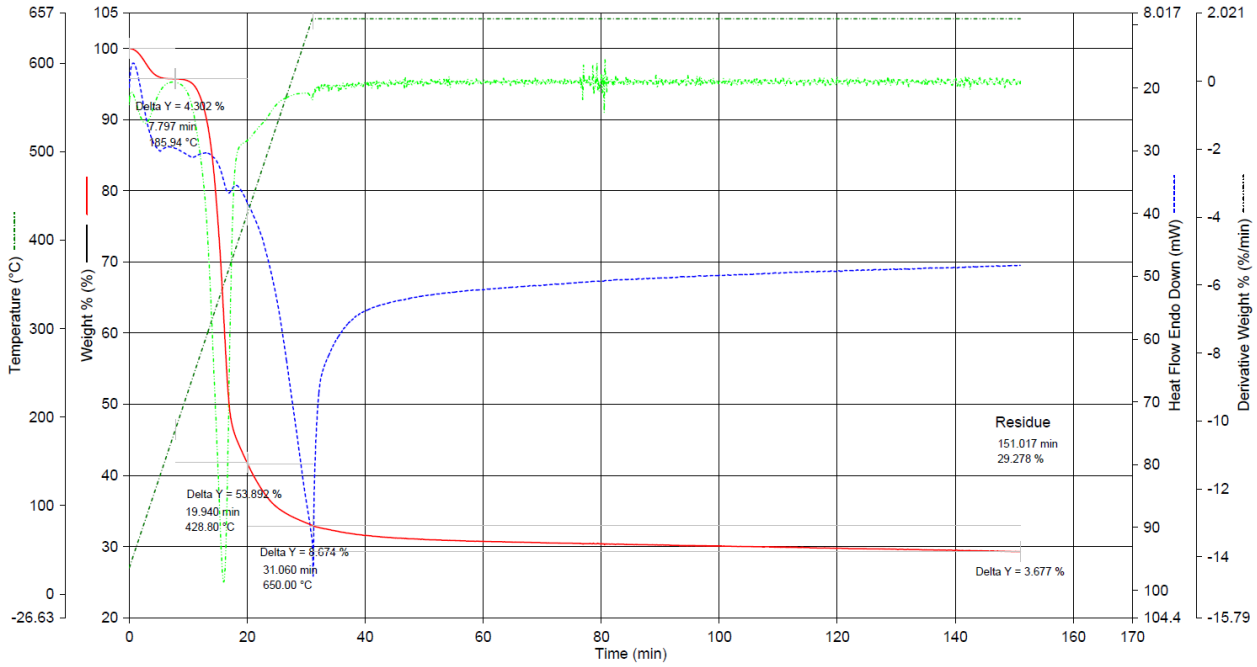

Figure 37. TGA-DTA results of digestate at 650 °C x 120 min at 20 °C/min.

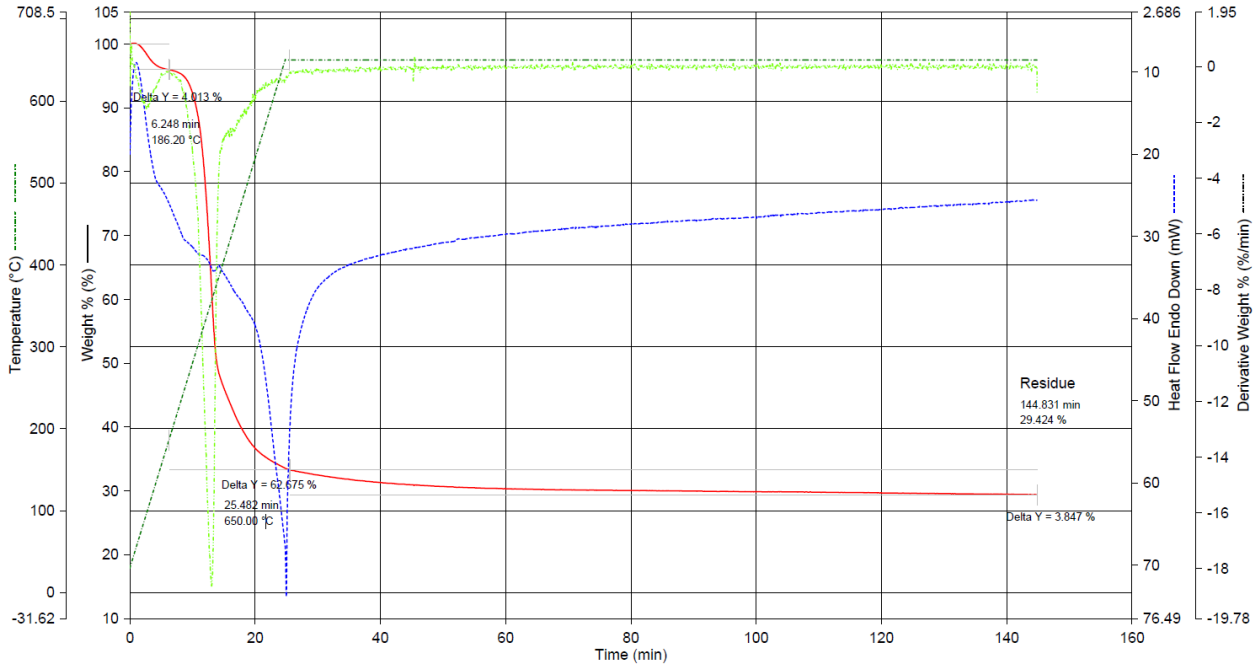

Figure 38. TGA-DTA results of digestate at 650 °C x 120 min at 25 °C/min.

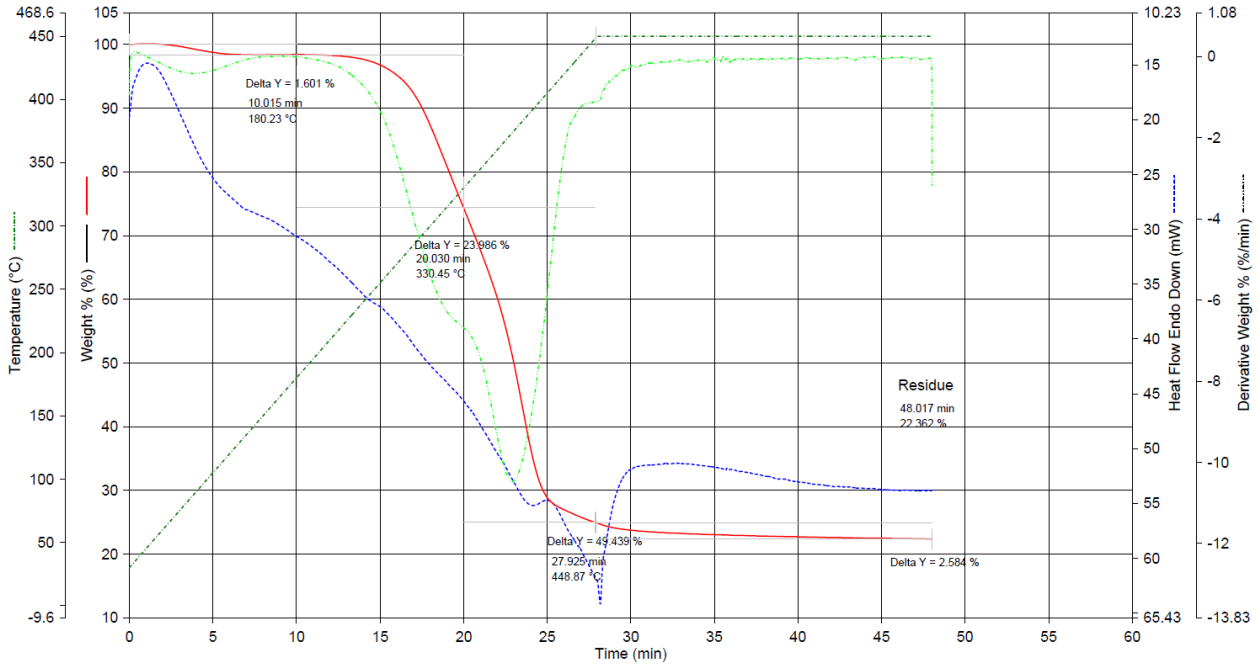

Figure 39. TGA-DTA results of prunings at 450 °C x 20 min at 15 °C/min.

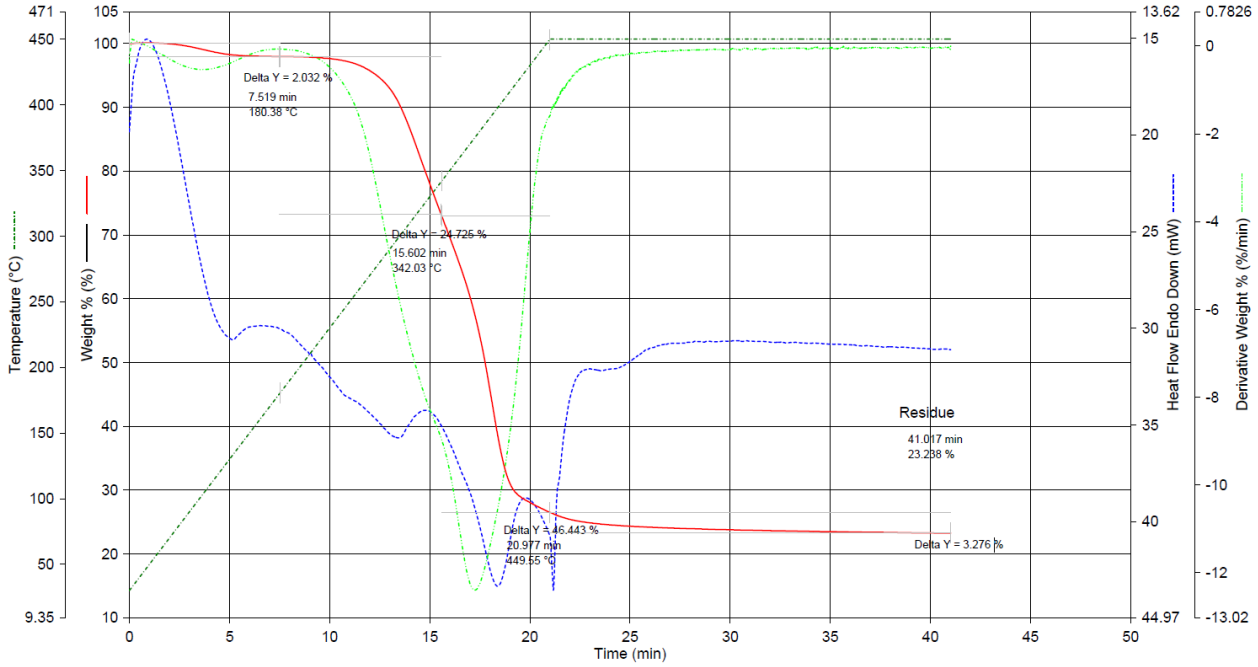

Figure 40. TGA-DTA results of prunings at 450 °C x 20 min at 20 °C/min.

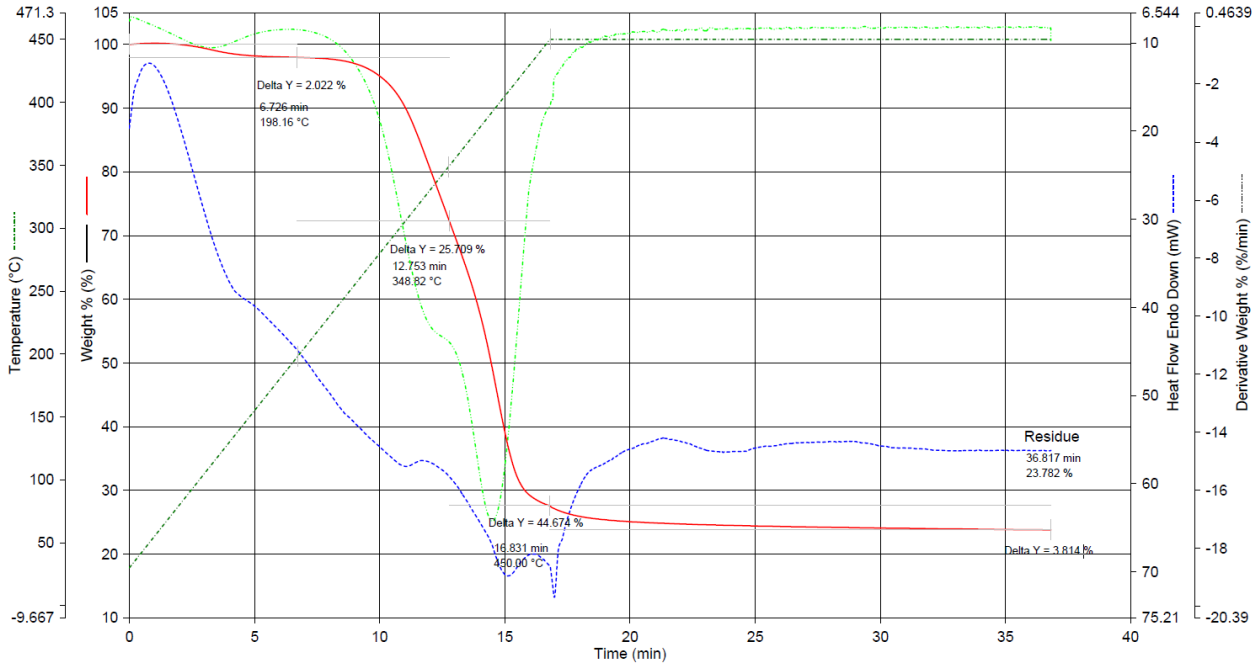

Figure 41. TGA-DTA results of prunings at 450 °C x 20 min at 25 °C/min.

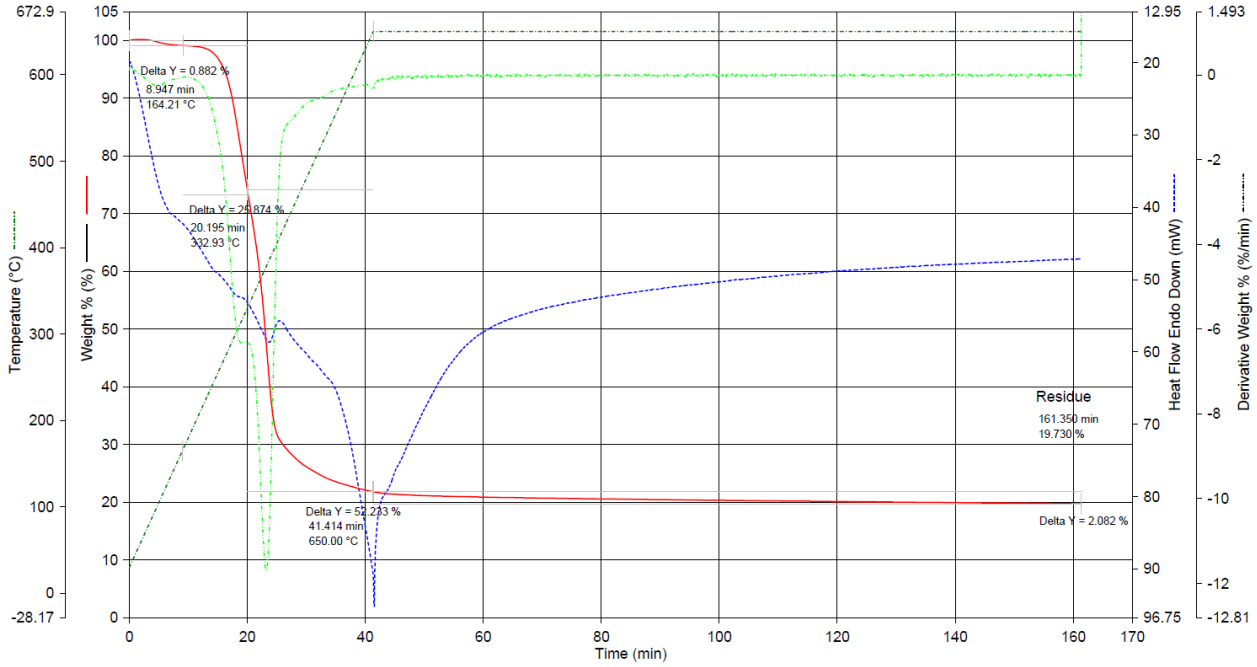

Figure 42. TGA-DTA results of prunings at 650 °C x 120 min at 15 °C/min.

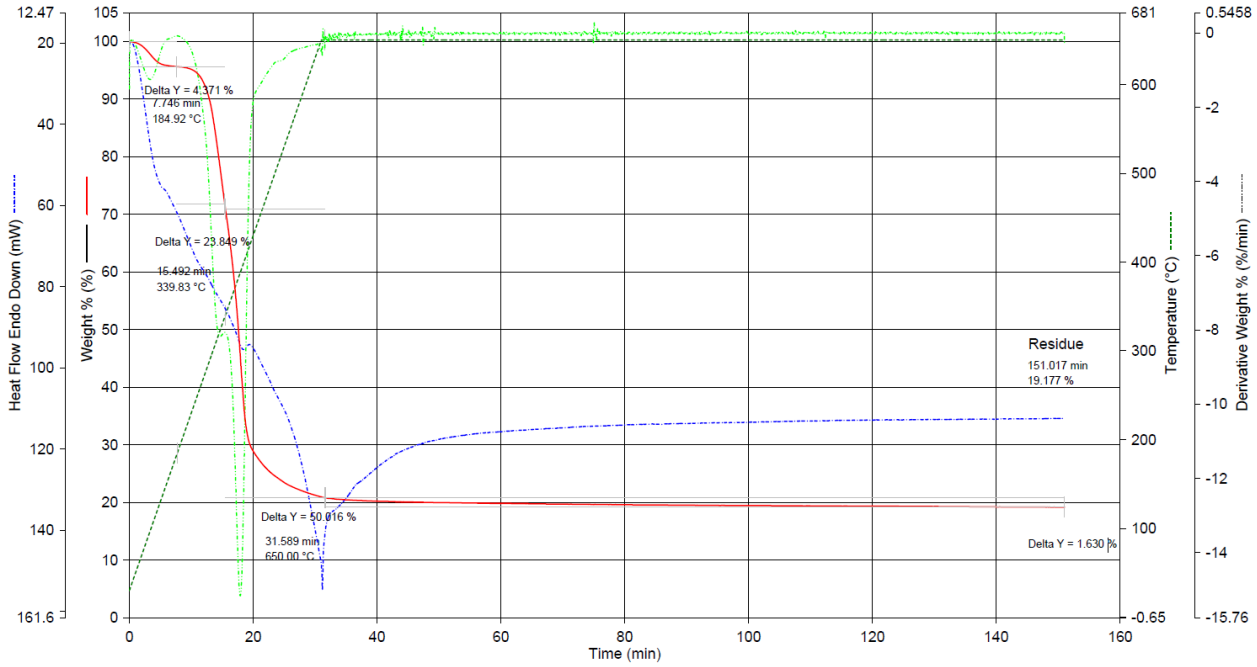

Figure 43. TGA-DTA results of prunings at 650 °C x 120 min at 20 °C/min.

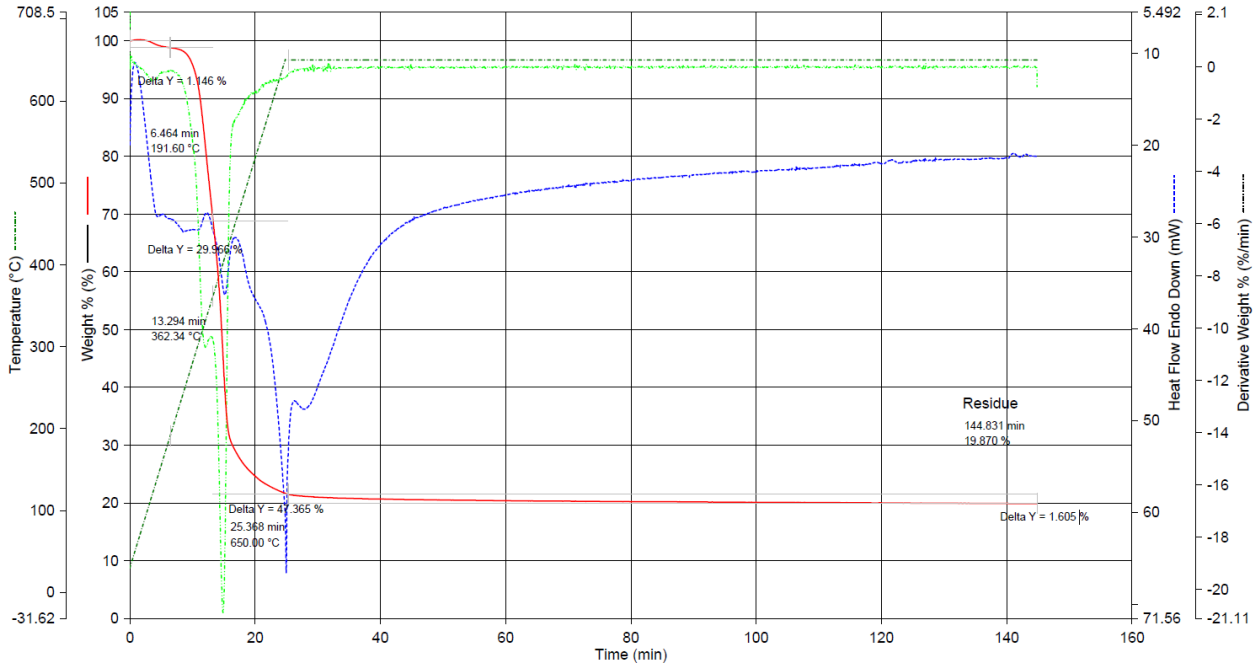

Figure 44. TGA-DTA results of prunings at 650 °C x 120 min at 25 °C/min.

Table 14 summarizes the results of the mass loss associated to the main transformations occurred in the four biomasses during the heating. In Table 15, the onset temperature of the pyrolysis process is reported.

From the mass loss analysis, prunings and OFMSW are the two biomasses that show the highest loss and the less yield whereas the civil mud is the sample with the highest residual mass among the whole matrixes.

Although prunings and OFMSW behaved similarly in term of mass loss, the former has a beginning temperature of pyrolysis process (i.e., onset temperature) higher than the latter, that seems to be the matrix that requires a lower thermal input to start its conversion into a char. On the other side, digestate is the sample requiring the highest temperature to begin the pyrolysis process.

Table 36 Mass loss due to moisture evaporation, pyrolysis during the heating rate and pyrolysis during the isothermal dwelling.

Samples	Temperature x Time [°C x min]	Heating rate [%]	Moisture [%]	Pyrolysis [%]	Isothermal [%]	Residue [%]
Digestate	450 x 20	15	2.702	53.578	3.444	40.276
		20	3.679	53.521	3.484	39.125
		25	4.005	54.262	4.231	37.139
	650 x 120	15	2.059	49.167	14.238	34.534
		20	4.302	62.566	3.677	29.278
		25	4.013	62.675	3.847	29.424
Prunings	450 x 20	15	1.061	69.419	2.584	22.362
		20	2.032	71.168	3.276	23.238
		25	2.022	70.383	3.814	23.782
	650 x 120	15	0.882	78.107	2.082	19.730
		20	4.371	73.865	1.630	19.177
		25	1.146	77.331	1.605	19.870
Civil mud	450 x 20	15	3.838	44.015	4.640	47.434
		20	3.933	42.465	5.871	47.356
		25	3.725	42.638	6.305	47.142
	650 x 120	15	2.516	58.479	1.567	42.894
		20	2.460	53.683	1.611	42.819
		25	2.411	53.079	1.600	42.769
OFMSW	450 x 20	15	0.117	71.921	3.554	24.264
		20	1.344	69.657	4.791	24.209
		25	1.274	68.548	6.264	23.967
	650 x 120	15	0.786	77.732	1.391	20.091
		20	3.209	76.478	1.199	19.093
		25	0.763	78.331	1.476	19.430

Table 37. Onset temperature for the pyrolysis process (°C)

Experimental condition	450 °C x 20 min			650 °C x 120 min		
Heating rate	15 °C/min	20 °C/min	25 °C/min	15 °C/min	20 °C/min	25 °C/min
Digestate	287.19	304.51	309.98	283.95	302.92	306.09
Prunings	278.52	285.85	292.61	273.55	286.14	292.96
Civil mud	248.67	258.00	266.76	250.39	258.78	268.33
OFMSW	211.63	230.51	239.95	218.96	226.79	228.08

In Figure 45 and Figure 46 the interpolation of experimental points according to the KAS method is reported while in Figure 47 the activation energy as a function of the conversion rate (commonly from 0.2 to 0.8) is reported.

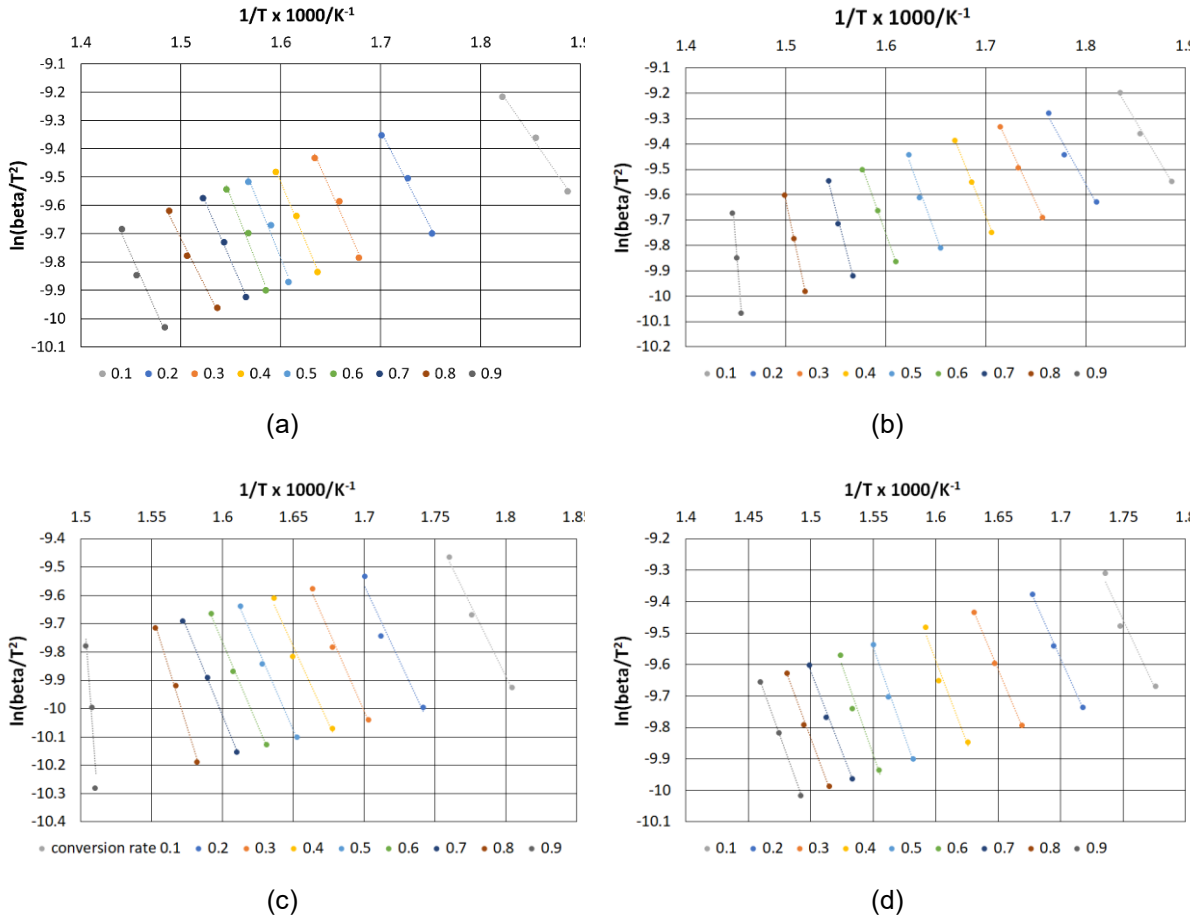

Figure 45. Linear interpolation of experimental points according to the KAS method for a) OFMSW; b) civil mud; c) digestate; d) prunings treated at 450 °C for 20 min.

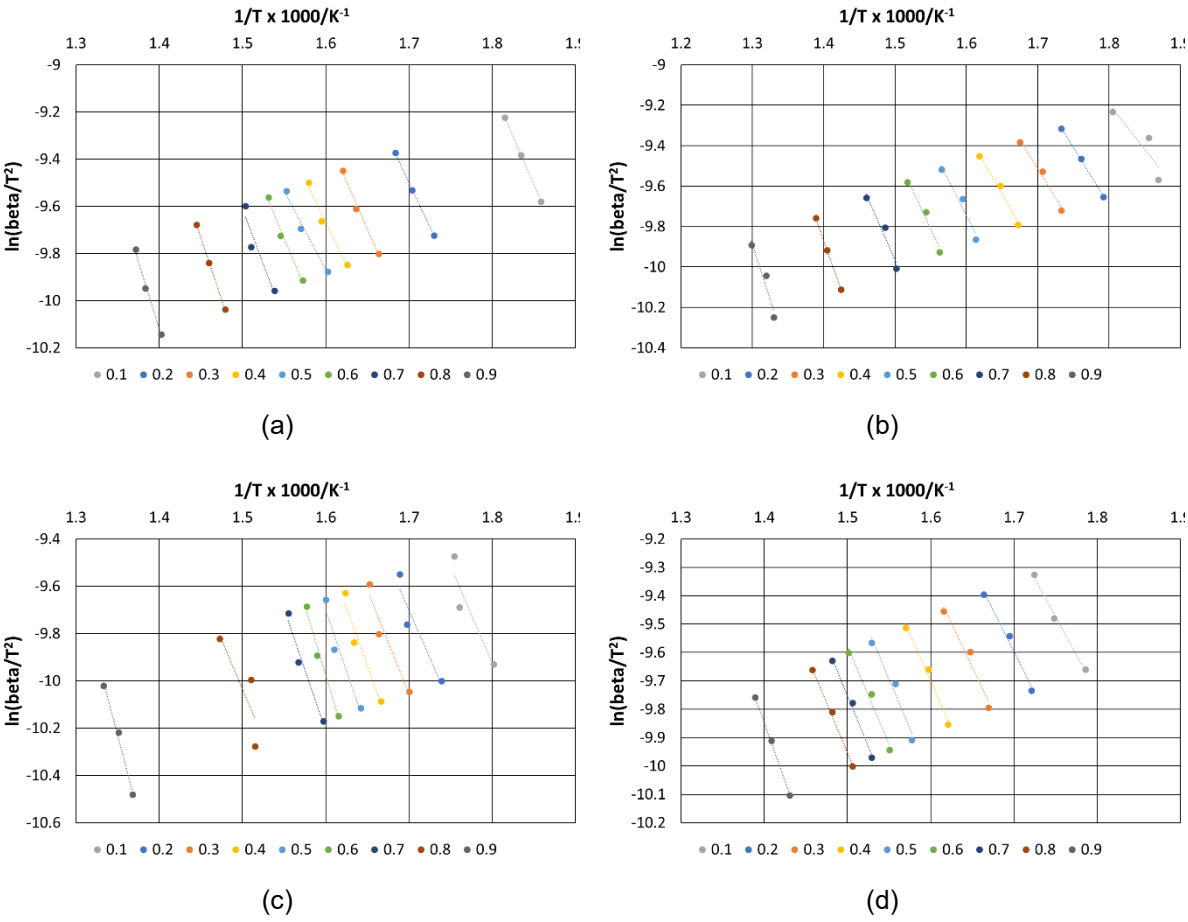

Figure 46. Linear interpolation of experimental points according to the KAS method for a) OFMSW; b) civil mud; c) digestate; d) prunings treated at 650 °C for 120 min.

As can be inferred from Figure 47 and Figure 37, the four biomasses have an activation energy very close each other and with limited variation by increasing the conversion rate. From the pyrolysis performed at 450 °C for 20 min, the digestate registered the highest activation energy, while OFMSW showed the lowest. However, by processing the biomasses at higher temperature (650 °C) the activation energy required for initiating the pyrolysis decreased for all the matrixes except the OFMSW. By the way, the heterogeneity of biomass streams may influence significantly the result of micro TGA-DTA due to the small mass of the sample investigated.

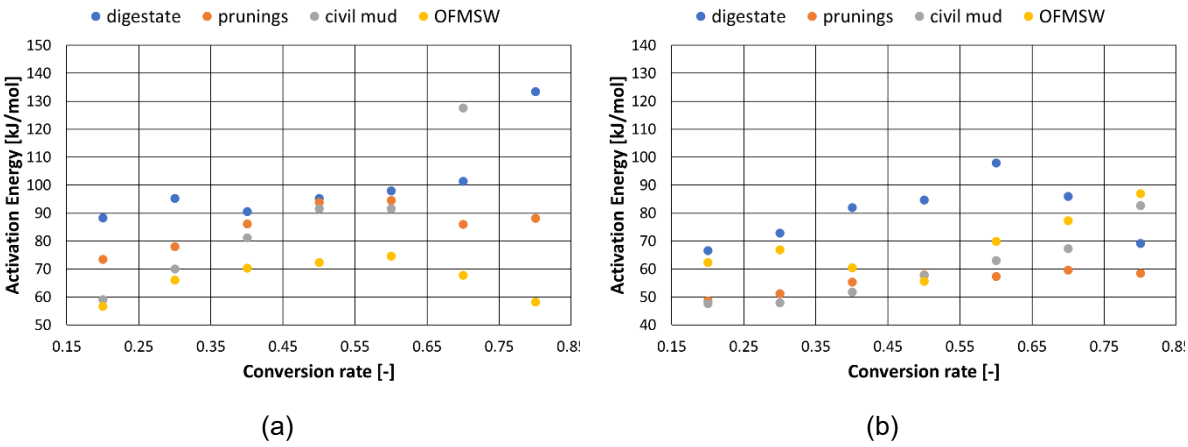

Figure 47. Activation energy as a function of conversion rate for test at a) 450 °C x 20 min and b) 650 °C x 120 min

Table 38. Average activation energy of the pyrolysis process as a function of the experimental conditions.

Experimental condition	450 °C x 20 min	650 °C x 120 min
Digestate	100.40 kJ/mol	79.99 kJ/mol
Prunings	85.80 kJ/mol	55.60 kJ/mol
Civil mud	96.39 kJ/mol	59.82 kJ/mol
OFMSW	66.70 kJ/mol	68.58 kJ/mol

8.1 Annex I conclusions

From the TGA-DTA analysis conducted on the four selected biomass streams, it is possible to conclude that:

- civil mud has the highest yield in terms of residual mass after the pyrolysis process (> 40 wt.%);
- onset temperature for pyrolysis initiation ranges from 210 °C to 310 °C moving from OFMSW to digestate;
- digestate has the highest activation energy among the four streams while OFMSW the lowest;
- by increasing the pyrolysis temperature, the activation energy decreases for all the biomasses except the OFMSW.

8.2 Annex I references

[1] T. Akahira, T. Sunose, *Res. Rep. Chiba Inst. Technol.* **1971**, 16, 22.